

THE PROCESSING AND INTERPRETATION
OF DEER LAKE SEISMIC DATA

CENTRE FOR NEWFOUNDLAND STUDIES

**TOTAL OF 10 PAGES ONLY
MAY BE XEROXED**

(Without Author's Permission)

FARAZI KAMALUDDIN AHMED



THE PROCESSING AND INTERPRETATION
OF DEER LAKE SEISMIC DATA

by



Farazi Kamaluddin Ahmed, M.Sc.

A thesis submitted in partial fulfilment
of the requirements for the degree of
Master of Science

Department of Earth Sciences (Geophysics)

Memorial University of Newfoundland

December 1983

St. John's

Newfoundland

ABSTRACT

Seismic data were collected along a 1.5km long section near Squires Pond Park. These data along with Shell data for the area provided refraction and reflection information on the subsurface structure of the area.

Computer programmes were developed and implemented to process the refraction and reflection data and the data were interpreted in terms of geologic structure. An ideal synthetic seismogram was constructed and compared with the stacked section, and a good correlation was obtained.

Two shallow reflectors and refractors at average depths about 75m and 175m were detected. The seismic interpretation agrees with the local geology and with the available gravity and magnetic interpretation.

Table of Contents

1	INTRODUCTION	1
1.1	Objective	1
1.2	Geology	3
1.3	Previous Geophysical Work	9
1.3.1	Gravity and Magnetics	9
1.3.2	Paleomagnetism	11
1.4	Present Survey	12
2	REFRACTION	14
2.1	Purpose of the Refraction Studies	14
2.2	Preliminary Velocity Determination	14
2.2.1	Collection of Data	14
2.2.2	Processing of Shell Data	16
2.2.3	Results from Shell Data	16
2.3	Squires Park line	18
2.3.1	Collection of Data	19
2.3.2	Processing of Data	19
2.3.3	Refraction Interpretation	35
3	REFLECTION	38
3.1	Objective	38
3.2	Reflection Data Collection	38
3.3	Data Processing	39
3.3.1	Static Correction	41
3.3.2	Mute	41
3.3.3	Filter	42
3.3.4	CDP Gather	48
3.3.5	Velocity Analysis †	50
3.3.6	Normal Moveout Correction	52
3.3.7	Stack	53
4	INTERPRETATION	54
4.1	Reflection	54
4.2	Refraction	57
4.3	Correlation with Geology, Gravity and Magnetics	58
5	SUMMARY AND CONCLUSIONS	60
5.1	Summary and Conclusions	60
5.2	Limitations and Suggestions for Further Work	61
6	APPENDIXES	63
	Appendix-1	63
	Appendix-2	64
	Appendix-3	68
	Appendix-4	70
	Appendix-5	73
	Appendix-6	76
	Appendix-7	78

7 COMPUTER PROGRAMMES
8 ACKNOWLEDGEMENTS
9 REFERENCES

79
96
98

LIST OF FIGURES

FIGURE		Page
1.1	Geology of Deer Lake Basin	2
1.2	Geology of eastern Canada and adjacent areas	4
2.1	Shot-point location map of Shell	15
2.2-2.13	Time-distance curve for shot 1 to 14 except shot 2 and 12	21-32
2.14	Refraction interpretation	36
3.1	Plot of demultiplexed data	(in pocket)
3.2	Plot of static corrected data	(in pocket)
3.3	Plot of muted data	(in pocket)
3.4	Plot of power spectrum before filter	43
3.5	Plot of filtered data	(in pocket)
3.6	Plot of power spectrum after filter	47
3.7	Stacking chart	49
3.8	Plot of CDP gather data	(in pocket)
3.9	Plot of data after NMO correction	(in pocket)
3.10	Plot of stacked data	(in pocket)
4.1	Plot of synthetic stacked data	(in pocket)

LIST OF TABLES.

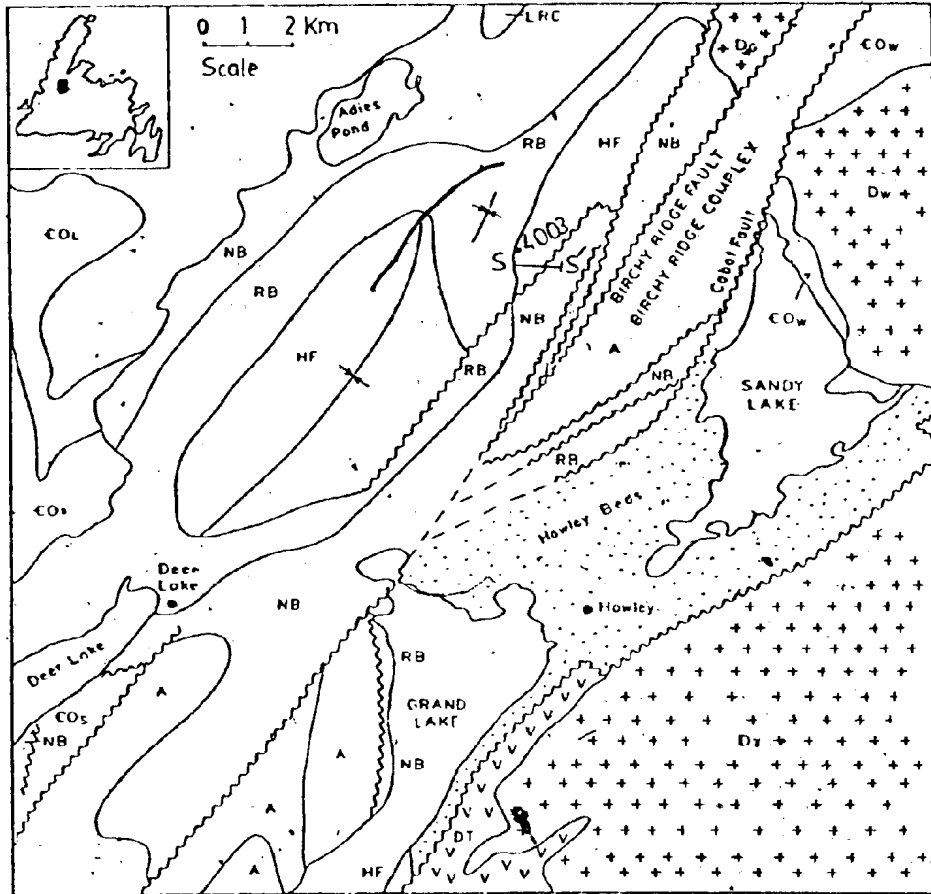
TABLE		Page
2.1	Average velocity from Shell seismic refraction data	17
2.2	Offset distance, intercept time, velocity, depth and crossover distance of different shots in Squires Park line	33
3.1	Stacking velocity for the second reflector at different CDP	52

1 INTRODUCTION

The present work is concerned with a seismic study of the Deer Lake Basin of west central Newfoundland. The basin is approximately bounded by latitudes $49^{\circ}00'N$ and $49^{\circ}30'N$ and longitudes $56^{\circ}50'W$ and $57^{\circ}30'W$. Economic interest in the basin arises from the discovery of oil shales and coal (Hatch, 1919), natural gas (Werner, 1955), and uranium associated with solid hydrocarbons (Hyde, 1979; O'Sullivan, 1979) in the basin.

1.1 Objective

The main aim of the present study was to process the seismic data and to interpret the final seismic sections in terms of geologic structure. As a major part of this work, computer programmes were developed to process the seismic data because of nonavailability of such programmes at Memorial University. The developed programmes were used in data processing in order to get the final seismic sections for interpretation. A major objective of the present investigation was to find the attitude, geometry and depth of the shallow reflectors and refractors below the Squires Park line which traverses part of the Humber Syncline (Hyde, 1979)(Fig. 1.1). The seismic interpretation of the Squires Park line will be correlated with the local geology and with the recently published gravity and magnetic interpretation of the area (Miller and Wright, 1984).



LEGEND

Carboniferous Sediments		Devonian Intrusives	Lower Paleozoics
[Stippled Box] Howley Beds	[Box with + + +] D ₆ Gull Pond	[Box with + + +] Granite	[Box with + + +] Cambro-Ordovician Clastics
[Wavy Line] Number Syncline	[Box with + + +] D _w Wild Cove Pond	[Box with V V V] Volcanics	[Box with + + +] Cambro-Ordovician White Bay Suite
[Box with HF] Humber Falls	[Box with + + +] D _t Topsails	[Box with 4003] Gravity Station	[Box with + + +] Cambro-Ordovician Limestones
[Box with RB] Rocky Brook			[Box with + + +] Precambrian Long Range Complex
[Box with NB] North Brook			
[Box with A] Anguille Group			
[Box with SS] Seismic line			

Fig. 1.1 Geology of Deer Lake Basin (After Hyde, 1979).

1.2 Geology

The Deer Lake Basin is a narrow elliptically shaped northeasterly trending basin in west central Newfoundland. The basin extends north to White Bay and is connected with the Bay St. George Basin to the south (Fig.1.2). The basin contains Carboniferous rocks (Hyde,1979; Haworth and Sanford,1976; Haworth et al.,1976) and is bounded on the northwest by the crystalline rocks of the Long Range Complex and on the east by the lower Paleozoic oceanic rocks of the Dunnage Zone (Williams,1979)(Fig.1.1)

The stratigraphic and structural development of the Deer Lake Basin has been recently studied by Hyde(1979,1983) and Knight(1982). Within the larger basinal framework, smaller sub-basins developed during different time intervals. For this reason, Carboniferous strata of variable age unconformably overlie pre-Carboniferous basement rocks from place to place in the basin. The age of the strata within the Deer Lake Basin can not be estimated with certainty, but most if not all, strata were deposited during the time span Tournaisian-Westphalian A (Hyde,1983).

Our main interest was the geology of the Humber Syncline in the Deer Lake Basin as the seismic line traverses this area and is described in detail.

The major part of the Deer Lake Basin is occupied by Carboniferous rocks which can be divided into two main parts based on the structure of the basin(Fig.1.1)(Hyde,1983). In the western half of the basin is the major northeast

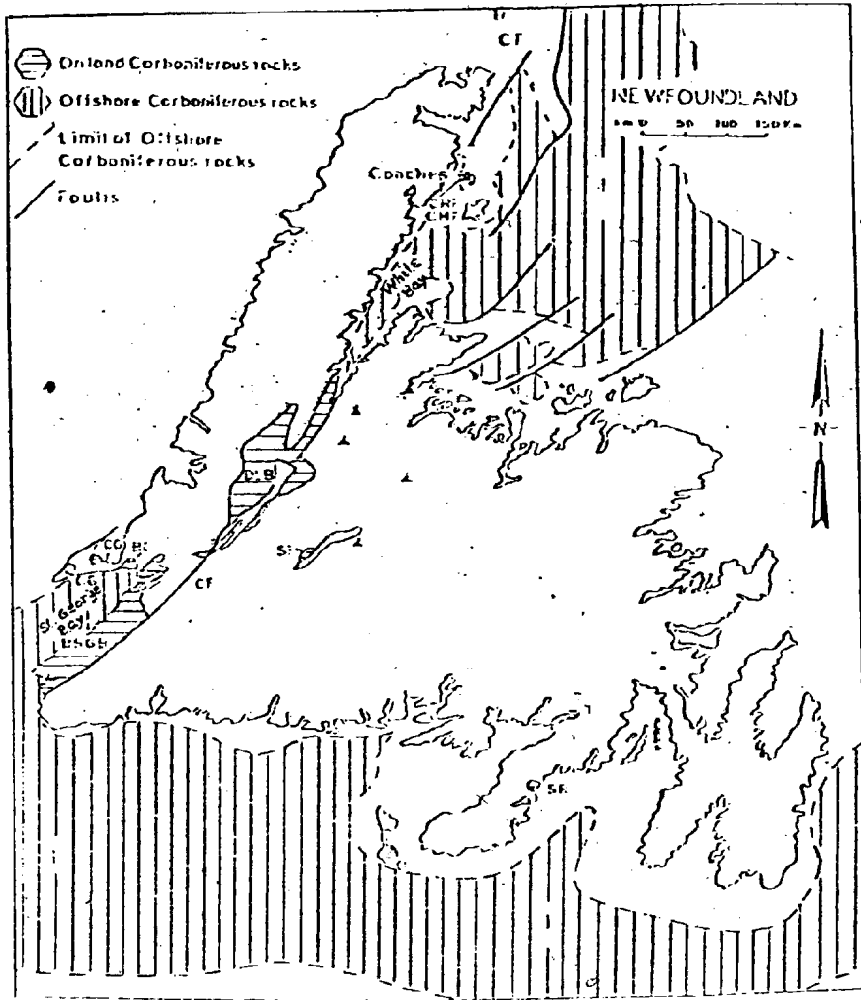


Fig. 1.2 After Sanford, B.V. et al. (1979) Geology of Eastern Canada and adjacent areas, Geological Survey Canada, Map 1401A.

trending Humber Syncline of the Deer Lake group rocks composed of North Brook, Rocky Brook, and Humber Falls Formations. In the eastern part of the basin the Deer Lake Group is represented by "Howley Beds" (Hacquebard et al., 1960). The Humber Syncline is fault bounded on the east by the Birchy Ridge Fault (Hyde, 1983). Small anticlinal and synclinal structures are found in the major syncline especially in the northern side of the Humber Falls formation. The Squires Park seismic line passes over this area (Fig. 1.1)

North Brook Formation: The oldest unit in the Humber Syncline is the North Brook Formation which unconformably overlies Lower Paleozoic metasedimentary strata in the western part of the basin. The stratigraphic thickness of this formation varies from a feather edge to possibly about 2000m elsewhere in the basin (Fig. 1.1) (Hyde, 1983). The North Brook formation is characterized by reddish, and to a lesser extent grey, sandstones, conglomerates and siltstones. This formation has all the characteristics of fluvial deposition.

Rocky Brook Formation: The Rocky Brook Formation is Viséan in age (Hyde, 1979) and is conformable with the North Brook Formation in such a way that the lower part of the Rocky Brook is interpreted to be intertonguing with and the facies equivalent to the upper portion of the North Brook Formation. The Rocky Brook Formation is about 1000m thick as a maximum, but 500-600m is more usual.

Hyde (1983) suggested that the Rocky Brook Formation can be

internally subdivided into a lower member(not shown in Fig.1.1) which contains mainly red, calcareous siltstones, grey to green siltstones and mudstones, and intercalated calcareous dolostones and dolomitic limestones. The upper member contrasts with the lower member in that it lacks red strata and is dominated by grey, green and black mudstones, and grey to green siltstones. Pyrite, oil shale and fossil fish are much more abundant in the upper member than in the lower member.

Humber Falls Formation: This formation having a maximum thickness of about 250m sharply overlies the Rocky Brook Formation in the western part of the Deer Lake Basin. The Humber Falls Formation is of Visean age and is composed of light grey to light green, pink, red, and orange, arkosic sandstones, pebble conglomerates, and red to grey siltstones and mudstones. Sedimentary features are present in this formation. The Humber Falls formation is thought to be the product of fluvial deposition.

Hyde(1983) defined a new unit known as "Little Pond Brook Formation", which was previously considered to be the younger Howley Formation(Belt,1969; Hyde and Ware,1981). The age of this formation is in between Visean to Namurian, which is quite distinct from the Westphalian A assemblage of the Howley Formation. The Little Pond Brook Formation gradationally overlies the lower member of the Rocky Brook Formation at Grand Lake(not shown in Fig.1.1), but also appears along the eastern side of the Grand Lake. Although

the Humber Falls Formation overlies the Rocky Brook Formation, the Little Pond Brook Formation has enough lithologic difference to remain as separate unit. It has the more abundant organic matter and greater lithologic heterogeneity that distinguishes the Little Pond Brook Formation from the Humber Falls Formation.

The Little Pond Brook Formation is about 750m thick and consists of sandstones, pebble to boulder conglomerates and siltstones. Its formation is interpreted to be another fluvial deposit in the Deer Lake Basin with drainage predominantly from the east.

Northwest of the Deer Lake Basin are the Precambrian rocks of the Long Range Complex consisting of metagabbro, gabbroic dikes, granitic gneiss and individual granitic plutons; and southwest of the basin are the Late Precambrian-Middle Ordovician rocks predominantly carbonates, variably recrystallized dolostone, dolostone breccia (including tremolite-phlogopite marble), limestone, quartzite, quartz-mica schist and mica schist (Hyde, 1983).

Southeast and northeast of the Deer Lake Basin are the pre-Carboniferous rocks. The rocks to the southeast consist of the Devonian volcanic rocks, reddish conglomerate and sandstone, whereas to the northeast are the Devonian Gull Lake intrusive and Wild Cove Pond intrusive suite that consists mainly of granite but also granodiorite, diorite and gabbro (Hyde, 1983).

The Howley Formation which Hyde considers the youngest

stratigraphic unit in the basin is Westphalian A age. It lies east of the Cabot Fault, west of the Topsails Igneous suite and south of the Wild Cove Pond Igneous suite. It is not considered part of the Deer Lake Group because of the age difference (Deer Lake Group mainly Viséan). Hyde(1979) suggests a maximum total stratigraphic thickness of 3100m if there has been no repetition by faulting or folding in an area of intermittent exposure. Neale and Nash(1963) considered the thickness to be 2440m based upon their stratigraphic interpretation. Miller and Wright(1984) interpret the thickness to be 1500m based on gravity and magnetics.

The Howley Formation consists of grey to red pebble conglomerates, and sandstone that are interbedded with siltstone and mudstones. Thin seams of bituminous coal are also present in the Howley Formation. This formation is interpreted to be a fluvial deposit (Hyde, 1983).

According to Hyde(1979) the history of the Deer Lake Basin can not be interpreted in terms of a single basin deposition. He suggested that the whole is a pull-apart basin into which sediments were deposited from the surrounding positive topographic features. The Humber Syncline is interpreted in this fashion but the Howley Formation genesis is poorly understood.

1.3 Previous Geophysical Work

In the past, several geological surveys had been conducted in the Deer Lake Basin but no regional geophysical work had been done in that area. Intense exploration geophysical surveys were conducted in limited areas. Recently, extensive gravity surveys were conducted (Miller and Wright, 1984) and paleomagnetic studies were done by Strong and Irving (1983).

1.3.1 Gravity and Magnetics

In the mid 1960s a gravity survey was conducted by the Dominion observatory with a mean station spacing of 13km (Weaver, 1967). From Weaver's survey a high positive gravity anomaly was observed in the Adies Pond area which correlates with gabbro and/or diorite mapped by Baird (1960). Weaver's survey also showed a pronounced eastward trending gravity low over the Howley Formation which was interpreted to be 5km thick compared with the geological estimate of 2440m from Neale and Nash (1963).

In 1981 and 1982 gravity data were collected extensively by a Memorial University team (Miller and Wright, 1984) in the Deer Lake Basin. The Bouguer anomaly map shows that there are strong positive anomalies in the northeast and southeast part of the basin which correlate with the Wild Cove Pond and Topsails igneous suites respectively. Miller and Wright (1984) also showed a positive anomaly in the northwest part of the basin which agrees with the mapping of Weaver's Adies Pond High and coincides with the location of the oldest crystalline rocks in the area.

A prominent northeast trend and the presence of east-west trend in the eastern portion of the Deer Lake Basin are observed in the regional trend map.

The features close to the surface were prominent on the residual anomaly map which shows slightly negative gravity features in the Humber Syncline coinciding with the geology of that area.

Miller and Wright (1984) also discussed the reduced magnetic data for the basin. They showed that the major magnetic anomalies were observed in the north of the basin which is dominated by an east-west trending high towards the northwest extension of the basin and found that the trend of this anomaly pattern is orthogonal to that of the major syncline area. Another positive magnetic anomaly having a north-south trend occurs in the central portion of the northern edge of the basin. They pointed out that both of these high magnetic anomalies terminate over Humber Falls rocks and both have uranium occurrences mapped on their flanks on Smyth and Martineau's map (Smyth and Martineau, 1982).

Miller and Wright (1984) used numerical two-dimensional gravity and magnetic modelling techniques to establish the thickness of various features of the Humber Syncline and the Howley Formation. They computed the gravity and magnetic results for the various geological models which evolved from Hyde's (1979) interpretation.

Their modelling results show that the main Humber Syncline

has a maximum thickness of 1200m. It is underlain on the west by a mafic/ ultramafic body and the east by material of higher than average density having a low magnetic susceptibility. Another result from the modelling is the constraint on the total vertical thickness of the Howley Formation. A good estimate of the Howley sediments thickness was made from the gravity and magnetic modelling and a maximum thickness of sediment was suggested to be 1500m (Miller and Wright, 1984) which disagrees with the estimates of Weaver(1967), Neale and Nash(1963) and Hyde(1979).

1.3.2 Paleomagnetism

Strong and Irving(1983) conducted paleomagnetic studies of the Deer Lake Basin sequence, and thereby obtained some indication of movements relative to other Carboniferous rocks of Newfoundland. They studied the samples of Carboniferous St. Lawrence Granite and the Spanish Room and Terrenceville Formations of the Burin Peninsula(Avalon Tectonic zone) of eastern Newfoundland, in addition to samples from Deer Lake Carboniferous Basin. Their data from four formations of the Deer Lake group all yield a consistent paleolatitude of about 20 degrees south, in agreement with the values determined from the early Carboniferous (Tournaisian) Terrenceville Formation of eastern Newfoundland on the eastern side of the Appalachian orogen. From the good agreement of the results, Strong and Irving suggested that there is no paleomagnetic evidence for

previously proposed 2000km displacement of the northern Appalachians from the south relative to cratonic North America during the Carboniferous (Kent and Opdyke, 1979), although it could have occurred earlier or it could have been smaller than could be detectable paleomagnetically.

1.4 Present Survey

The present seismic survey was conducted during August 1981 by members of the Earth Sciences department of Memorial University. Seismic data were collected on a profile SS' along the road in the Squires Park area, north of Miller & Wright's (1984) gravity profile AB (Fig.1.1). Both the refraction and reflection data were obtained on the same records using shots consisting of 1kg of dynamite buried at depths from 1-3m. The near-offset of the geophone was 25m. A single geophone was placed every 50m along the line using 24 geophone locations per spread with the total spread length of 1175m from the shot to the last geophone. Fourteen shots were detonated at every second geophone location, that is, at an interval of 100m giving a total coverage of approximately 1.4km. Out of these 14 shots, shot number 2 and 12 were noise shots. The data were digitally recorded using a DAS recording system with a sample every 1ms. The elevations of the shots and the geophones were measured with respect to the elevation of the gravity station 4003 (Fig.1.1).

In this thesis, the refraction data (Chapter 2), and the

reflection data (Chapter 3) are discussed. The processed data are interpreted geologically and compared with the available gravity and magnetic results (Chapter 4).

2 REFRACTION

2.1 Purpose of the Refraction Studies

The purpose of the preliminary seismic refraction study was to determine the representative velocities of the different formations in the Deer Lake Carboniferous basin from Shell seismic data (Westfield Minerals Ltd, 1981). The main objective of the refraction study along the Squires Park line which traverses part of the Humber Syncline was to determine the depth of the basement from the first break information and hence to find the internal structure of the beds.

2.2 Preliminary Velocity Determination

In the preliminary refraction study, the velocity of the different formations in the Deer Lake Carboniferous basin was determined from Shell seismic data. The data collection, the processing of these data and finally, the results obtained from the data which give the velocity of different formations in the Deer Lake basin are discussed below.

2.2.1 Collection of Data

In May 1981, seismic refraction tests were conducted by Shell (Westfield Minerals Ltd, 1981) at twelve locations in the Deer Lake basin (Fig.2.1). Two shots, one at each end of the spread were recorded in each location except at location 1. Five single shots were recorded in location 1. One

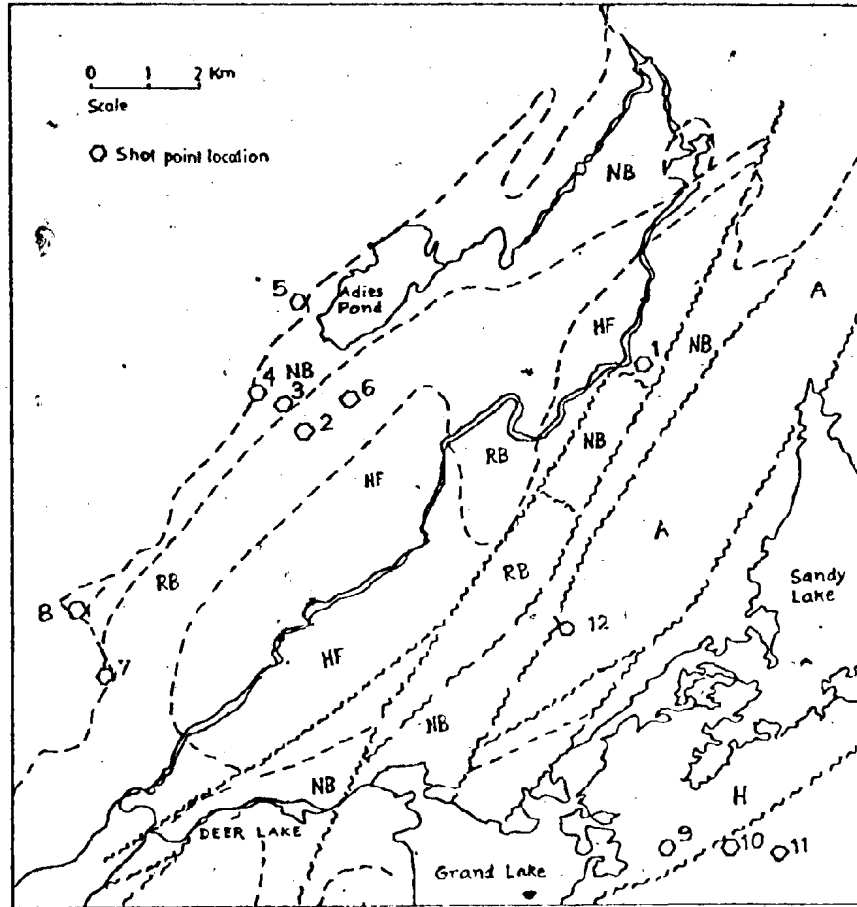


Fig. 2.1 Shot point location map (After Westfield Minerals Ltd., 1981).

kilogram of dynamite was used in each shot. The offset to the nearest geophone was 25m and single geophones were spaced every 25m along the line using 12 geophone locations in each spread. The data were digitally recorded with sampling every 1ms and the record length for each shot was 1sec. The average gain of each trace was 60db. There was no instrumental delay in recording and no filters were used.

2.2.2 Processing of Shell Data

The Shell seismic refraction data were processed from the plots of the data. The first refraction arrival was marked on the field plot of the refraction data for each shot in every location of the Deer Lake basin and the time-distance curve was drawn through the first arrivals. No corrections were made for elevation differences since no elevation data was available. The velocity of the upper layer was determined from the inverse slope of the time-distance curve. The average velocity and the range of the velocity of different formations were computed. Their values were tabulated in Table-2.1.

2.2.3 Results from Shell Data

The results of Shell seismic refraction data which show the range and the average velocity of the different Formations of the Deer Lake basin are given below (Table-2.1).

Shot Point Location nos.	Formation	Range of Velocity(m/s)	Average Velocity(m/s)
1	Humber Falls	2800-3200	3000
2,6,7	Rocky Brook	3200-4650	3925
3,4	North Brook	4400-4650	4525
5,8	Precambrian	6600-7140	6870
10,11	Devonian	4500-5400	4950
9	Howley	4160	4160
12	Anguille Group	4880	4880

Table-2.1 Average velocity from Shell seismic refraction data.

Our main interest was to consider the velocity of the Humber Falls, Rocky Brook and North Brook Formations because the Squires Park line traverses this area. The velocity of these formations was found to be significantly different from each other (Table-2.1). These velocities play an important role in both of our refraction and reflection studies.

The average velocity of the Humber Falls Formation was 3000m/s which overlies the Rocky Brook Formation of higher velocity of approximately 4000m/s. The average velocity of the North Brook Formation is about 4500m/s. On the basis of these velocity contrasts, the velocity contours were chosen to determine the layering in seismic refraction studies.

There are various implications of the velocity of Humber Falls, Rocky Brook and North Brook Formations in reflection studies. Firstly, the upper layer average velocity 3000m/s was used in determining the static correction in both refraction and reflection data. Secondly, these velocities played an important role in estimating the stacking velocity

for the Normal Moveout correction. And finally, they were used to calculate the reflection coefficient for the synthetic modelling in reflection interpretation.

The velocity of the other formations gave an idea of geology of the entire Deer Lake Basin. The velocity of the Howley Formation was 4160m/s. It was less than the velocity of the Devonian intrusive and Anguille Group Formations whose values were 4950m/s and 4880m/s respectively. These results were consistent with Hyde's interpretation which considered the Howley Formation as the youngest unit (Hyde, 1983). The Precambrian rocks of Long Range Complex had the maximum velocity in the range of 6660-7140m/s. The higher velocity in Precambrian rocks was reasonable as it consists of compact high density metamorphic rocks such as quartzite, mica schists etc. (Hyde, 1983).

2.3 Squires Park line

The Squires Park line traverses part of the Humber Syncline. The refraction and reflection data of the present study were collected together along that line. The refraction data were processed and interpreted and are discussed in this chapter.

2.3.1 Collection of Data

In August 1981, seismic refraction data were collected by a team from Memorial University along the Squires Park line. The offset of the nearest geophone was 25m and single geophone was placed every 50m along the line using 24 geophone locations per spread. Fourteen shots were detonated at every second geophone location with an interval of 100m giving a total coverage of about 1.4 km. Shot number 2 and 12 were misfires and all the shots consist of 1kg of dynamite buried at 1 to 3m depth. The data were digitally recorded with sampling every 1ms. The shot and the geophone elevations were measured with respect to the elevation of the gravity station 4003 (Fig.1.1.) and their values were tabulated (Appendix-1).

2.3.2 Processing of Data

At first, the seismic refraction data were static corrected in the data processing. The purpose of the static correction was to eliminate the effect of differing surface elevation.

The technique for static correction was to correct the data to a "datum elevation" (datum plane) by removing the calculated travel times from the source to the datum and from the geophone to the datum.

The static correction is

$$\Delta t_o = \Delta t_s + \Delta t_g \quad (2.1)$$

where $\Delta t_s = \frac{E_s - E_d}{V_{av}}$, is the source correction

and $\Delta t_g = \frac{E_G - E_d}{V_{av}}$, is the geophone correction.

E_s and E_G are the elevation of source and geophone and E_d is the datum elevation which was chosen 40m below the gravity station 4003 in order to be below the lowest elevation geophone. The average velocity to the datum, $V = 3000\text{m/s}$ used for the static correction which was obtained from preliminary refraction survey of Shell (Westfield Minerals Ltd, 1981)(Section 2.2.3).

Since for each shot 24 traces were recorded, the shot correction was common to every trace in the record and the individual geophone correction was computed for each trace. For the 14 shots in Squires Park line, the total number of traces was 336 and each of them was static corrected.

The corrected data were plotted as travel times versus offset distance of the geophones. These time-distance curves are shown in figures 2.2 to 2.13. The velocity of each layer was determined from the inverse slope of the static corrected first break data for all shots. Their values were tabulated in Table-2.2.

Assuming horizontal layering, the depth to the interfaces were calculated by using the relations (Appendix-2)

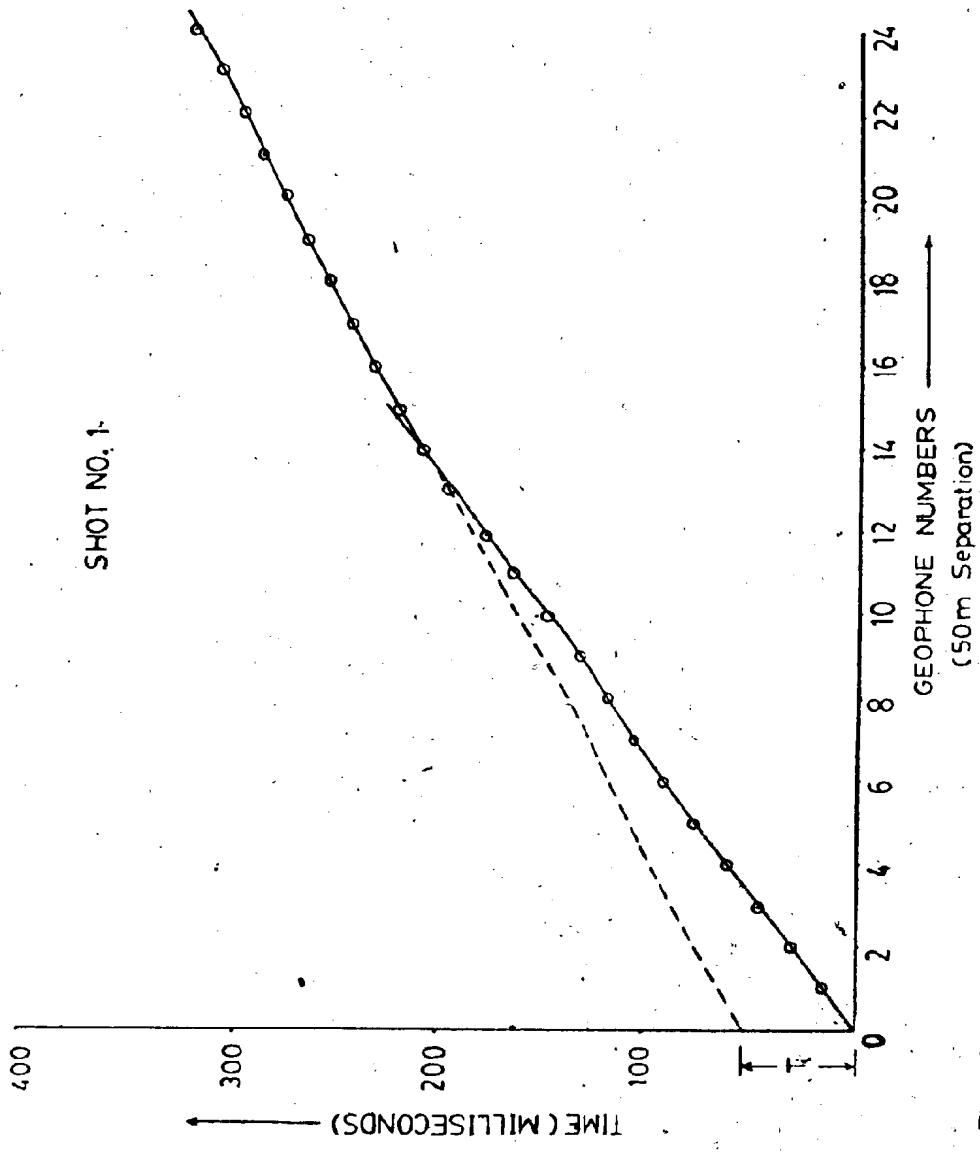


Fig.2.2 Time-distance curve

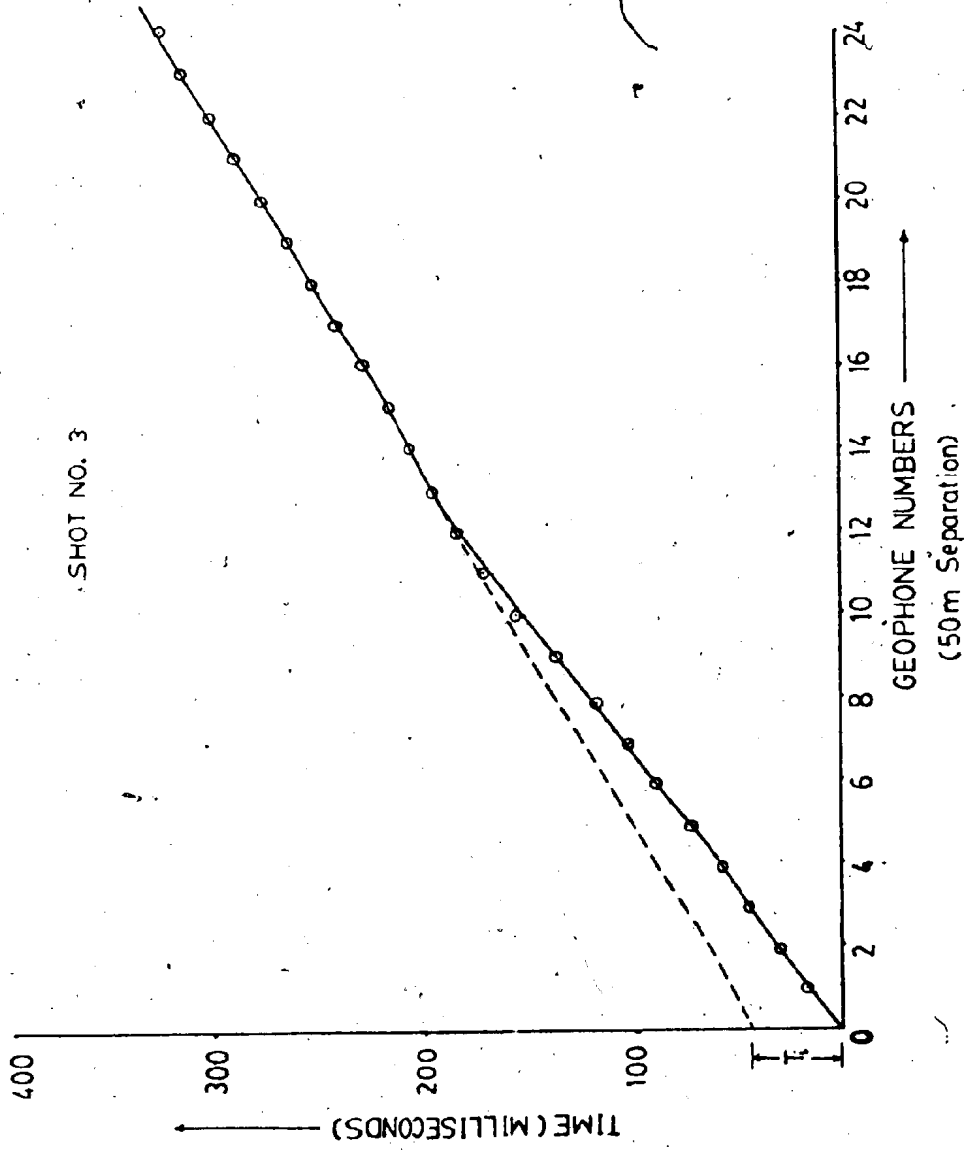


Fig.2.3 Time-distance curve

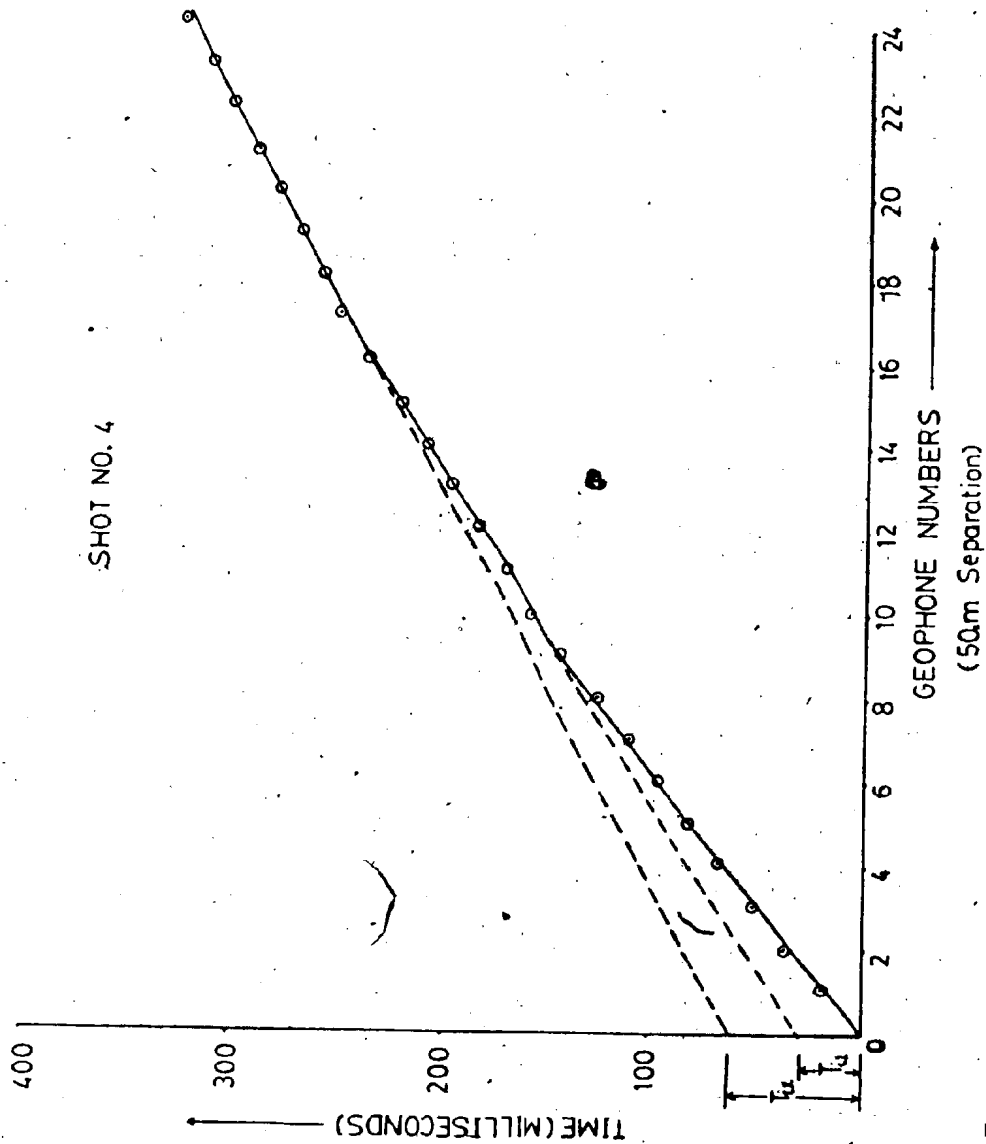


Fig. 2.4 Time-distance curve

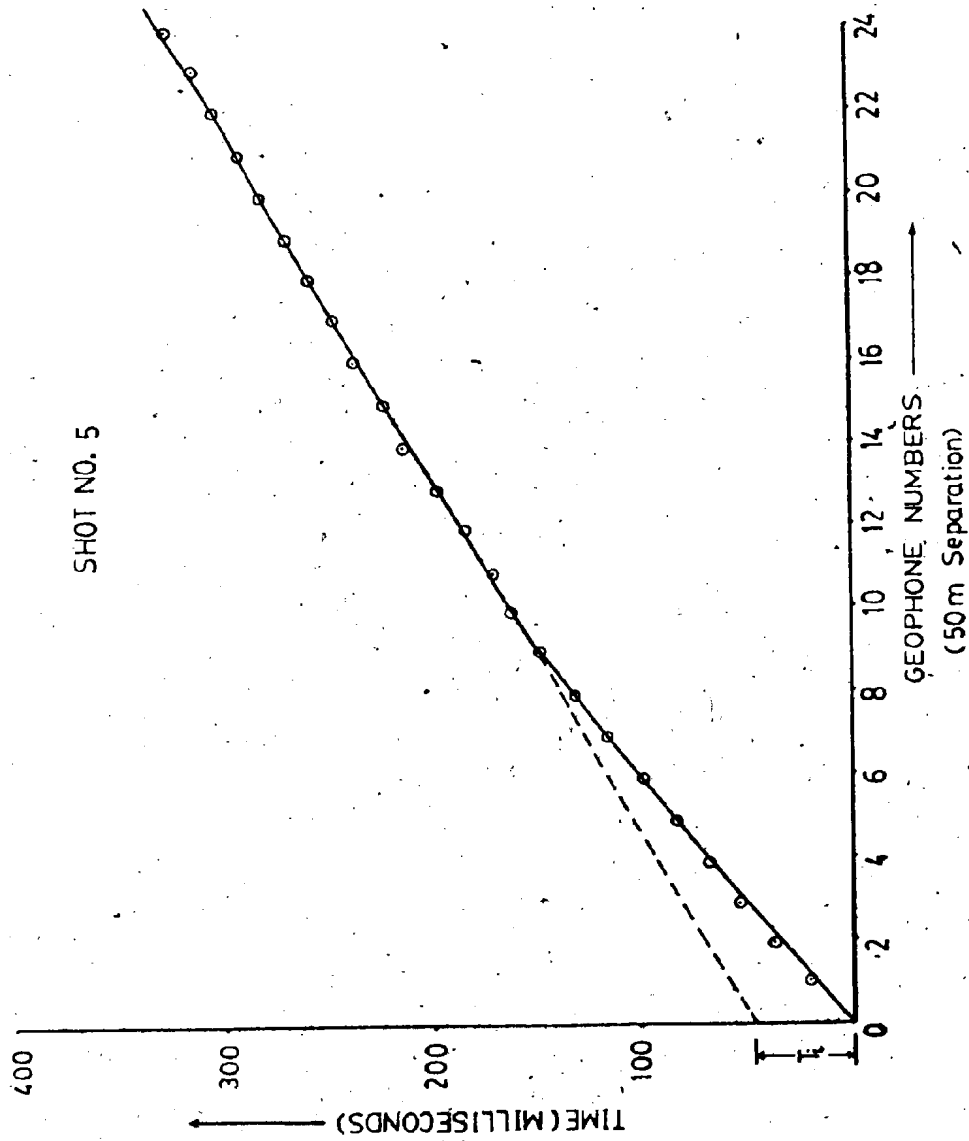


Fig. 2.5 Time-distance curve

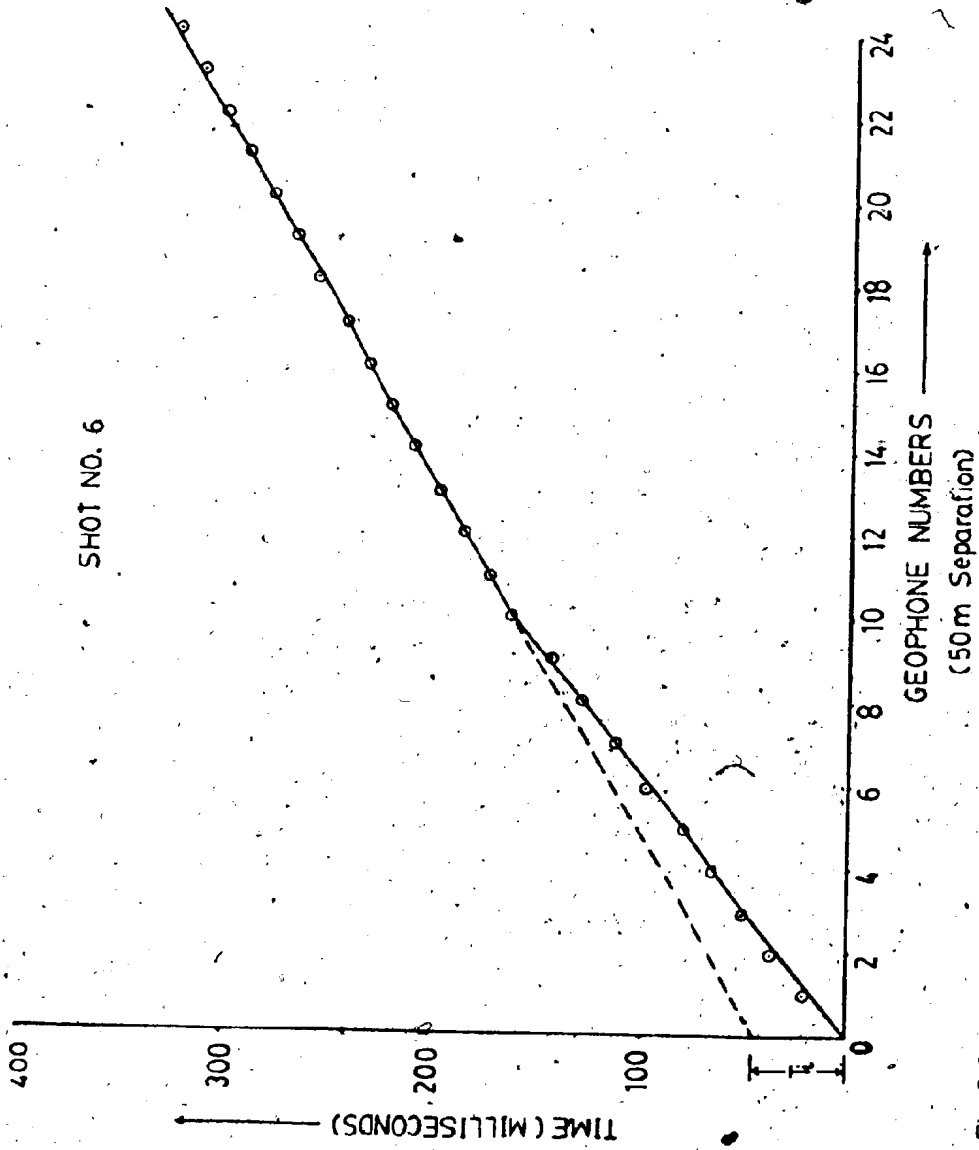


Fig. 2.6 Time-distance curve

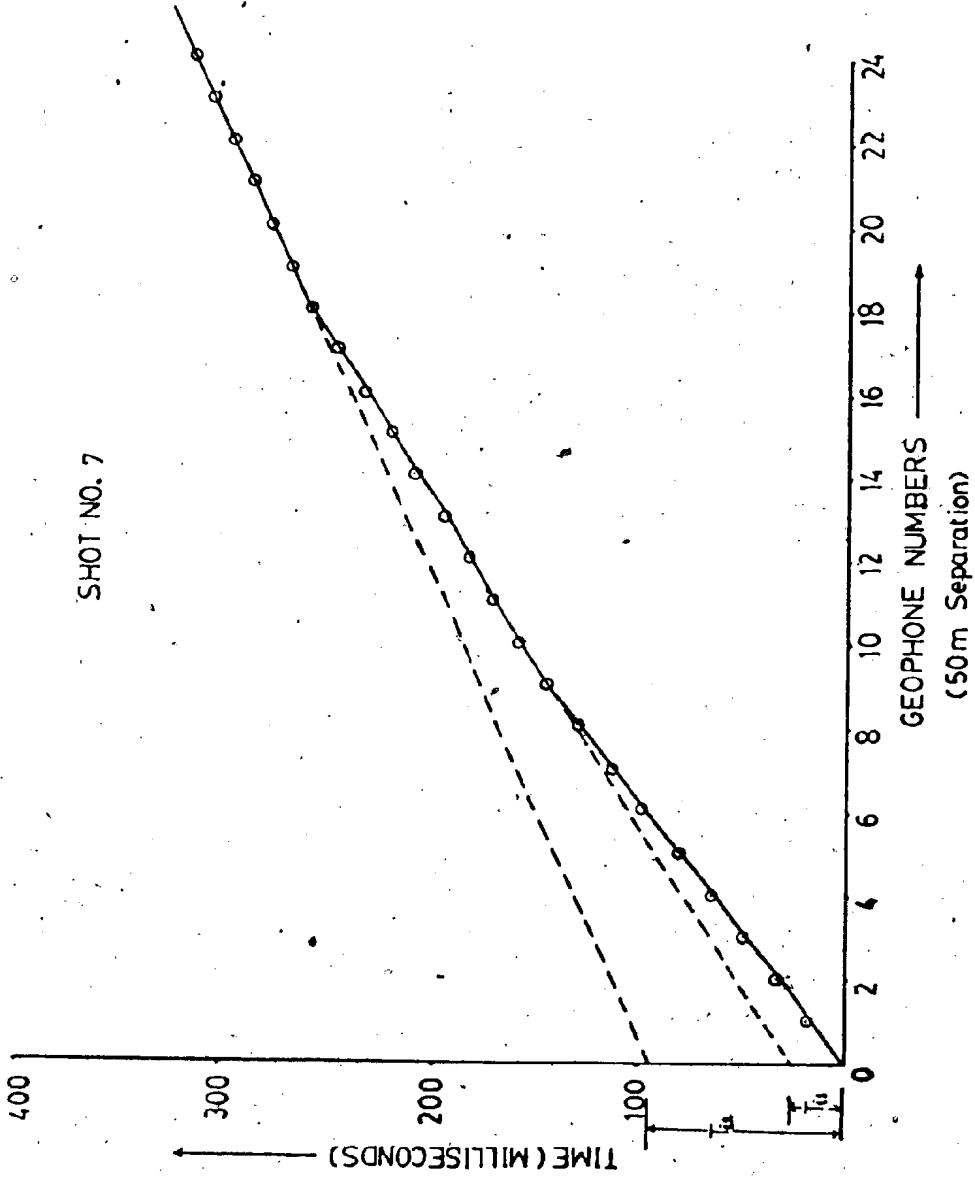


Fig.2.7 Time-distance curve

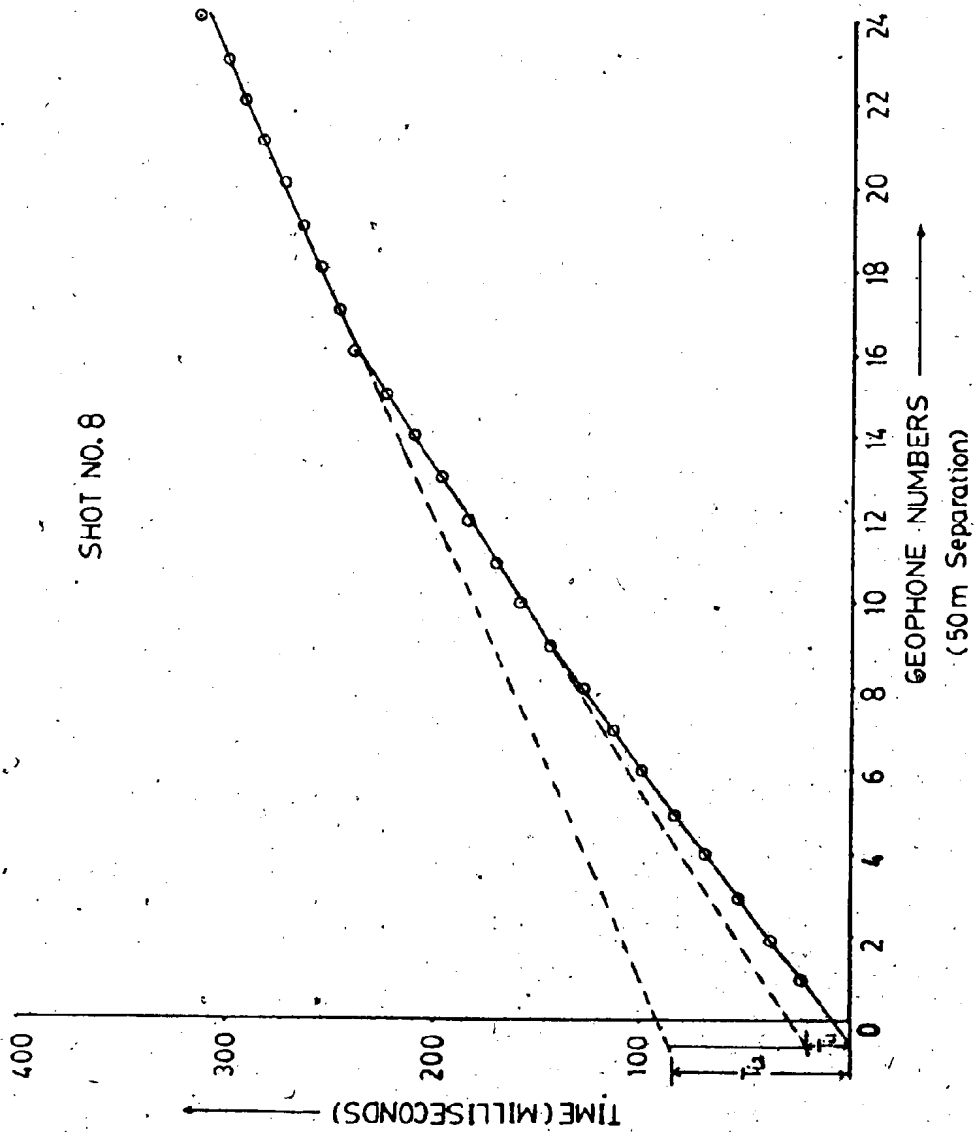


Fig. 2.8 Time-distance curve

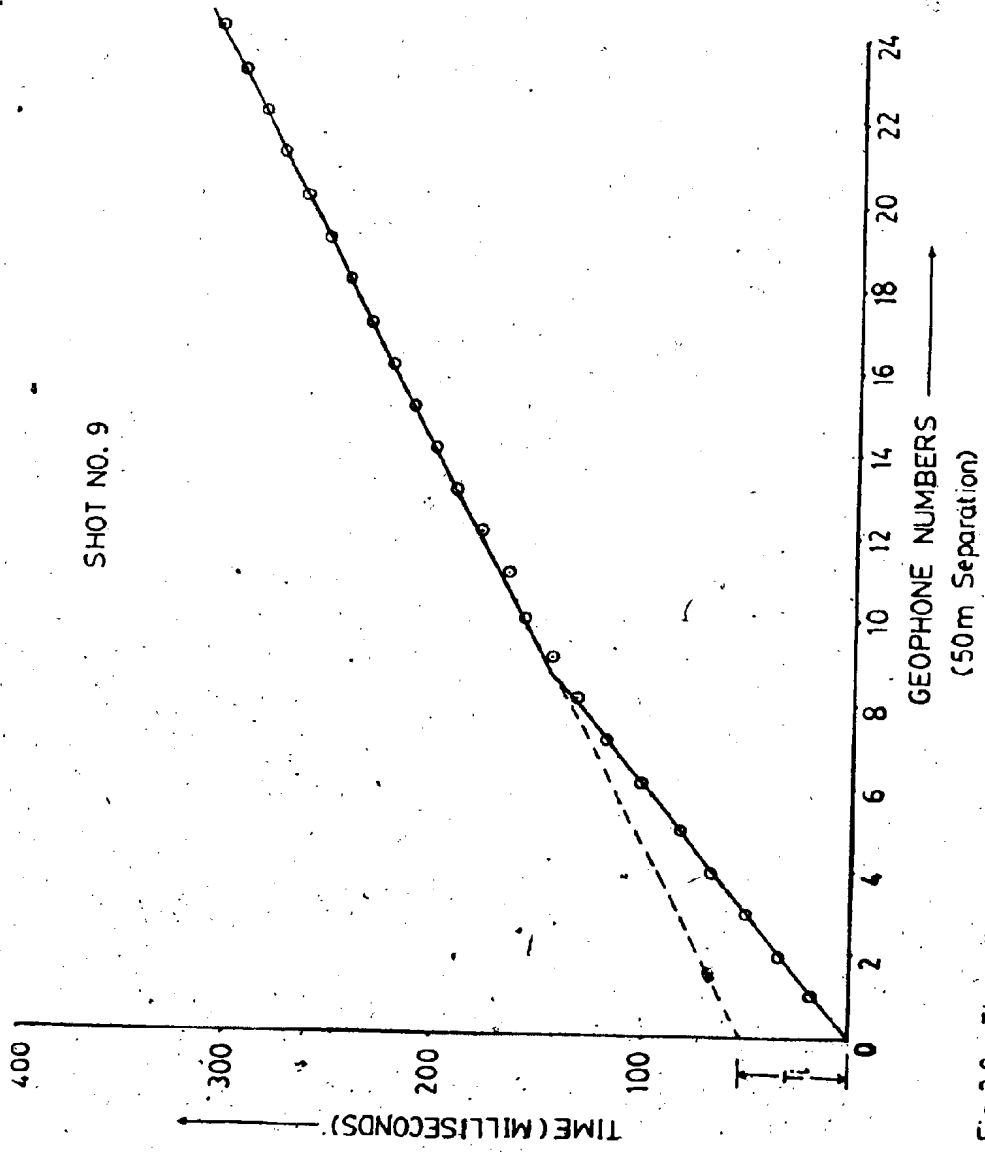


Fig.2.9 Time-distance curve

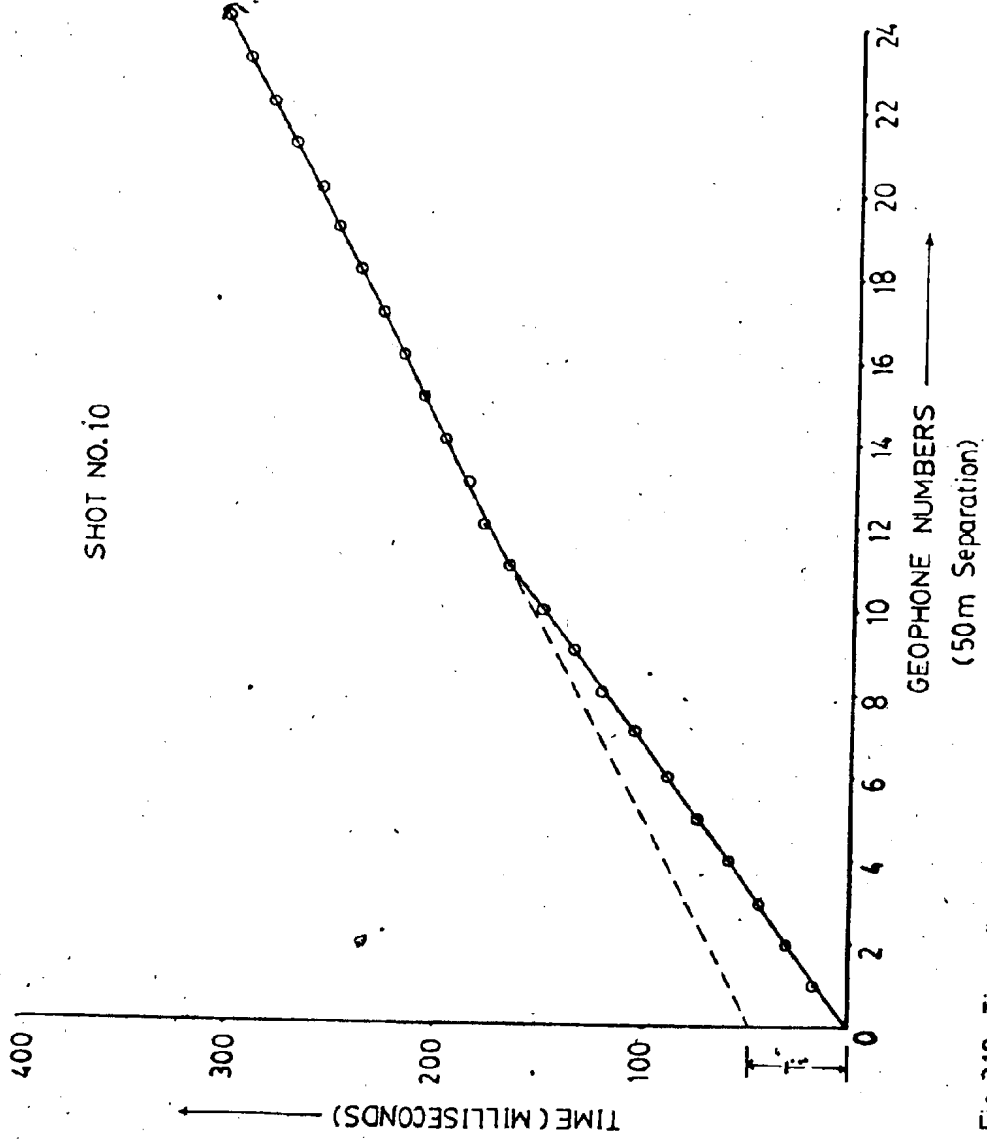


Fig.2.10 Time-distance curve

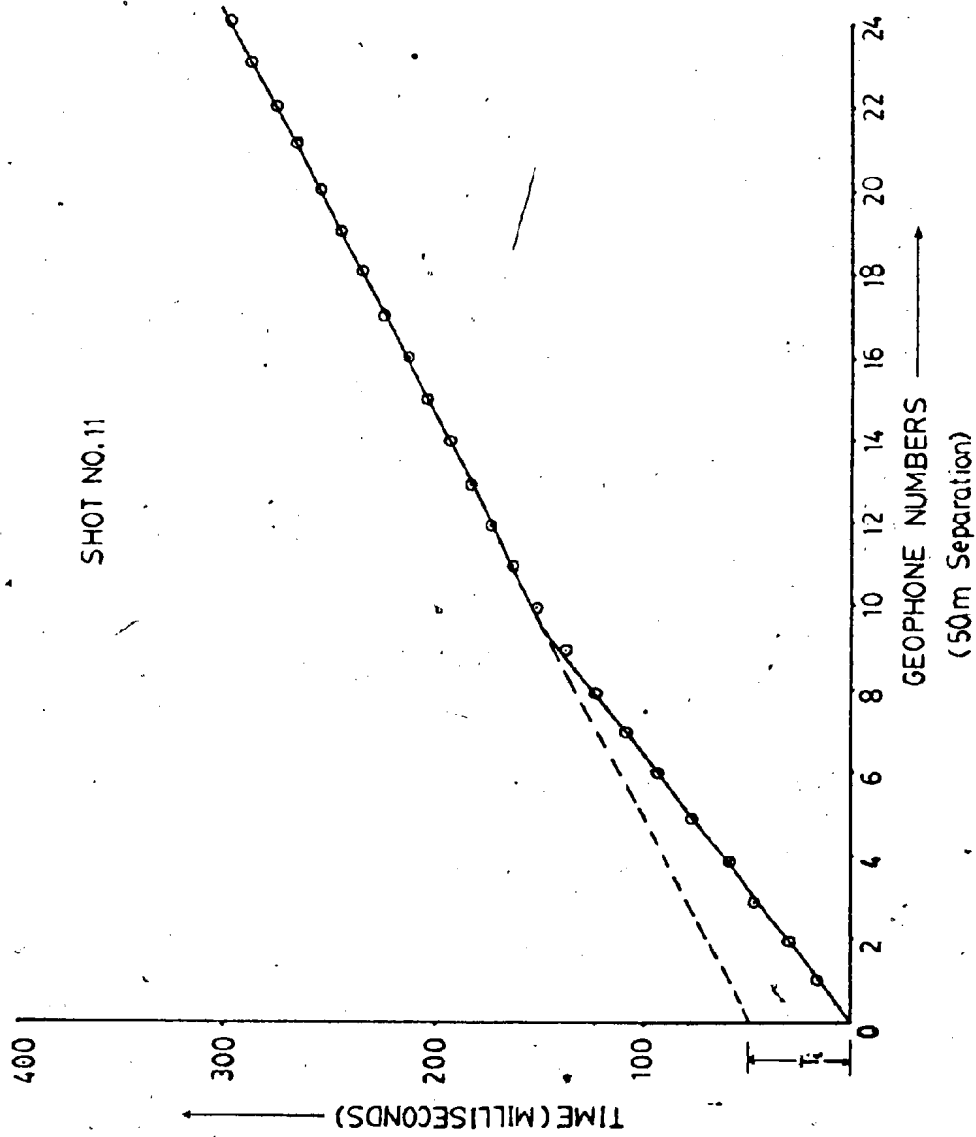


Fig. 2.11 Time-distance curve

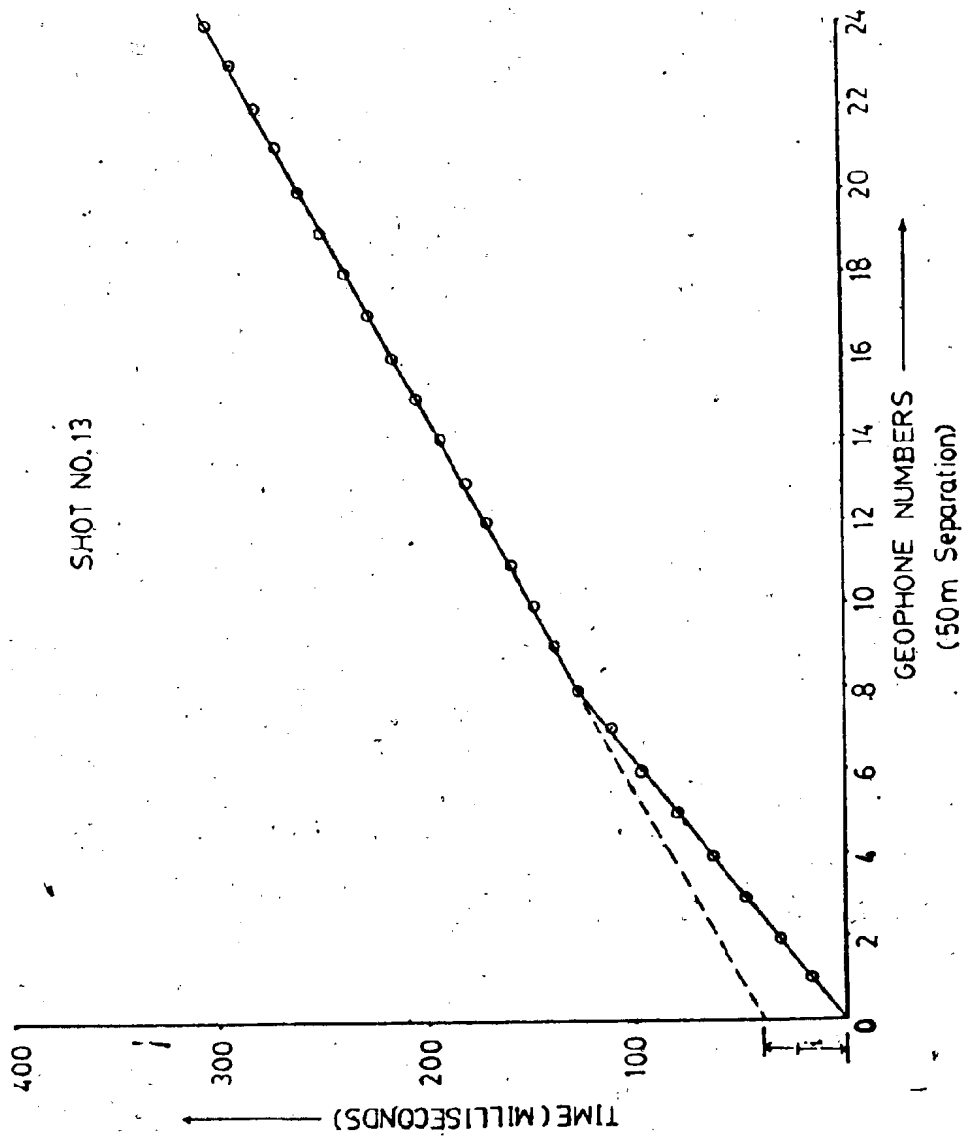


Fig. 2.12 Time-distance curve

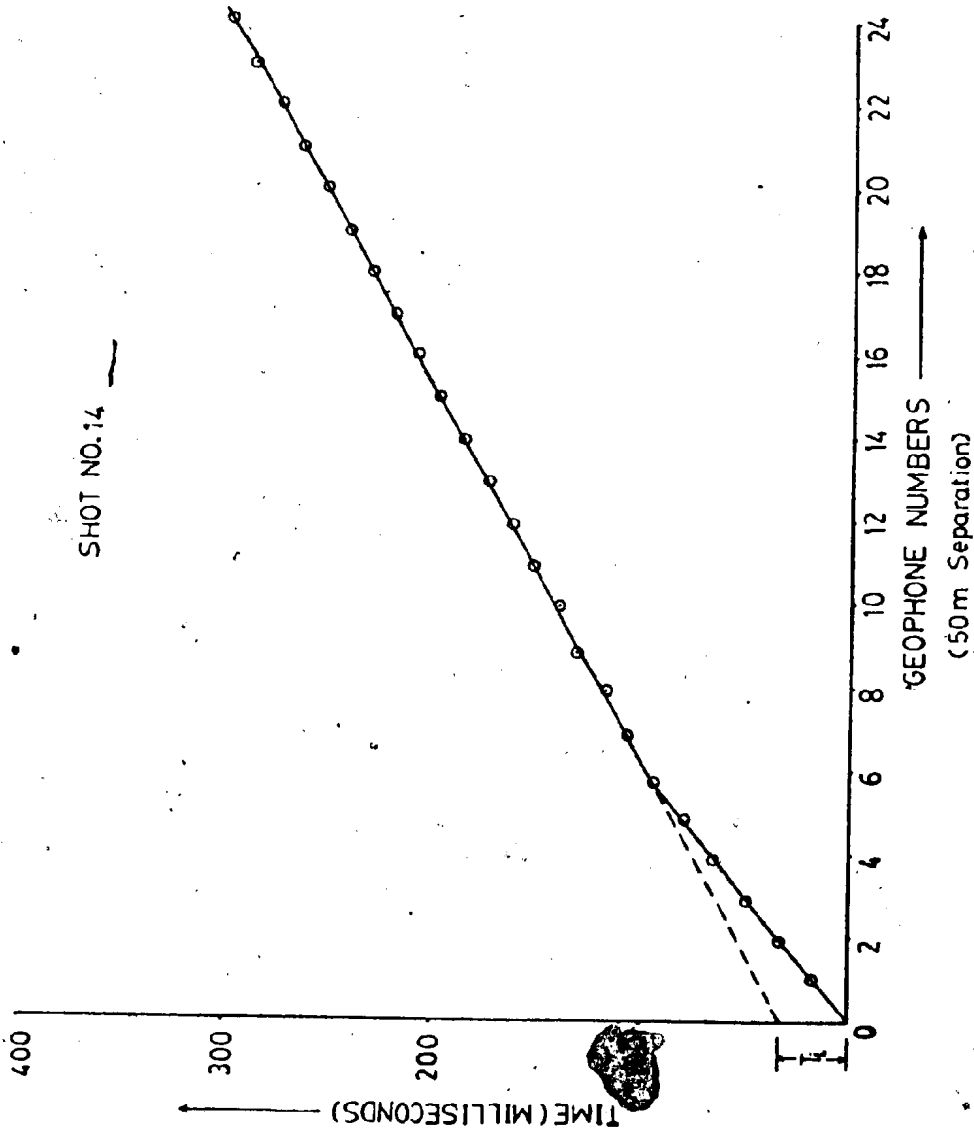


Fig. 2.13 Time-distance curve

TABLE 2.2 Offset distance, intercept time, velocity, depth and crossover distance of different shots in Squires Park line.

SHOT POINT NO.	OFFSET DISTANCE IN METERS		INTERCEPT TIME(S) IN SEC		VELOCITIES IN M/SEC			THICKNESS IN METERS		CROSSOVER DISTANCE IN METERS	
	x _{off 1}	x _{off 2}	T _{i1}	T _{i2}	V ₀	V ₁	V ₂	z ₀	z ₁	computation	graph
1	148	-	.052	-	3388	4546	-	132	-	695	700
-											
3	151	-	.041	-	3304	4167	-	116	-	654	625
4	101	266	.028	.060	3100	3846	4464	74	97	450	465
5	97	-	.044	-	2961	4118	-	94	-	464	450
6	96	-	.046	-	3012	4231	-	95	-	481	500
7	94	171	.028	.094	3036	3894	6372	75	124	428	435
8	127	258	.022	.086	3209	3611	5263	65	139	545	475
9	86	-	.051	-	3014	4643	-	101	-	438	425
10	116	-	.048	-	3268	4552	-	113	-	556	550
11	86	-	.048	-	3146	4762	-	101	-	445	475
-											
13	79	-	.038	-	3125	4508	-	82	-	387	400
14	57	-	.030	-	2959	4327	-	61	-	280	290

$$z = \frac{T_i}{2} \frac{v_1 v_0}{(v_1^2 - v_0^2)^{1/2}} \quad (2.2)$$

(Two layer case)

$$z_1 = \frac{1}{2} (T_{i2} - 2z_0 \frac{(v_2^2 - v_0^2)^{1/2}}{v_2 v_0}) \frac{v_1 v_2}{(v_2^2 - v_1^2)^{1/2}} \quad (2.3)$$

(Three layer case)

where T_i and T_{i2} are the intercept times obtained from the time-distance curves for the two-layer and three-layer cases.

It was necessary to compute the offset distance for each shot to locate the exact horizontal position from which the refraction starts. These distances were computed (Appendix-3) by using the relation

$$x_{\text{off}} = z_0 \tan i_c \quad (2.4)$$

where z_0 is the depth of the interface and $i_c = \sin^{-1}(v_0/v_1)$, the critical angle of refraction and their values were tabulated (Table-2.2).

The velocity contrast at the boundary of the layers was plotted against the shot numbers taking care of depth and offset distance (Fig.2.14). From this plot it was clearly observed that two distinct layers were present at about 3000m/s and 4000m/s velocity contrasts. At these velocities, two contours were drawn and were interpreted in the next section.

2.3.3 Refraction Interpretation

The results of the refraction data of Squires Park line are shown in Fig.2.14. From the velocity contours of this plot, it was observed that the average depth to the interface between the first and second layers was about 90m and the average depth to the interface between the second and third layers was 170m. It was also observed that there was an anticlinal shaped interface with the first layer interface cresting at shot 6 and two sharp changes of velocity near shot 7 and in between shots 10 and 11. The 4000m/s velocity contour interface roughly followed the first layer except, in between shot 6 and 10 where a distinct change was observed.

The nature of the velocity contours of the section (Fig.2.14) indicate that two major features are evident. Firstly, there is an anticline cresting at shot 6 and a gentle westward dip of the Deer Lake Group rocks. The formation beneath the anticline is Humber Falls which overlies the Rocky Brook of higher velocity. Secondly, there are faults at shot 7 and in between shots 10 and 11 with a gentle syncline in between the faults. The velocity contours observed in between the two faults were interpreted to mean that the layers of this part were uplifted. The formation beneath this section was Humber Falls overlying the Rocky Brook.

A change in velocity gradient was observed from shot 11 to 14 indicating the presence of a compact, high density

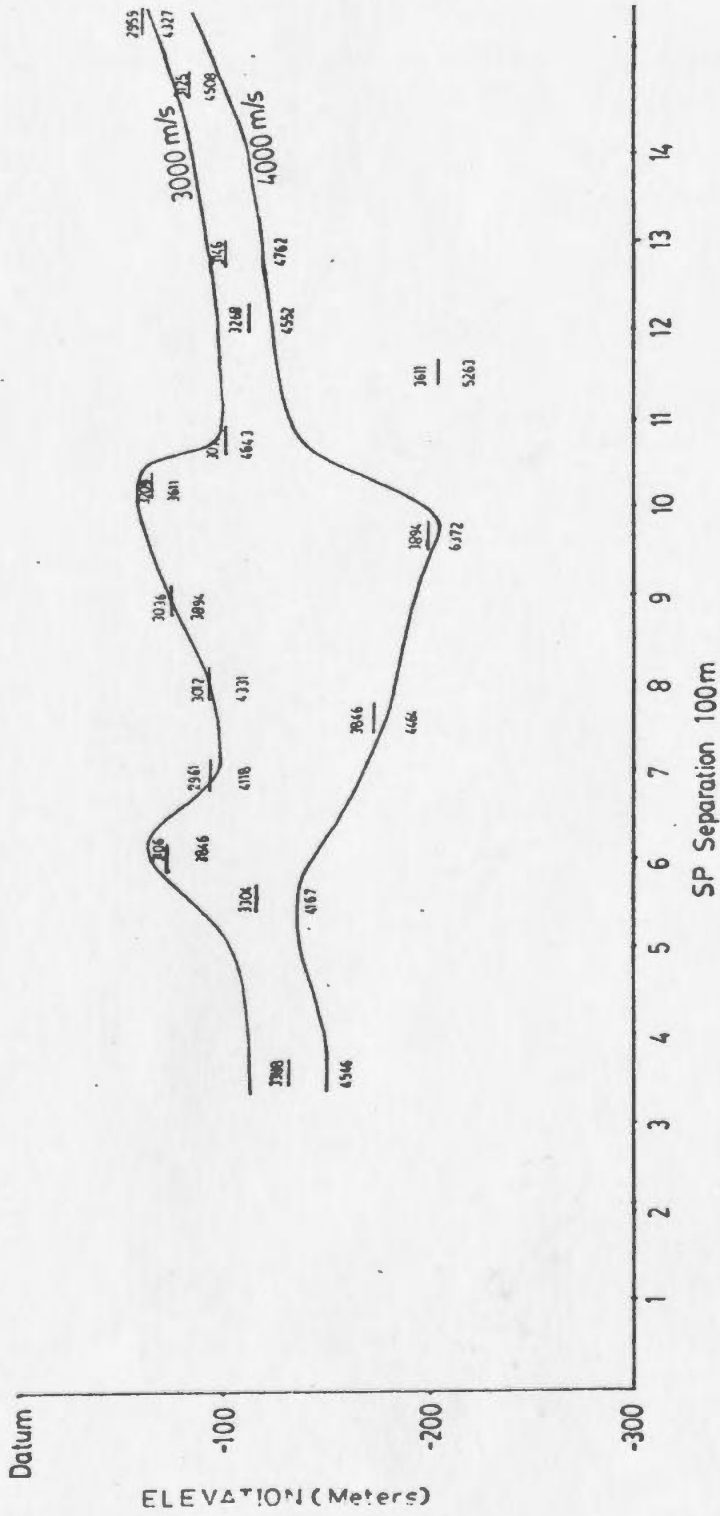


Fig. 2.14 Refraction interpretation

formation. The velocity beneath that part was higher than the velocity of the other part. It was interpreted that the formation beneath this section was North Brook with a gentle dip towards the fault line which agrees with the local geology (Hyde, 1981).

3 REFLECTION

3.1 Objective

The main objective of the seismic reflection study was to interpret the stacked section for the determination of depth and attitude of reflectors and to delineate the configuration and internal structure of the part of the Humber Syncline basin over which the Squires Park line traverses. Computer programmes were developed for the data processing sequence (Section 3.3) and implemented to obtain the final stacked section. In order to obtain the stacked section, the reflection data were processed to enhance the signal to noise ratio. In order to achieve the goal of the reflection study, high resolution (1 msec sample) data were collected which could precisely determine the configuration and geometry of the reflectors.

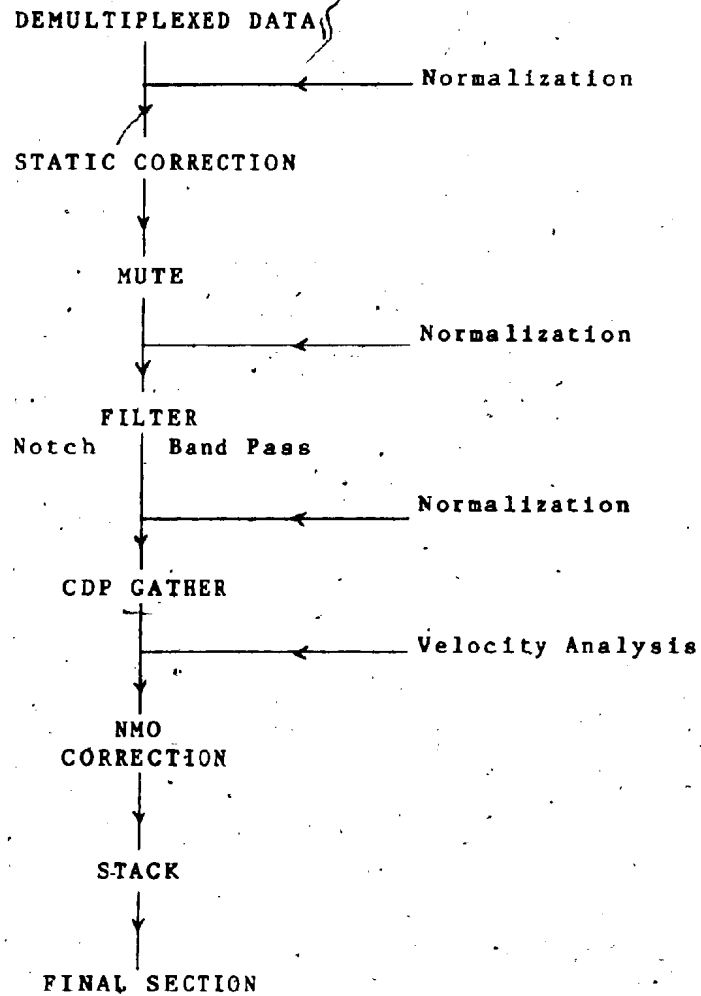
3.2 Reflection Data Collection

On the Squires Park line, the reflection and refraction data were collected together. The reflection data were recorded in Common-depth-point (CDP) gather with the coverage of 600% or 6-fold (Mayne, 1962). The reflector was assumed to be horizontal and the subsurface coverage was half of the surface coverage. First, shot 1 was detonated and the seismic signal was recorded by the geophone groups 1 to 24. The subsurface coverage extended below geophone 1 to 12. Secondly, shot 2 was detonated and the geophone groups 3 to

26 recorded the seismic signal with the subsurface coverage below geophone 3 to 14. The change of the geophone group was done by moving the seismic cable. Thirdly, shot 3 was detonated and the seismic signal was recorded by the geophone groups 5 to 28 with the subsurface coverage below geophone 5 to 16 and, so on. The data were recorded with high time resolution, that is, sampled every 1 msec using a DAS recording system.

3.3 Data Processing

The objective of the seismic reflection data processing was to improve the quality of the data and to present the data in a form that was convenient for geologic interpretation. The data recorded in the field were in a multiplexed format. At first, the data were demultiplexed in order to change the trace order and after demultiplexing the traces were in record order, that is, the traces of each record were together. The demultiplexing was done by Sefel(Calgary). The demultiplexed data were normalized. The normalization was done by dividing each sample of the data by the largest absolute value of the sample for each trace. The normalized data were plotted (Fig. 3.1). Since there were two misfires having shot number 2 and 12, the traces of these shots were not further processed. These traces were eliminated by zeroing out before NMO correction. All the other demultiplexed data were processed following the sequence of processing as given below.

SEQUENCE OF PROCESSING

The programmes for this processing sequence were developed and are presented in Section 7.

3.3.1 Static Correction

The first step of our processing was to apply a static correction to the normalized demultiplexed data. This correction was done only for the difference in surface elevation since there was no weathered layer (Low velocity Layer) in the Squires Park area.

The basic technique for static correction was to correct the data to datum elevation (datum plane) by removing the calculated travel times from the source to the datum and from the geophone to the datum. The detailed technique of static correction has been discussed in Section 2.3.2. This correction was done for all the 24 traces with each of 14 shots, that is, for all the 336 traces. The static corrected traces are shown in Fig. 3.2.

3.3.2 Mute

It was observed in the plots of the data (Fig. 3.2) that there were other events besides the primary reflections on the record. The amplitude of these events was higher than that of the primary reflections. It was necessary to remove these events from the record as our interest was to consider the primary reflections only.

The most prominent other events were the refracted waves whose amplitude was larger than that of our primary reflections. The refracted waves were eliminated from the records by muting the traces, that is, by zeroing out those portions of each trace that contained refracted waves. The

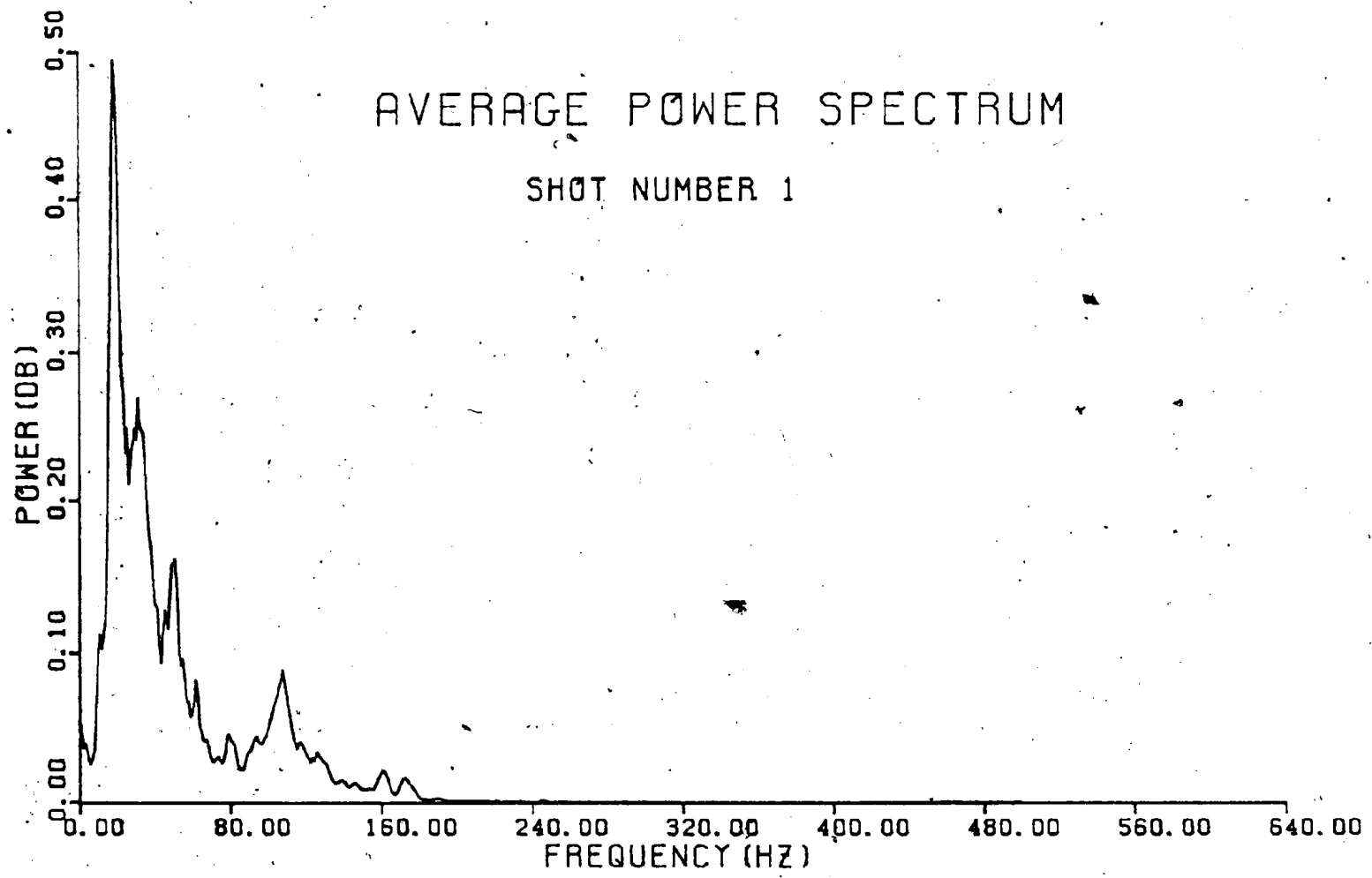
data also contained "air waves". This was the energy that had traveled from the source to the receivers through the air at the velocity of sound in the air (about 330m/s). The air waves were also muted out from the record. Then the muted data were renormalized and the traces were plotted (Fig.3.3). As can be seen from these traces the reflection events are now prominent. Note for example the events numbered A & B.

3.3.3 Filter

The purpose of the filtering in seismic reflection work is to remove noise, in other words, signal with undesirable frequencies from the record, leaving the primary reflections having geological meaning. Before the filters were chosen, an average power spectrum for each shot was calculated and plotted. A sample plot for shot 1 is shown in figure 3.4. From this figure it is clear that there was an interference effect with the power line frequency at 60Hz. To eliminate this effect, the 60Hz band rejection filter (or notch filter) was used. To exclude the noise which was mainly due to surface waves (ground roll), a band pass Butterworth filter was used with a cut of low frequency 20Hz and high frequency 120Hz.

Notch Filter

The notch filter (Truxal, 1955) was designed to reject 60Hz interference in data. To design this filter, a Z-diagram (Kanasewich, p.249) was considered on which 60Hz frequency



43

FIG. 3.4 PLOT OF POWER SPECTRUM BEFORE FILTER

was plotted around the unit circle (Appendix-4). The frequency corresponding to an angle of $\pm\Omega$ on the unit circle was

$$\Omega = \pm \frac{60}{f_N} \cdot 180 = \pm 21.6^\circ \quad (3.1)$$

where $f_N = 1/2\Delta T = 500\text{Hz}$ is the Nyquist frequency, since the sampling interval $\Delta T = 1\text{msec}$. This frequency plays an important role in designing filter because the power spectrum above this frequency is folded back which is known as aliasing (Kanasewich, p.110-114).

Two poles just outside the unit circle were considered so that the signal spectrum was not affected away from 60Hz.

The Z-transform of the impulse response function was given by (Appendix-4)

$$W = \frac{Y(z)}{X(z)} = \frac{0.9899(z^2 - 1.8596z + 1)}{1 - 1.8406z + 0.9800z^2} \quad (3.2)$$

where $Y(z)$ is the output and $X(z)$ is the input series.

The recursive relation for the output becomes

$$Y_n = 0.9899 X_n + 1.8408 X_{n-1} + 0.9899 X_{n-2} \\ + 1.8406 Y_{n-1} - 0.9800 Y_{n-2} \quad (3.3)$$

Using the above recursive relation(3.3), the filtered

output was obtained but with a phase shift. To get rid of this problem, that is, to get a zero phase shift rejection filter, the output from this process was reversed and passed through the same filter again. Then the output vector was reversed to obtain the desired zero phase shift data.

Band-pass Butterworth filter

The purpose of choosing the band-pass filter was to eliminate the surface waves from the data. The low cut frequency was chosen as 20Hz for the elimination of surface waves and the high cut frequency was chosen 120Hz, considering the significant contribution in the average power spectrum up to that frequency.

There are number of techniques available for designing band-pass recursion filters (Kaiser, 1963; Whittlesey, 1964; Robertson, 1965; Holtz and Leondes, 1966). The most suitable technique for designing a class of filters known as Butterworth band-pass was chosen (Guillemin, 1957, p.588-591). This filter has 8 poles in the S-plane and was applied in forward and reverse directions to have a zero phase filter.

A bilinear Z-transform was used in designing the filter to prevent aliasing problems (Golden and Kaiser, 1964). The Z-transform of the impulse response has the form (Appendix-5)

$$F(z) = (1-z^2)^4 / (B_1(z)B_2(z)B_3(z)B_4(z)) \quad (3.4)$$

$$\text{where } B_j = 1 - D_{2j-1}z + D_{2j}z^2$$

$$j = 1, 2, 3, 4$$

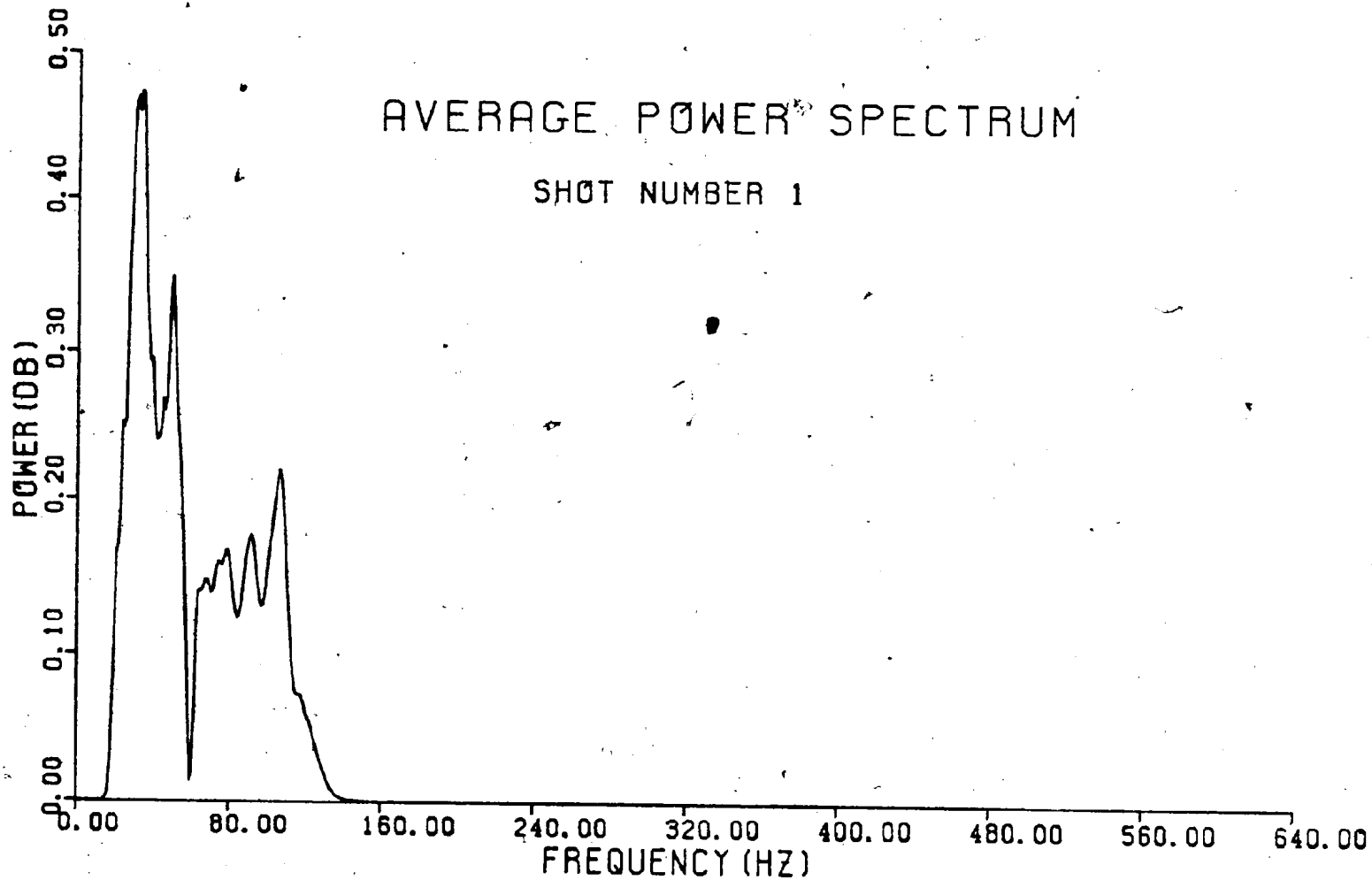
and the coefficients D_{2j-1} and D_{2j} were determined by the low and high pass cut-off frequencies. The impulse response of the filter (equation(3.4)) was equivalent to the cascaded product of four filters

$$F(z) = F_1(z)F_2(z)F_3(z)F_4(z) \quad (3.5)$$

where terms like F_1 have the form

$$F_1(z) = (1-z^2) / (1-D_1z + D_2z^2) \quad (3.6)$$

Since the filter was cascaded four times in succession to produce the Z-transform output, recursive equations for programming were developed and used (Appendix-5). A Fortran subroutine for the zero phase shift Butterworth filter which was given by Ganly (Kanasewich, p.274-277) was used in the programming for filtering the data and the output is normalized and plotted (Fig.3.5). The average power spectrum of filtered data was calculated and one of them is shown(Fig.3.6). From Fig.3.6, it was evident that both of our chosen filters worked properly since the 60Hz peak and the frequencies below 20Hz and above 120Hz are attenuated on



47

FIG. 3.6 PLOT OF POWER SPECTRUM AFTER FILTER

this spectrum compared with the amplitude on the previous spectrum(Fig.3.4).

3.3.4 CDP Gather

The purpose of the "CDP Gather" was to rearrange the traces from shot point order to depth point order. The traces of the Squires Park line were sorted or gathered into depth point order before stacking. All the traces of the first depth point were followed by all the traces of the second depth point and so on.

Since the shots were at an interval of two geophones and a 24-geophone group was used, a maximum coverage of 6-fold was possible. The number of fold coverage increases the signal to noise ratio by n , where n is the number of fold coverage. In order to achieve subsurface coverage up to below the shot 4, east of which there is an anticline structure(Section 2.3.3), 4-fold and 5-fold coverage were also considered; and a total number of 44 reflection points throughout the line of survey was obtained. Finally, CDP gather was obtained with the help of stacking chart (Fig.3.7) (Mayne, 1962) and individual traces were plotted(Fig.3.8).

STACKING CHART

SHOT POINT NOS.	DEPTH POINT NOS.																																																																																			
	1	2	3	4	5	6	7	8	9	10	11	12	13	14	15	16	17	18	19	20	21	22	23	24	25	26	27	28	29	30	31	32	33	34	35	36	37	38	39	40	41	42	43	44																																								
1	13	14	15	16	17	18	19	20	21	22	23	24																																																																								
2	9	10	11	12	13	14	15	16	17	18	19	20	21	22	23	24																																																																				
3	5	6	7	8	9	10	11	12	13	14	15	16	17	18	19	20	21	22	23	24																																																																
4	1	2	3	4	5	6	7	8	9	10	11	12	13	14	15	16	17	18	19	20	21	22	23	24																																																												
5					1	2	3	4	5	6	7	8	9	10	11	12	13	14	15	16	17	18	19	20	21	22	23	24																																																								
6									1	2	3	4	5	6	7	8	9	10	11	12	13	14	15	16	17	18	19	20	21	22	23	24																																																				
7													1	2	3	4	5	6	7	8	9	10	11	12	13	14	15	16	17	18	19	20	21	22	23	24																																																
8																	1	2	3	4	5	6	7	8	9	10	11	12	13	14	15	16	17	18	19	20	21	22	23	24																																												
9																					1	2	3	4	5	6	7	8	9	10	11	12	13	14	15	16	17	18	19	20	21	22	23	24																																								
10																									1	2	3	4	5	6	7	8	9	10	11	12	13	14	15	16	17	18	19	20																																								
11																													1	2	3	4	5	6	7	8	9	10	11	12	13	14	15	16																																								
12																																	1	2	3	4	5	6	7	8	9	10	11	12																																								
13																																					1	2	3	4	5	6	7	8																																								
14																																									1	2	3	4																																								

Fig. 3.7 Stacking chart.

3.3.5 Velocity Analysis

The main objective of the velocity analysis was to determine the velocity function which will yield the best normal moveout correction and the auxiliary objective of the velocity analysis was to identify lithology.

It was observed that the reflection seismic record for each shot looks like a hyperbola (Fig. 3.8) (Telford et al., 1976 p. 261)

$$T^2 = T_0^2 + x^2/v_{rms}^2 \quad (3.7)$$

where $T_0 = 2D/v_{rms}$ is the vertical two-way travel time and D and v_{rms} are the depth and rms velocity to the reflector respectively.

The relation (3.7) gives a straight line if T is plotted against X and the velocity can be determined from the slope ($1/v_{rms}$).

The normal moveout (NMO) is the difference between the reflection time at an offset X and the reflection time zero offset and is given by

$$\Delta T = T - T_0 \quad (3.8)$$

Substituting the value of T from equation (3.7) in equation (3.7) and simplifying (Appendix-6)

$$\Delta T \approx x^2/2v_{rms}^2 T_0 \quad (3.9)$$

It is evident from the above relation that for a particular offset, the normal moveout time depends on velocity (V_{NMO}). Our aim was to determine this velocity, known as stacking velocity, by measuring the NMO.

To determine the stacking velocity of the first reflector, the least squares method (Kossack et al., p.399-401) was applied. For each CDP reflection, the arrival times for different offset X was known from the CDP gather section (Fig.3.8). Using the different values of offset X and the corresponding values of arrival time T in equation(3.9), the vertical two-way travel time T and the velocity V were determined for the first reflector. It was found that the velocity was almost constant for each CDP and its value was equal to 3000 ± 200 m/s. This velocity agrees with the velocity of the upper layer Humber Syncline which was obtained from Shell seismic refraction results.

To estimate the stacking velocity for the second reflector, the vertical two-way travel time T was taken to be 112ms which was estimated from refraction(Fig.2.14). This value of T was used in equation(3.9) for different offset. The different values of V ranging from 3700m/s to 4300m/s with an interval of 100m/s were considered and the moveout time was calculated. This moveout time was applied to the traces to get the best alignment of the traces. The same procedure was repeated for all the common depth points. Different velocities were found (Table-3.1) to be best for the different CDP. These different velocities are caused by

local changes in the lithology and geometry of the reflector.

CDP Nos.	Stacking Velocity(m/s)	CDP Nos.	Stacking Velocity(m/s)
1	4000	23	3700
2	3900	24	3800
3	4100	25	3700
4	4000	26	3900
5	4000	27	3800
6	3700	28	3700
7	3700	29	3800
8	3900	30	4300
9	4300	31	4300
10	3800	32	4300
11	3700	33	3800
12	4000	34	4200
13	4000	35	4000
14	4200	36	3800
15	3700	37	4000
16	3900	38	4200
17	4000	39	4100
18	4000	40	4300
19	3700	41	4100
20	3800	42	4000
21	4000	43	4300
22	3700	44	4100

Table-3.1 Stacking velocity for the second reflector at different CDP.

3.3.6 Normal Moveout Correction

The normal moveout correction was done before stacking the traces. It was noticed that the reflection event on the seismic record is curved. This occurs because the ray-path from the source to the geophone with some offset is longer than that with no offset. The difference in the arrival time for a reflection on a zero-offset trace and an offset trace is called normal moveout(NMO).

The NMO correction was computed by using the stacking velocity (discussed in section 3.3.5) in equation(3.9) for each trace. This correction was done by shifting the reflection up by that amount and the traces were found to be aligned for each reflection point. The data after NMO correction is shown in Fig.3.9.

3.3.7 Stack

After the necessary corrections of the traces, all that remained was to stack the data, that is, to sum all the traces for each common depth point, resulting in a single stacked trace being output for each depth point. Each individual trace in the stacked line is actually the sum of all the traces at a depth point. Because of the different fold coverage, not all depth points contain the same number of traces. To compensate for this and to insure that all stacked traces have the same overall level, each stacked trace is scaled according to the number of traces in the depth point. For the first four depth points, each gathered trace consisting of 4 traces was multiplied by $1/4$ when stacked. For the next four depth points, each stacked trace consisting of 5 traces was multiplied by $1/5$ when stacked. The remaining 36 depth points, that is depth point number 9 to 44, each point consisting of 6 traces was multiplied by $1/6$ when stacked. After stacking, the final section was plotted (Fig.3.10) and this section was interpreted in the next chapter.

4 INTERPRETATION

The second purpose of this thesis was to interpret the seismic data, that is the transformation of the seismic information into geological terms for the Squires Park line which traverses part of the Humber Syncline of the Deer Lake Basin. The interpretation of both seismic reflection and refraction data is discussed in this chapter. The interpretation of the seismic data is correlated with the interpretation of geology (Hyde, 1979; 1983) and with the interpretation of the gravity and magnetics data (Miller and Wright, 1984).

4.1 Reflection

A two-dimensional geological interpretation of the reflection seismic data of the Squires Park line was done from the final (stacked) section (Fig. 3.10). The reflection events having the highest-amplitude troughs (or peaks) are easily identified in this section. The troughs of the reflection events of the different traces were found to follow each other except at two places, where an abrupt change was observed. The trough to trough of the reflection events were joined and it was clear that there were two shallow reflectors along the seismic line. The average depths of the reflectors were estimated to be about 75m and 175m assuming velocity of the first and second reflectors 3000m/s and 4000m/s respectively (Section 2.3.3) based on the refraction velocities and stacking velocity for the

layers. Two major structures are evident from the stacked section (Fig.3.10). Firstly, an anticlinal structure cresting at shot 6 was observed. Secondly, two faults at about shot 7 and 11 are evident where there is an abrupt discontinuity in the reflection events. The beds, east of shot 7 and west of shot 11 are uplifted. There were vertical throws of about 70m and 120m in both the faults of the first and second reflectors which show that the faults appear to be growing rapidly with depth. There was no diffraction pattern in the stacked section (Fig.3.10), since the faults are at shallow depth. It was observed that the uplifted bed has a gentle synclinal structure and the reflectors below shot 11 to 14 have a gentle updip indicating higher velocity at lower depth towards the end of the profile.

To interpret the stacked section (Fig.3.10) geologically, a synthetic stacked section was generated assuming a simple geologic model. This model was based on the local geology and the refraction information. The synthetic stacked section was generated assuming a two-reflector model at an average depth of 75m and 175m with the presence of the two major structures discussed earlier.

To generate synthetic stacked section means to generate synthetic seismograms (Peterson et al. 1955) which are artificial reflection records made by convolution of the reflectivity function with a source pulse. The two-way zero offset times from the source to the reflectors were calculated for each shot by assuming the velocity 3000m/s

and 4000m/s for the first and second reflector and a locally horizontal reflecting surface. The travel time was digitized with 1ms interval which is same as the sampling interval of our field data. Since the reflectors are at shallow depth and the change of velocity from the first to the second layer is large, the travel time of the second reflector is lower than twice the travel time of the first reflector and hence, multiples were not included in generating the synthetic stacked section. The reflectivity was calculated (Appendix-7) at the two layer boundaries at 75m and 175m depth assuming velocities 3000m/s, 4000m/s and 5000m/s with the corresponding densities 2.5 gm/c.c, 2.54 gm/c.c and 2.7 gm/c.c respectively. A 50-Hz Ricker wavelet instead of minimum phase wavelet was chosen as the source pulse because good Ricker wavelet was observed in the plot of the data after filtering(Fig.3.5). The chosen 50-Hz frequency is within the usual seismic range and is consistent with the frequency band used in reflection data processing(Section 3.3.3).

The synthetic stacked section is plotted(Fig.4.1) and compared with the original stacked section(Fig.3.10). The nature of the two plots was almost identical. From these it was evident that there are two reflectors with an average depth of about 75m and 175m with the presence of two major structures. Firstly, an anticline cresting at shot 6 with the slanting surface of about 25 and secondly, two vertical faults near shot 7 and 11 with an uplift of bed in between

the faults having fault throws about 70m and 120m of the first and second reflector, respectively.

4.2 Refraction

The seismic refraction data were interpreted from the velocity contours (Fig. 2.14). The refraction interpretation has been discussed in detail in section 2.3.3. It was interpreted from the velocity contours that there are two interface of the layers at average depths 90m and 170m and that of the other two major structures, discussed in the reflection interpretation, are present. A discrepancy of 15m is observed in the first layer depth (Section 4.1), because the velocity contrast was drawn at discrete shot point locations which gives certain error in interpolating the velocity contour for depth calculation. Moreover, depth calculation by refraction time-distance curve gives an approximate idea about the depth of different layers since here we used the assumption of horizontal layering but the data indicate dipping layers. The two major structures which are present: an anticline cresting at shot 6 and faults at shot 7 and in between shots 10 and 11 with a gentle syncline in between the faults. The formation beneath the anticline is Humber Falls which overlies the higher velocity Rocky Brook. These formations are identified on the basis of their velocities 3000m/s and 4000m/s respectively (section 2.2.3). The layers in between the faults are uplifted and the formation beneath this area is also Humber Falls overlying

the Rocky Brook on the basis of their velocities. There was an updip gradual change in velocity from shot 11 to shot 14. The formation beneath this part is North Brook, which has higher density and velocity than the other two formations (Section 2.3.3), with a gentle dip towards the fault line agreeing with the local geology as explained by Hyde (1983).

4.3 Correlation with Geology, Gravity and Magnetics

The seismic data for both reflection and refraction were correlated with the local geology (Hyde, 1979; 1983) and with the gravity and magnetics data (Miller and Wright, 1983). According to Hyde, the part of the Humber Syncline Basin which our seismic line traverses is composed of three rock groups, namely, North Brook, Rocky Brook and Humber Falls formations. From reflection as well as refraction interpretation it was evident that there is a fault in the vicinity of our shot 11 and east of the fault, from shot 11 to 14 there is updip slope of the North Brook formation whose density is higher than that of the other formations. This interpretation correlates with the geology of that area (Hyde, 1983).

Hyde's (1983) geology also suggests that there are synclinal and anticlinal structures in the major Humber Syncline with the Humber Falls formation overlying the higher density Rocky Brook formation. An anticline cresting at shot 6 was observed on the seismic data from the

interpretation of both reflection and refraction data and there are two layers with velocity 3000m/s and 4000m/s beneath this structure which agrees with the velocity of the corresponding layer of the Humber Falls and Rocky Brook formations (Section 2.2.3) and also agrees with the local geology (Hyde, 1983).

It is interpreted from both reflection and refraction data that there is another fault near shot 7 and the bed in between the two faults at shot 7 and 11 is uplifted. From refraction interpretation, it was clear that there is a gentle synclinal structure in the uplifted bed agreeing with the Miller and Wright's (1984) residual anomaly map which shows slightly negative gravity features in the Humber Syncline coinciding with the Humber Falls overlying the higher density Rocky Brook formation in that area.

It is clear from the present seismic interpretation that all the seismic data of the Squires Park line are in agreement with the interpretation of the local geology (Hyde, 1983) and with the gravity and magnetics data (Miller and Wright, 1984).

5 SUMMARY AND CONCLUSIONS

5.1 Summary and Conclusions

A seismic study of the Deer Lake Basin of Newfoundland was undertaken. High resolution data (1msec) were acquired along the Squires Park line in the Humber Syncline by using 6-fold CDP technique.

A preliminary refraction study was done from Shell seismic data and the representative velocity of the different formations of the Humber Syncline was used in data processing and interpretation.

Prior to reflection interpretation, refraction data were processed and interpreted in order to estimate the geologic structure in the Squires Park line area.

In the reflection study, programmes were developed and implemented to use the conventional data processing sequence in order to get the final stacked section for interpretation. An ideal synthetic seismogram was constructed based on the available geological and geophysical information. A comparison was made between the synthetic and the original stacked sections and a good correlation was observed. On the basis of the refraction as well as the reflection interpretation, the following conclusions were drawn:

1. There are two reflectors at average depths of about 75m and 175m.
2. There is an anticline cresting at shot 6.

3. The formation beneath the anticline is Humber Falls overlying the higher velocity Rocky Brook.

4. Two vertical faults are present at shot 7 and 11 with an uplift of beds in between the faults having fault throws about 70m and 120m of the first and second reflector, respectively.

5. A gentle synclinal structure is present in the uplifted bed and the formation beneath this structure is Humber Falls overlying the Rocky Brook.

6. There are gentle updip reflectors below shot 11 to 14 with the presence of compact and high density North Brook formation beneath this area.

The above conclusions are in agreement with the local geology and with the interpretation of the available gravity and magnetic data.

5.2 Limitations and Suggestions for Further Work

These are the following limitations of the present work:

1. A two-dimensional seismic interpretation is done since the data were available in a single line.

2. The quality of data in some traces was not good, so the noise could not be reduced to the optimum level.

3. Migration technique was not applied to the data and, therefore, accurate position and shape of the anticline and faults was not possible to determine.

It is suggested that quality seismic data should be acquired in different lines for three-dimensional seismic

interpretation of the entire Humber Syncline. It is also suggested that the migration technique should be applied before interpretation for the accurate determination of the structure.

6 APPENDIXES

1 Appendix-1

Shot elevation from survey data.

Shot Numbers	Shot Elevation E (meters)	Shot Numbers	Shot Elevation E (meters)
1	-0.94	8	-10.26
2	-2.46	9	-12.42
3	-5.11	10	-13.19
4	-5.62	11	-16.39
5	-7.30	12	-17.26
6	-8.05	13	-19.57
7	-10.38	14	-21.15

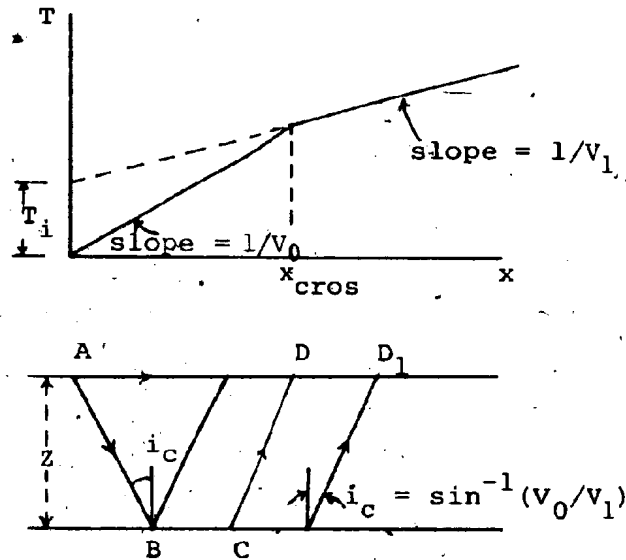
Geophone elevation from survey data.

Geophone Locations	Geophone Elev. E(m)	Geophone Locations	Geophone Elev. E(m)
1	-1.32	26	-20.76
2	-2.60	27	-21.41
3	-3.12	28	-21.91
4	-4.45	29	-22.52
5	-5.24	30	-23.23
6	-5.49	31	-24.08
7	-6.04	32	-25.09
8	-6.88	33	-25.65
9	-7.49	34	-25.77
10	-7.86	35	-26.90
11	-8.63	36	-26.61
12	-9.80	37	-26.93
13	-10.35	38	-27.04
14	-10.29	39	-27.51
15	-10.80	40	-28.32
16	-11.88	41	-28.54
17	-12.61	42	-28.17
18	-12.99	43	-27.63
19	-13.99	44	-26.94
20	-15.59	45	-26.47
21	-16.61	46	-26.23
22	-17.04	47	-26.06
23	-17.84	48	-25.97
24	-18.99	49	-26.82
25	-19.97	50	-28.61

Appendix-2

Two-Media Case (After Dobrin, 1976)

Consider two-media with respective velocities of V_0 and V_1 , separated by a horizontal discontinuity at depth z .



The direct wave travels from shot to detector near the earth's surface at a velocity of V_0 , so that $T = x/V_0$. This is represented on the plot of T versus x as a straight line which passes through the origin and has a slope of $1/V_0$. The wave refracted along the interface at depth z , follows the path $ABCD$ making a critical angle i_c with the horizontal.

The total time along the refraction path $ABCD$ is

$$T = T_{AB} + T_{BC} + T_{CD}$$

which can be written as

$$T = z/v_0 \cos i_c + (x - 2z \tan i_c)/v_1 + z/v_0 \cos i_c$$

$$\text{where } \sin i_c = v_0/v_1, \quad \cos i_c = (1 - v_0^2/v_1^2)^{1/2}$$

$$\text{and } \tan i_c = v_0/(v_1^2 - v_0^2)^{1/2}$$

After simplification, the time-distance relation finally becomes

$$T = x/v_1 + 2z(v_1^2 - v_0^2)^{1/2}/v_1 v_0$$

On a plot T versus x, this is the equation of a straight line which has a slope of $1/v_1$ and which intercept the T axis ($x=0$) at a time

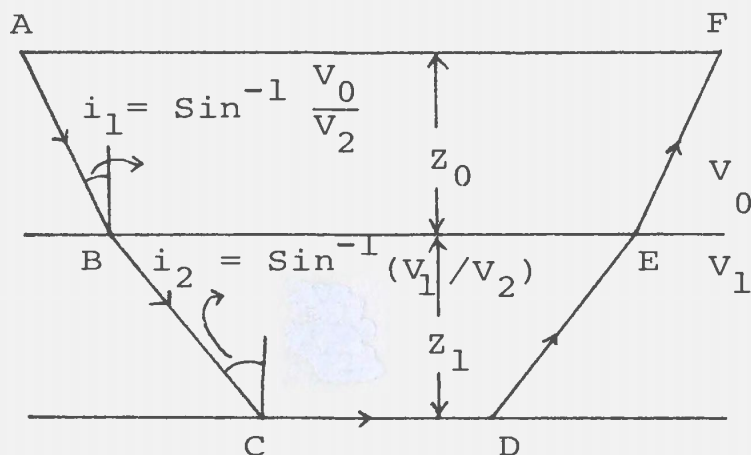
$$T_i = 2z(v_1^2 - v_0^2)^{1/2}/v_1 v_0$$

T_i is known as the intercept time.

From the above relation the depth z becomes

$$z = (T_i/2) v_0 v_1 / (v_1^2 - v_0^2)^{1/2}$$

Three-Media Case (After Dobrin, 1976)



Consider three-media with velocities v_0, v_1 , and v_2 ($v_2 > v_1 > v_0$). Then the ray corresponding to the least travel time takes an angle $i_1 = \sin^{-1}(v_0/v_2)$ with the vertical in the uppermost layer and an angle $i_2 = \sin^{-1}(v_1/v_2)$ with the vertical in the second layer.

The total travel time from A to F is

$$T = T_{AB} + T_{BC} + T_{CD} + T_{DE} + T_{EF}$$

$$\text{Since } T_{AB} = T_{EF} = z_0/v_0 \cos i_1 = (z_0/v_0)/[1 - (v_0/v_2)^2]^{1/2}$$

$$T_{BC} = T_{DE} = z_1/v_1 \cos i_2 = (z_1/v_1)/[1 - (v_1/v_2)^2]^{1/2}$$

The total travel time becomes

$$T = (2z_0/v_0)/[1 - (v_0/v_2)^2]^{1/2} + (2z_1/v_1)/[1 - (v_1/v_2)^2]^{1/2} + CD/v_2$$

where $CD = x - 2z_0 \tan i_1 - 2z_1 \tan i_2$

$$= x - 2z_0 (v_2^2 - v_0^2)^{1/2}/v_2 v_0 + 2z_1 (v_2^2 - v_1^2)^{1/2}/v_2 v_1$$

Rearranging terms, we get

$$T = x/v_2 + 2z_0 (v_2^2 - v_0^2)^{1/2}/v_2 v_0 + 2z_1 (v_2^2 - v_1^2)^{1/2}/v_2 v_1$$

The intercept time (at $x=0$)

$$T_{i2} = 2z_0 (v_2^2 - v_0^2)^{1/2}/v_2 v_0 + 2z_1 (v_2^2 - v_1^2)^{1/2}/v_2 v_1$$

Solving for z_1 , we get

$$z_1 = 1/2 [T_{i2} - 2z_0 (v_2^2 - v_0^2)^{1/2}/v_2 v_0] v_2 v_1 / (v_2^2 - v_1^2)^{1/2}$$

The depth to the lower interface is the sum of z_1 and z_0 , where z_0 is computed by two-media case.

Appendix-3

Crossover Distance

The crossover distance is the distance at which the direct wave and the refracted wave meet each other. At distance less than this, the direct wave traveling along the top of the v_0 layer reaches the detector first. At greater distances, the wave refracted by the interface arrives before the direct wave.

Therefore, the time distance relation of the direct wave, $T_0 = x/v_0$ and the refracted wave,

$$T_1 = x/v_1 + 2z(v_1^2 - v_0^2)^{1/2}/v_1 v_0$$

are equal at x_{cros}

$$\text{Hence, } x_{\text{cros}}/v_0 = x_{\text{cros}}/v_1 + 2z(v_1^2 - v_0^2)^{1/2}/v_1 v_0$$

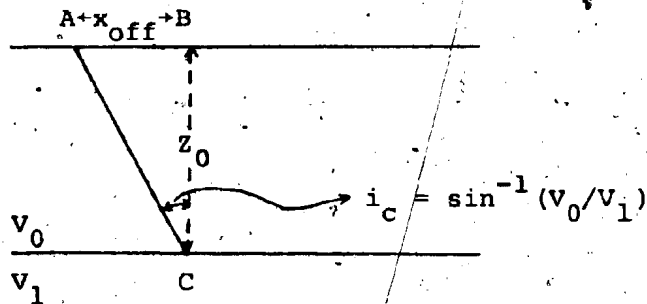
$$\text{and } z = v_0 v_1 x_{\text{cros}} (1/v_0 - 1/v_1) / 2(v_1^2 - v_0^2)^{1/2}$$

Simplifying and solving for x , we obtain

$$x_{\text{cros}} = 2z(v_1 + v_0)^{1/2}/(v_1 - v_0)^{1/2}$$

Offset Distance (After Dobrin, 1976)

Consider two-media with velocities v_0 and v_1 separated by a horizontal discontinuity at depth z_0 .



The offset distance, x_{off} is given by

$$x_{\text{off}} = z_0 \tan i_c$$

where i_c is the critical angle of refraction and $\sin i_c = v_0/v_1$.

The value of

$$\tan i_c = \sin i_c / \cos i_c = v_0 / (v_1^2 - v_0^2)^{1/2}$$

Therefore,

$$x_{\text{off}} = z_0 v_0 / (v_1^2 - v_0^2)^{1/2}$$

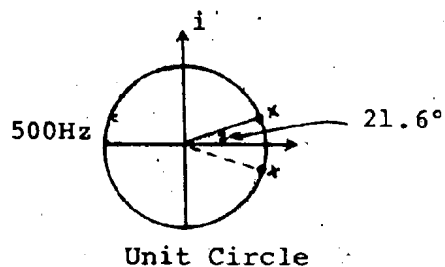
Appendix-4

Notch Filter

A notch filter can be designed directly with the help of a Z-diagram on which frequencies are plotted around the unit circle. The objective was to design a filter for rejecting 60Hz frequency by locating zeroes of the filter at the points on the Z-plane unit circle corresponding to that frequency. To reject 60Hz with data of 1ms intervals, the Z-plane points which correspond to that frequency occur on the unit circle at angles $\pm \Omega$, determined as follows:

$$\Omega = \pm (60/f_N) 180 = \pm 21.6^\circ$$

where $f_N = 500\text{Hz}$ is the Nyquist frequency.



The location of the zeroes in the Z-plane are denoted by α_1 and α_2 .

$$\alpha_1 = \cos 21.6^\circ + j \sin 21.6^\circ$$

$$\alpha_2 = \cos 21.6^\circ - j \sin 21.6^\circ$$

or,

$$\alpha_1 = 0.9288 + j 0.3685$$

$$\alpha_2 = 0.9288 - j 0.3685$$

In order not to disturb the signal spectrum away from 60Hz, two poles just outside the unit circle (say $r=1.01$ and $\Omega = +21.6^\circ$) and close to the two zeroes are located. Then the poles are located at

$$\beta_1 = 1.01 (\cos 21.6^\circ + j \sin 21.6^\circ)$$

$$\beta_2 = 1.01 (\cos 21.6^\circ - j \sin 21.6^\circ)$$

or

$$\beta_1 = 0.9391 + j 0.3722$$

$$\beta_2 = 0.9391 - j 0.3722$$

The Z-transform of the impulse response function with a static gain G , to insure a gain of unity at the Nyquist frequency is

$$W(z) = G[(z-\alpha_1)(z-\alpha_2)]/[z-\beta_1)(z-\beta_2)]$$

Rearranging and separating real and imaginary parts yield

$$W(z) = \frac{G[z^2 - (\alpha_1 + \alpha_2)z + \alpha_1\alpha_2]}{1 - (\beta_1 + \beta_2)z/\beta_1\beta_2 + z^2/\beta_1\beta_2}$$

$$\text{where } G = \frac{[1 + (\beta_1 + \beta_2 + 1)/\beta_1\beta_2]}{2 + (\alpha_1 + \alpha_2)}$$

Substituting the values of α 's and β 's in the above equations, the impulse response becomes

$$W(z) = Y(z)/X(z) = \frac{0.9899(z^2 - 1.8596z + 1)}{1 - 1.8406z + 0.9800z^2}$$

where $Y(z)$ and $X(z)$ are the output and input series.

The recursive relation for the output is

$$Y_n = 0.9899(X_n - 1.8596X_{n-1} + X_{n-2}) - 0.9800Y_{n-2} + 1.8406Y_{n-1}$$

$$\text{i.e. } Y_n = a_0X_n + a_1X_{n-1} + a_2X_{n-2} + b_1Y_{n-1} + b_2Y_{n-2}$$

where $a_0 = 0.9899$, $a_1 = 1.8408$, $a_2 = 0.9899$, $b_1 = 1.8406$ and $b_2 = -0.9800$.

The initial value of the output Y_0 was determined from the initial value of the input data X , that is at $n=0$, $Y_0 = a_0 X_0$ and the all other terms are zero. When $n=1$, $Y_1 = a_0 X_1 + a_1 X_0 + b_1 Y_0$, and the other terms are zeros and, so on.

Appendix-5

Band-pass filter

The recursion filtering (Golden and Kaiser, 1964; Shanks, 1967) involves a feedback loop using the polynomial of the Z-transform of the impulse response of recursive filter is of the type

$$F(z) = \frac{N(z)}{D(z)} = \frac{N_0 + N_1 z + N_2 z^2 + \dots + N_n z^n}{1 + D_1 z + D_2 z^2 + \dots + D_m z^m}$$

where N and D's are the coefficients.

Since $F(z) = Y(z)/X(z)$, where $Y(z)$ and $X(z)$ are the output and input series, the recursive relation of the output is

$$Y_n = \sum_{i=0}^n N_i X_{n-i} - \sum_{j=1}^m D_j Y_{n-j}$$

The band-pass Butterworth filter having lower and upper cutoff frequencies of 20Hz and 120Hz, respectively and having 8 poles in the Z-plane was chosen. The filter was applied in forward and reverse directions so as to have zero phase.

This filter has four S-plane zeroes at $S=0$, and eight S-plane poles at

$$S = -36.60 \pm j 123.97$$

$$S = -134.44 \pm j 98.90$$

$$S = -218.28 \pm j 739.30$$

$$S = -480.89 \pm j 353.80$$

and the transfer function is of the form

$$F(s) = \frac{s^4}{g_8 s^8 + g_7 s^7 + \dots + g_1 s + g_0}$$

where g_i are constants.

Using bilinear Z-transform (Golden and Kaiser, 1964).

$$S = \frac{2}{\Delta T} \frac{1 - z}{1 + z}$$

where $\Delta T = 1 \text{ms}$, sampling interval; the transfer function of the filter becomes

$$F(z) = (1 - z^2)^4 / (B_1(z)B_2(z)B_3(z)B_4(z))$$

$$\begin{aligned} \text{where } B_1 &= 1 - 1.91361z + 0.92966z^2 \\ B_2 &= 1 - 1.74003z + 0.76443z^2 \\ B_3 &= 1 - 1.24588z + 0.68060z^2 \\ B_4 &= 1 - 1.16038z + 0.38739z^2 \end{aligned}$$

The transfer function $F(z)$ may be written as a cascaded product of four filters

$$F(z) = F_1(z)F_2(z)F_3(z)F_4(z)$$

where terms like $F_1(z)$ have the form

$$F_1(z) = (1 - z^2)/(1 - D_1z + D_2z^2)$$

where D 's are coefficients.

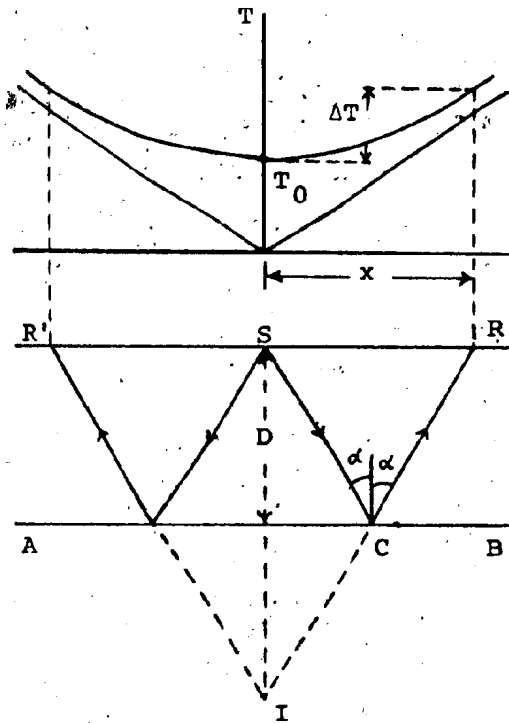
The filter is cascaded four times (Kanasewich, 1981, p. 243-244) in succession produces a Z-transform output and the recursive equations for programming are

$$\begin{aligned} c_n &= x_n - x_{n-2} + 1.91361 c_{n-1} - 0.929665 c_{n-2} \\ d_n &= c_n - c_{n-2} + 1.74003 d_{n-1} - 0.76443 d_{n-2} \\ e_n &= d_n - d_{n-2} + 1.24588 e_{n-1} - 0.68060 e_{n-2} \\ Y_n &= e_n - e_{n-2} + 1.16038 Y_{n-1} - 0.38739 Y_{n-2} \end{aligned}$$

Appendix-6

Normal moveout in horizontal reflector (After Telford et al., 1976).

Consider a horizontal reflector AB at a depth D below the shot point S. Energy leaving S along the direction SC will be reflected in such a direction that the angle of reflection equals the angle of incidence.



Denoting the average velocity by V_{rms} , the travel time T for the reflected wave is $(SC + CR)/V_{rms}$. However, $SC = CI$ so that IR is equal to the length of the actual path, SCR . Therefore, $T = IR/V_{rms}$ and in terms of offset X , we can write

$$v_{rms}^2 T^2 = X^2 + 4D^2$$

The travel times for a geophone at the shot i.e. at $X=0$, we obtain

$$T_0 = 2D/v_{rms}$$

$$\text{or, } 4D^2 = T_0^2 v_{rms}^2$$

Substituting the value of $4D^2$ in the above equation and dividing all throughout by v_{rms}^2 , we get

$$T^2 = T_0^2 + X^2/v_{rms}^2$$

To obtain Normal Moveout (NMO) ΔT , we substitute $T = T_0 + \Delta T$:

$$(T_0 + \Delta T)^2 = T_0^2 + X^2/v_{rms}^2$$

After simplifying

$$\Delta T \doteq X^2/2 v_{rms}^2 T_0$$

Appendix-7

To calculate the reflectivity at the interfaces of the layers below the Squires Park line in Humber Syncline, the density and velocity of different formations must be used. There are three layers, Humber Falls, Rocky Brook and North Brook formations in that area. Their densities are 2.5 gm/c.c, 2.54 gm/c.c and 2.7 gm/c.c respectively with the corresponding velocities 3000m/s, 4000m/s and 5000m/s respectively. The reflectivity or the reflection coefficient of the interface of the layers (Waters, 1981, p.26)

$$\begin{array}{l}
 \rho_1 = 2.5 \text{ gm/c.c, } V_1 = 3000 \text{ m/s} \\
 \hline
 R_1 \\
 \rho_2 = 2.54 \text{ gm/c.c, } V_2 = 4000 \text{ m/s} \\
 \hline
 R_2 \\
 \rho_3 = 2.7 \text{ gm/c.c, } V_3 = 5000 \text{ m/s}
 \end{array}$$

$$R_i = (\rho_{i+1} V_{i+1} - \rho_i V_i) / (\rho_{i+1} V_{i+1} + \rho_i V_i)$$

$$i = 1, 2.$$

where ρ_i and V_i denote the density and velocity.

Using the values of ρ and V 's in the above equation, $R_1 = 0.51$ and $R_2 = 0.141$ are determined.

7 COMPUTER PROGRAMMES

PROGRAM FOR STATIC CORRECTION

```

C   STATIC CORRECTION OF THE DEER LAKE DATA
C   DIMENSION=IRAHD(336),M(336),X(1000),Y(1000)
C
C   INTEGER*2 HEAD(200)
C
C   OPEN(UNIT=4,FILE='MFA0:',RECL=121,BLOCKSIZE=12100,
C   * STATUS='OLD',RECORDTYPE='FIXED',READONLY)
C
C   READ(3,115) HEAD(1),HEAD(2),HEAD(3)
C   WRITE(6,105) HEAD(1),HEAD(2),HEAD(3)
115  FORMAT(1X,I6,I5,I6)
105  FORMAT(1X,'REEL NO ',I6,10X,'NO OF TRACES '
C   *,I4,10X,'DEL TIM',I6)
C
C   READ(2,109)(M(II),II=1,336)
C   WRITE(6,109)(M(II),II=1,336)
109  FORMAT(16I5)
C   K=361
C   II=1
C
C   READ(3,117) IRAHD(1),IRAHD(3),IRAHD(4)
C   WRITE(6,107) IRAHD(1),IRAHD(3),IRAHD(4)
117  FORMAT(1X,I6,I5,I6)
107  FORMAT(1X,'TRA NO ',I5,10X,'FIELD REC NO '
C   *,I5,'FIELD TRA NO',I5)
C
C   READ(8)(X(I),I=1,1000)
C   LKK=M(II)+1
C   N=0
C   DO 90 JM=LKK,1000
C   N=N+1
90   Y(N)=X(JM)
C   J=1000-M(II)
C   WRITE(9)(Y(I),I=1,J)
C
C   II=II+1
C   K=K+1
C   IF(K.LT.697) GO TO 1
C
C   STOP
C   END

```

PROGRAM FOR MUTING THE DATA

```

C   MUTING THE STATIC CORRECTED NORMALIZED DATA
DIMENSION IRAHD(336),M(336),X(1000),GD(24),
*V(14),DELT(14),Y(1000)
INTEGER*2 HEAD(200)

C
C
READ(3,115) HEAD(1),HEAD(2),HEAD(3)
WRITE(6,105) HEAD(1),HEAD(2),HEAD(3)
115  FORMAT(1X,16,15,16)
105  FORMAT(1X,'REEL NO ',16,10X,'NO OF TRACES '
*,14,10X,',DEL TIM ',16)
READ(2,109)(M(II),II=1,336)
109  FORMAT(16I5)
READ(5,104)(GD(J),J=1,24)
104  FORMAT(10F8.1)
READ(5,106)(V(I),I=1,14)
106  FORMAT(10F8.3)
READ(5,102)(DELT(I),I=1,14)
102  FORMAT(10F8.1)
      K=361
      II=1
      AIRV=1.35

C
DO 60 II=1,14
DO 60 J=1,24
T1=(GD(J)/V(II))+DELT(II)
T2=GD(J)/AIRV
LT1=T1
LT2=T2
READ(3,117) IRAHD(1),IRAHD(3),IRAHD(4)
WRITE(6,107) IRAHD(1),IRAHD(3),IRAHD(4)
117  FORMAT(1X,16,15,16)
107  FORMAT(1X,'TRA NO ',15,10X,'FIELD REC NO '
*,15,'FIELD TRA NO',15)
      N=1000-M(II)

C
READ(8)(X(I),I=1,N)

C
DO 40 IJ=1,N
Y(IJ)=X(IJ)
40  CONTINUE

C
DO 50 IK=1,LT1
Y(IK)=0.0
50  CONTINUE

```



```

C      IF(LT2.LE.N) GO TO 3
      GO TO 70
3      DO 70 IM=LT2,N
      Y(IM)=0.0
70     CONTINUE
C
      WRITE(9)(Y(I),I=1,N)
      II=II+1
      K=K+1
60     CONTINUE
      STOP
      END

```

PROGRAM FOR NOTCH FILTER(60 HZ REJECTION)

```

C      60 HZ REJECTION USING NOTCH FILTER IN TIME DOMAIN.
C
      DIMENSION IRAHD(336),M(336),X(-1:1000),Y(-1:1000)
      *,YY(-1:1000),Z(-1:1000),ZZ(1000)
      INTEGER*2 HEAD(200)
C
      READ(3,115) HEAD(1),HEAD(2),HEAD(3)
      WRITE(6,105) HEAD(1),HEAD(2),HEAD(3)
115     FORMAT(1X,I6,I5,I6)
105     FORMAT(1X,'REEL NO ',I6,10X,'NO OF TRACES
      *,I4,10X,'DEL TIM',I6)
      READ(2,109)(M(II),II=1,336)
109     FORMAT(16I5)
      L=361
      II=1
1      READ(3,117) IRAHD(1),IRAHD(3),IRAHD(4)
      WRITE(6,107) IRAHD(1),IRAHD(3),IRAHD(4)
117     FORMAT(1X,I6,I5,I6)
107     FORMAT(1X,'TRA NO ',I5,10X,'FIELD REC NO
      *,I5,'FIELD TRA NO',I5)
      N=1000-M(II)
C
      READ(8)(X(I),I=1,N)

```

```

C
A1=0.9899
A2=-1.8408
A3=0.9899
B2=1.8406
B3=-0.98
C
DO 20 I=1,N
J=I-1
IF(J.GE.1) GO TO 30
X(J)=0.0
Y(J)=0.0
30 CONTINUE
K=I-2
IF(K.GE.1) GO TO 40
X(K)=0.0
Y(K)=0.0
40 CONTINUE
C
Y(I)=(A1*X(I))+(A2*X(J))+(A3*X(K))+(B2*Y(J))
*(B3*Y(K))
20 CONTINUE
C
C PASSING THE IN REVERSE ORDER
C
DO 50 IJ=1,N
YY(IJ)=Y(N-IJ+1)
50 CONTINUE
C
DO 60 IK=1,N
IL=IK-1
IF(IL.GE.1) GO TO 70
YY(IL)=0.0
Z(IL)=0.0
70 CONTINUE
IM=IK-2
IF(IM.GE.1) GO TO 80
YY(IM)=0.0
Z(IM)=0.0
80 CONTINUE
Z(IK)=(A1*YY(IK))+(A2*YY(IL))+(A3*YY(IM))
*(B2*Z(IL))+(B3*Z(IM))
60 CONTINUE
C
C REVERSING THE DATA AGAIN
C
DO 90 IN=1,N
ZZ(IN)=Z(N-IN+1)
90 CONTINUE
C
WRITE(9)(ZZ(I),I=1,N)
II=II+1
L=L+1
IF(L.LT.697) GO TO 1
C
STOP
END

```

PROGRAM OF FFT FOR THE POWER SPECTRUM

```

C   TO CALCULATE POWER SPECTRUM BY USING FFT.
    DIMENSION IRAHD(336),M(336),V(1024),X(1024)
    * ,POWER(1024)
    * INTEGER*2 HEAD(200)
    * COMPLEX X
C
    READ(3,115) HEAD(1),HEAD(2),HEAD(3)
    WRITE(6,105) HEAD(1),HEAD(2),HEAD(3)
115  FORMAT(1X,I6,I5,I6)
105  FORMAT(1X,'REEL NO ',I6,10X,'NO OF TRACES
    * ,I4,10X,'DEL TIM',I6)
    READ(2,109)(M(II),II=1,336)
109  FORMAT(16I5)
    K=361
    II=1
    N=10
    SIGN=1.0
C
1   READ(3,117) IRAHD(1),IRAHD(3),IRAHD(4)
    WRITE(6,107) IRAHD(1),IRAHD(3),IRAHD(4)
117  FORMAT(1X,I6,I5,I6)
107  FORMAT(1X,'TRA NO ',I5,10X,'FIELD REC NO
    * ,I5,'FIELD TRA NO',I5)
    NN=1000-M(II)
    READ(8)(V(I),I=1,NN)
C
    DO 55 IJ=1,NN
55   X(IJ)=CMPLX(V(IJ),0.0)
C
    L=NN+1
    DO 2 J=L,1024
    X(J)=CMPLX(0.0,0.0)
2   CONTINUE
    CALL NLOGN(N,X,SIGN)
    DO 3 I=1,1024
    A=REAL(X(I))
    B=AIMAG(X(I))
    AMP=SQRT(A**2+B**2)
3   POWER(I)=(AMP)**2
    WRITE(9)(POWER(I),I=1,1024)
    II=II+1
    K=K+1
    IF(K.LT.697) GO TO 1
C
    STOP
    END

```

```

SUBROUTINE NLOGN(N,X,SIGN)
C NMAX=LARGEST VALUE OF N TO BE PROCESSED
C NONDUMMY DIMENSION M(NMAX)
C DIMENSION M(1024)
C DIMENSION X(2**N)
C DIMENSION X(2)
C COMPLEX X,WK,HOLD,Q
C LX=2**N
C DO 1 I=1,N
1 M(I)=2**(N-I)
C DO 4 L=1,N
C NBLOCK=2**(L-1)
C LBLOCK=LX/NBLOCK
C LBHALF=LBLOCK/2
C K=0
C DO 4 IBLOCK=1,NBLOCK
C FK=K
C FLX=LX
C V=SIGN*6.2831853*FK/FLX
C WK=CMPLX(COS(V),SIN(V))
C ISTART=LBLOCK*(IBLOCK-1)
C DO 2 I=1,LBHALF
C J=ISTART+I
C JH=J+LBHALF
C Q=X(JH)*WK
C X(JH)=X(J)-Q
C X(J)=X(J)+Q
2 CONTINUE
C DO 3 I=2,N
C II=I
C IF (K.LT.M(I)) GO TO 4
3 K=K-M(I)
4 K=K+M(II)
C K=0
C DO 7 J=1,LX
C IF (K.LT.J) GOTO 5
C HOLD=X(J)
C X(J)=X(K+1)
C X(K+1)=HOLD
5 DO 6 I=1,N
C II=I
C IF (K.LT.M(I)) GOTO 7
6 K=K-M(I)
7 K=K+M(II)
C IF (SIGN.LT.0.0) RETURN
C DO 8 I=1,LX
8 X(I)=X(I)/FLX
C RETURN
C END

```

PROGRAM FOR AVERAGING THE POWER SPECTRUM

```
C   AVERAGE POWER SPECTRUM
C   DIMENSION IRAHD(336),V(512,24),SUM(512),AVPW(512)
C
C   INTEGER*2 HEAD(200)
C
C   READ(3,115) HEAD(1),HEAD(2),HEAD(3)
C   WRITE(6,105) HEAD(1),HEAD(2),HEAD(3)
115  FORMAT(1X,16,15,16)
105  FORMAT(1X,'REEL NO ',16,10X,'NO OF TRACES '
      *,14,10X,'DEL TIM',16)
C   DO 81 IX=1,14
C   READ(4,210) ISPNO
C   WRITE(6,220) ISPNO
210  FORMAT(15)
220  FORMAT(20X,'SHOT NUMBER',15)
C   DO 80 IY=1,24
C   READ(8)(V(I,IY),I=1,512)
80   CONTINUE
C
C   DO 12 J=1,512
C   SUM(J)=0.0
C   DO 12 I=1,24
C   SUM(J)=SUM(J)+V(J,I)
12   CONTINUE
C
C   DO 13 K=1,512
C   AVPW(K)=SUM(K)/24.
13   CONTINUE
C
C   WRITE(9)(AVPW(I),I=1,512)
81   CONTINUE
C   STOP
C   END
```

PROGRAM FOR THE BAND PASS FILTER

```

C   BUTTERWORTH BAND PASS FILTER(20 HZ TO 120 HZ)
      DIMENSION IRAHD(336),M(336),X(1000),D(8)
      *,XC(3),XD(3),XE(3)
      INTEGER*2 HEAD(200)
      COMPLEX P(4),S(8),Z1,Z2
C
      READ(3,115) HEAD(1),HEAD(2),HEAD(3)
      WRITE(6,105) HEAD(1),HEAD(2),HEAD(3)
115  FORMAT(1X,I6,I5,I6)
105  FORMAT(1X,'REEL NO',I6,10X,'NO OF TRACES
      *,I4,10X,'DEL TIM',I6)
      READ(2,109)(M(II),II=1,336)
109  FORMAT(16I5)
      L=361
      II=1
C
      F1=20.0
      F2=120.0
      DELT=1.0
C
C
      TWOPI=6.2831853
C
      DT=DELT/1000.0
      TDT=2.0/DT
      FDT=4.0/DT
      ISW=1
      P(1)=CMPLX(-.3826834,.9238795)
      P(2)=CMPLX(-.3826834,-.9238795)
      P(3)=CMPLX(-.9238795,.3826834)
      P(4)=CMPLX(-.9238795,-.3826834)
      W1=TWOPI*F1
      W2=TWOPI*F2
      W1=TDT*TAN(W1/TDT)
      W2=TDT*TAN(W2/TDT)
      HWID=(W2-W1)/2.0
      WW=W1+W2
C
      DO 19 I=1,4
      Z1=P(I)*HWID
      Z2=Z1*Z1-WW
      Z2=CSQRT(Z2)
      S(I)=Z1+Z2
19   S(I+4)=Z1-Z2
C

```

```

G=.5/HWID
G=G*G
G=G*G
DO 29 I=1,7,2
B=-2.0*REAL(S(I))
Z1=S(I)*S(I+1)
C=REAL(Z1)
A=TDT+B+C/TDT
G=G*A
D(I)=(C*DT-FDT)/A
29 D(I+1)=(A-2.0*B)/A
G=G*G

C
111 READ(3,117) IRAHD(1),IRAHD(3),IRAHD(4)
WRITE(6,107) IRAHD(1),IRAHD(3),IRAHD(4)
117 FORMAT(1X,I6,I5,I6)
107 FORMAT(1X,'TRA NO',I5,10X,'FIELD REC NO'
*,I5,'FIELD TRA NO',I5)
N=1000-M(I)
READ(8)(X(I),I=1,N)
CALL FILTER(X,N,D,G,IG)
WRITE(9)(X(I),I=1,N)
II=II+1
L=L+1
IF(L.LT.697) GO TO 111
STOP
END

C
C FILTER IN FORWARD DIRECTION
C
SUBROUTINE FILTER(X,N,D,G,IG)
DIMENSION X(1000),D(8),XC(3),XD(3),XE(3)
XM2=X(1)
XM1=X(2)
XM=X(3)
XC(1)=XM2
XC(2)=XM1-D(1)*XC(1)
XC(3)=XM-XM2-D(1)*XC(2)-D(2)*XC(1)
XD(1)=XC(1)
XD(2)=XC(2)-D(3)*XD(1)
XD(3)=XC(3)-XC(1)-D(3)*XD(2)-D(4)*XD(1)
XE(1)=XD(1)
XE(2)=XD(2)-D(5)*XE(1)
XE(3)=XD(3)-XD(1)-D(5)*XE(2)-D(6)*XE(1)
X(1)=XE(1)
X(2)=XE(2)-D(7)*X(1)
X(3)=XE(3)-XE(1)-D(7)*X(2)-D(8)*X(1)

```

C

```

DO 39 I=4,N
XM2=XM1
XM1=XM
XM=X(I)
K=I-((I-1)/3)*3
GO TO(34,35,36),K
34 M=1
M1=3
M2=2
GO TO 37
35 M=2
M1=1
M2=3
GO TO 37
36 M=3
M1=2
M2=1
37 XC(M)=XM-XM2-D(1)*XC(M1)-D(2)*XC(M2)
XD(M)=XC(M)-XC(M2)-D(3)*XD(M1)-D(4)*XD(M2)
XE(M)=XD(M)-XD(M2)-D(5)*XE(M1)-D(6)*XE(M2)
39 X(I)=XE(M)-XE(M2)-D(7)*X(I-1)-D(8)*X(I-2)
C
C FILTER IN REVERSE DIRECTION
C
XM2=X(N)
XM1=X(N-1)
XM=X(N-2)
XC(1)=XM2
YC(2)=XM1-D(1)*XC(1)
XC(3)=XM-XM2-D(1)*XC(2)-D(2)*XC(1)
XD(1)=XC(1)
XD(2)=XC(2)-D(3)*XD(1)
XD(3)=XC(3)-XC(1)-D(3)*XD(2)-D(4)*XD(1)
XE(1)=XD(1)
XE(2)=XD(2)-D(5)*XE(1)
XE(3)=XD(3)-XD(1)-D(5)*XE(2)-D(6)*XE(1)
X(N)=XE(1)
X(N-1)=XE(2)-D(7)*X(1)
X(N-2)=XE(3)-XE(1)-D(7)*X(2)-D(8)*X(1)
C
DO 49 I=4,N
XM2=XM1
XM1=XM
J=N-I+1
XM=X(J)
K=I-((I-1)/3)*3
GO TO (44,45,46),K
44 M=1
M1=3
M2=2
GO TO 47
45 M=2

```



```

M1=1
M2=3
GO TO 47
46 M=3
M1=2
M2=1
47 XC(M)=XM-XM2-D(1)*XC(M1)-D(2)*XC(M2)
XD(M)=XC(M)-XC(M2)-D(3)*XD(M1)-D(4)*XD(M2)
XE(M)=XD(M)-XD(M2)-D(5)*XE(M1)-D(6)*XE(M2)
49 X(J)=XE(M)-XE(M2)-D(7)*X(J+1)-D(8)*X(J+2)
IF(1G.NE.1) RETURN
DO 59 I=1,N
59 X(I)=X(I)/G
RETURN
END

```

PROGRAM FOR CDP GATHER(6-FOLD)

```

C CDP GATHER(6-FOLD)
DIMENSION CDPNO(36), M(336), X(1000)
INTEGER CDPNO
IA=20
IB=40
IC=60
ID=80
IE=100
IF=120
C
J=1
LL=0
3 L=1
C
2 READ(1,15) CDPNO(J)
15 FORMAT(15)
WRITE(6,19) CDPNO(J)
C
READ(2,25)(M(II), II=1,336)
25 FORMAT(16I5)
K=1
II=1
1 N=1000-M(II)
READ(8)(X(I), I=1,N)
C

```

```

IAA=IA+LL+L
IBB=IB+LL+L
ICC=IC+LL+L
IDD=ID+LL+L
IEE=IE+LL+L
IFF=IF+LL+L
C
IF(K.EQ. IAA) GO TO 100
IF(K.EQ. IBB) GO TO 100
IF(K.EQ. ICC) GO TO 100
IF(K.EQ. IDD) GO TO 100
IF(K.EQ. IEE) GO TO 100
IF(K.EQ. IFF) GO TO 100
C
GO TO 200
C
100 CONTINUE
NN=N+1
DO 50 I=NN,1000
50 X(I)=0.0
WRITE(9)(X(I),I=1,1000)
WRITE(6,89) M(II)
C
200 II=II+1
K=K+1
IF(K.LT.337) GO TO 1
C
REWIND 8
REWIND 2
J=J+1
L=L+1
IF(L.LT.5) GO TO 2
C
LL=LL+24
IF(LL.LT.193) GO TO 3
19 FORMAT(10X,'COMMON DEPTH POINT NO',15)
89 FORMAT(15)
C 99 FORMAT(5F16.5)
STOP
END

PROGRAM FOR THE ELIMINATION OF NOISE TRACES
-----

C TO ELIMINATE THE TRACES OF NOISE SHOT AFTER NMO
DIMENSION X(1000), NUMBER(20)
C OPEN(UNIT=2,FILE='NSTEL.DAT',TYPE='NEW')
DATA (NUMBER(I),I=1,20)/2,8,14,20,25,31,37,43,
*150,156,162,168,173,179,185,191,196,202,208,214/
K=1

```

```

1.  READ(8)(X(I), I=1,1000)
    IFLAG=0
    DO 20 I=1,20
    IF(K.EQ.NUMBER(I)) IFLAG=1
20  CONTINUE
    IF(IFLAG.EQ.1) GO TO 30
    GO TO 50
30  CONTINUE
    C
    DO 40 J=1,1000
    X(J)=0.0
40  CONTINUE
    C
C50  WRITE(2,19)(X(I), I=1,1000)
50  WRITE(9)(X(I), I=1,1000)
    K=K+1
    IF(K.LT.217) GO TO 1
    C
C19  CLOSE(UNIT=2, STATUS='SAVE')
    FORMAT(8F10.5)
    STOP
    END

```

PROGRAM FOR THE DETERMINATION OF VELOCITY BY L.S. METHOD

```

C
C THE VELOCITY AND TWT AT ZERO OFF-SET
C BY LEAST SQUARE METHOD.
C
C DIMENSION OFFSET(6), Y(6), X(6)
C DATA(OFFSET(I), I=1,6)/25., 225., 425., 625., 825., 1025./
C H=500.
C V=3000.
C N=6
C
C DO 30 I=1,6
C Y(I)=(4*(H**2)+(OFFSET(I)**2))/(V**2)
C X(I)=OFFSET(I)**2
30 CONTINUE
C
C SUMX=0.0
C SUMY=0.0
C SUMXY=0.0
C SUMXX=0.0
C

```

```

DO 40 I=1,N
SUMX=SUMX+X(I)
SUMY=SUMY+Y(I)
SUMXY=SUMXY+(X(I)*Y(I))
SUMXX=SUMXX+(X(I)**2)
40 CONTINUE
C
B=(SUMXY-(SUMX*SUMY)/N)/(SUMXX-(SUMX**2)/N)
A=(SUMY/N)-B*(SUMX/N)
C
VEL=SQRT(ABS(1./B))
TWT=SQRT(A)
C
WRITE(6,50) VEL, TWT
50 FORMAT(10X,'VELOCITY=',F5.0,'M/S',10X,'VERTICAL
* TWT=',F8.3,'SEC')
STOP
END

```

0

SAMPLE PROGRAM FOR THE VELOCITY SCAN

```

C VELOCITY SCAN FOR FIRST CDP TRACES
DIMENSION X(6),TO(7),IDELTIM(6,7),M(6),Y(1000),Z(1000)
OPEN(UNIT=1,FILE='VLST1.DAT',TYPE='NEW')
V=3.0
DATA(X(I),I=1,6)/1025.,825.,625.,425.,225.,25./
DATA(TO(J),J=1,7)/60.,66.,72.,78.,84.,90.,96./
DATA(M(II),II=1,6)/18,18,18,18,19,18/
C
DO 30 J=1,7
DO 30 I=1,6
IDELTIM(I,J)=((X(I)**2)/(2*TO(J)*(V**2)))
* - ((X(I)**4)/(8*(TO**3)*(V(J)**4)))
C PRINT *,IDELTIM(I,J)
30 CONTINUE
C
J=1
2 II=1
3 N=1000-M(II)
READ(8)(Y(I),I=1,N)
LKK=IDELTIM(II,J)+1
NN=0
DO 90 JM=LKK,N
NN=NN+1
90 Z(NN)=Y(JM)

```

```

L=N-IDELTIM(II,J)
WRITE(1,18) L
WRITE(9)(Z(I),I=1,L)
II=II+1
IF(II.LT.7) GO TO 3
REWIND 8
J=J+1
IF(J.LT.8) GO TO 2
CLOSE(UNIT=1,STATUS='SAVE')
C
18 FORMAT(16I5)
C 19 FORMAT(8F10.5)
STOP
END

```

PROGRAM FOR THE NORMAL MOVEOUT(NMO) CORRECTION

```

C PROGRAM FOR NMO
DIMENSION X(216),TO(216),IDELTIM(216),Y(1000),Z(1000)
V=3.0
READ(3,15)(X(I),I=1,216)
15 FORMAT(6F8.0)
C
READ(4,17)(TO(I),I=1,216)
17 FORMAT(12F5.0)
C
DO 30 I=1,216
IDELTIM(I)=(X(I)**2)/(2*TO(I)*(V**2))
30 CONTINUE
C
WRITE(6,18)(IDELTIM(I),I=1,216)
18 FORMAT(6I12)

```

```

C
  I=1
  3  N=1000
    READ(8)(Y(II),II=1,N)
    LKK=IDELTIM(I)+1
    NN=0
    DO 90 JM=LKK,N
    NN=NN+1
  90  Z(NN)=Y(JM)
C
    L=N-IDELTIM(I)+1
    DO 50 IK=L,N
  50  Z(IK)=0.0
    WRITE(9)(Z(J),J=1,1000)
    I=I+1
    IF(I.LT.217) GO TO 3
  C16  FORMAT(6I5)
  C19  FORMAT(8F10.5)
    STOP
    END

```

PROGRAM FOR STACKING THE DATA

```

C  STACKING PROGRAM
  DIMENSION X(6,1000), SUM(1000)
  OPEN(UNIT=8,FILE='NSTEL.DAT',TYPE='OLD')
  DO 30 K=1,36
  READ(8,15)((X(I,J),J=1,1000),I=1,6)
  DO 40 J=1,1000
  SUM(J)=0.0
  DO 50 I=1,6
  SUM(J)=SUM(J)+X(I,J)
  50  CONTINUE
  SUM(J)=SUM(J)/6.0
  40  CONTINUE
C    PRINT *, 'HEADING'
  WRITE(9)(SUM(J),J=1,1000)
  30  CONTINUE
  15  FORMAT(8F10.5)
    STOP
    END

```

SAMPLE PROGRAM FOR PLOTTING THE SEISMIC TRACES

```

C   PLOTTING OF DEMULTIPLEX NORMALIZED DATA OF DEER LAKE
C   DIMENSION X(1002),Y(1002)
C   CALL PLOTS(0.0,6)
C   CALL FACTOR(1.0)
C   CALL PLOT(2.0,2.0,-3)
C   CALL SCALE( )
C   CALL AXIS(0.0,0.0,15HTIME IN SECONDS,15,4.0,90.,1.000,-0.25)
C   CALL AXIS( )
C   CALL SYMBOL(12.5,4.7,0.21,18HDEMULPLEXED DATA,0.0,18)
C   CALL SYMBOL(0.0,-0.5,0.14,34HFIG.3.1 PLOT OF DEMULPLEXED DATA,
C   *0.0,34)
C
C   DO 50 I=1,14
C   XL=1.92*(I-1)
C   CALL SYMBOL(XL,4.2,0.14,7HSP= ,0.0,7)
C   VAL=I
C   CALL NUMBER(XL+0.5,4.2,0.14,VAL,0.0,-1)
50  CONTINUE
C
C   X(1)=1.000
C   DO 51 I=2,1000
51  X(I)=X(I-1)-0.001
C   CALL SCALE(X,8.0,1000,1)
C   X(1001)=0.000
C   X(1002)=0.25
C   Y(1001)=-1.00
C   Y(1002)=12.5
C
C   K=361
C   II=1
C   N=1000
1   READ(8)(Y(I),I=1,N)
C
C   CALL LINE(Y,X,1000,1,0.2)
C   CALL PLOT(0.08,0.0,-3)
C   II=II+1
C   K=K+1
C   IF(K.LT.697) GO TO 1
C   CALL PLOT(12.0,0.0,999)
C   STOP
C   END

```

8 ACKNOWLEDGEMENTS

I wish to acknowledge with thanks the following individuals and organizations for their help in the completion of this work:

My supervisor, Dr. H.G. Miller, for his constant guidance and many suggestions during the course of work.

Dr. J.A. Wright, Department of Earth Sciences for many useful suggestions about data treatment and analysis.

Dr. C.R. Barnes, Head of the Department of Earth Sciences for the use of departmental equipment and facilities.

Dr. R.S. Hyde of the Department of Earth Sciences for valuable discussions about the geology of the area and for the use of personal notes.

Dr. D.F. Strong, Department of Earth Sciences for using his manuscript about the paleomagnetic information of the area.

Mr. Greg Bennett of Computing Services, MUN for his help in computer programming and plotting.

Mr. P.R. Mohanty and J.N. Prasad, graduate students of the Department of Earth Sciences for discussions during the course of work.

Mrs. Gerri Starkes, Department of Earth Sciences for typing the mathematical part of the thesis.

Further, I express my appreciation to Memorial University of Newfoundland, for providing me with financial support in the form of fellowship and assistantship; to the Shell Resources Canada for providing support for this study as

research grant to Memorial University Earth Sciences team consisting of Drs. R.N. Hiscott, Dr. H.G. Miller, Dr. J.A. Wright and Dr. D.F. Strong; Department of Mines and Energy, Government of Newfoundland and Labrador for supplying geological maps.

I am also grateful to the University of Chittagong, Bangladesh for granting me study leave for my studies abroad.

Finally, I am very much indebted to my wife, Farida, and members of my family for their exemplary patience and constant encouragement, without which this work would not have been possible.

9 REFERENCES

- Baird, D.M., 1960, Geological map of Sandy Lake (west half), Newfoundland. Geological Survey of Canada, Map 47-1959.
- Belt, E.S., 1969, Newfoundland Carboniferous stratigraphy and its relation to the Maritimes and Ireland: Amer. Assoc. Pet. Geologists Memoir 12, M. Kay (Edition), p.734-753.
- Dobrin, M.B., 1976, Introduction to Geophysical Prospecting, 3rd Edition, McGraw-Hill Publishing Co., Toronto.
- Gold, R.M., and Kaiser, J.F., 1964, Design of a side-band sampled data filter. The Bell telephone Technical Journal, pp.1533-1547.
- Guillemin, E.A., 1957, Synthesis of passive networks: New York, John Wiley and Sons, Inc.
- Hacquebard, P.A., Brass, M.S. and Donaldson, J.R., 1960, Distribution and stratigraphic significance of small spore genera in the upper Carboniferous of the Maritime provinces of Canada: 4th International Carboniferous Stratigraphy and Geology Cong., Heerlen, 1958, Comptes Rendus, V.1, P.237-45.
- Hatch, H.B., 1919, Deer Lake, Humber River and Grand Lake

Shell. Report to Reid Newfoundland Co. on file with
with Nfld. Dept. Mines and Energy.

Haworth, R.T. and Sanford, B.V., 1976, Paleozoic geology of
the southeast Gulf of Saint Lawrence Geological
Survey of Canada, Paper 76-1A, pp.1-6.

Haworth, R.T., Poole, W.H., Grant, A.C. and Sanford, B.V.,
1976, Marine Geoscience survey north east of Nfld.
Geological Survey of Canada, Paper 76-1A, pp.7-15.

Holtz, H., and Leondes, C.T., 1966, The synthesis of recursive
digital filters: Jour. ACM, V.13, no.2, pp.262-280.

Hyde, R.S., 1983, Geology of the Carboniferous Deer Lake
Basin, Nfld. Dept. of Mines and Energy Map 82-7,
1:100,000.

Hyde, R.S., 1979, Geology of Carboniferous strata in portions
of the Deer Lake Basin, western Newfoundland: Nfld.
Dept. of Mines and Energy Report 79-6, p.43.

Hyde, R.S. and Ware, M.J., 1981, Geology of portions of the
Cormack(12H/6) and Silver Mountain(12H/11) map-areas
, Nfld. Dept. of Mines and Energy Map 8011, 1:50,000.

Kaiser, J.F., 1963, Design methods for sampled data filters:
Proc. First Allerton Conference on Circuit and
System theory, p.221-236.

Kanasewich, E.R., 1981, Time Sequence Analysis in Geophysics,

3rd Edition, The University of Alberta Press.

- Kent, D.V. and Opdyke, N.D., 1979, The early Carboniferous paleomagnetic field of North America and its bearing on tectonics of the northern Appalachians. Earth and Planetary Science Letters, 44, pp. 365-72.
- Knight, I., 1982, Geology of the Carboniferous Bay St. George Sub-basin: Nfld. Dept. of Mines and Energy Map 82-1, 1:125,000.
- Kossack, C.F. and Claudia, I.H., 1975, Introduction to Statistics and Computer Programming, Pilot Edition, p.400-405.
- Mayne, W.H., 1962, Common Reflection Point horizontal data stacking techniques, Geophysics, Vol. XXVII, No. 6, Part-II, pp.927-938.
- Miller H.G. and Wright J.A., 1984, Gravity and magnetic interpretation of the Deer Lake Basin, Newfoundland. In press, Canadian Journal of Earth Sciences, Jan. 1984 ed.
- Neale, E.R.W. and Nash, W.A., 1963, Sandy Lake (east half) Newfoundland. Geological Survey of Canada Map 62-28.
- O'Sullivan, J., 1979, Report on geological, geochemical and geophysical surveys, Northgate Exploration Ltd., Project 721 Cornack.

Peterson, R.A., Philippone, W.R. and Coker, F.B., 1955, The synthesis of seismograms from Well Log Data, Geophysics, Vol. 20, p.516-538.

Robertson, H.H., 1965, Approximate design of digital filters: Technometrics, V.7, no.3, p.387-403.

Shanks, J.J., 1967, Recursion filters for digital processing, Geophysics, vol. 32, p.33-51.

Smyth, W.R. and Martineau, Y., 1982, Geology Sandy Lake, Mineral Development Division, Dept. of Mines and Energy, Government of Newfoundland and Labrador, Map 82-54.

Strong, D.F. and Irving, E.C., 1983, Paleomagnetism of the Carboniferous Deer Lake Group, western Newfoundland no evidence for mid-Carboniferous displacement of "Acadia". Preprint, paper submitted to Earth and Planetary Science Letters, Sept., 1983.

Telford, W.M., Geldart, L.P., Sheriff, R.E. and Keys, D.A., 1976, Applied Geophysics, Cambridge University Press, Cambridge.

Truxal, J.G., 1955, Automatic feedback control system syntheses. McGraw-Hill, p. 531.

Waters, K.H., 1981, Reflection Seismology, John-Wiley & sons, Toronto, p.26.

Weaver, D.F., 1967, A geological interpretation of the Bouguer anomaly field of Newfoundland Publications of the Dominion Observatory, Ottawa. V.35, p.223-51.

Werner, H.J., 1955, The geology of the Humber Valley, Nfld. Private report to Newkirk Mining Co. on file Mineral Development Div., Nfld. Dept. of Mines and Energy.

Westfield Minerals Ltd., 1981, Geology of Deer Lake, Nfld. (Unpublished Geology map).

Whittlesey, J.R.B., 1964, A rapid method for digital filtering: Comm. ACM, V.7, no.9, p.552-556.

Williams, H., 1979, Appalachian Orogen in Canada. Canadian Journal of Earth Sciences, vol.16, pp.792-802.

1 of

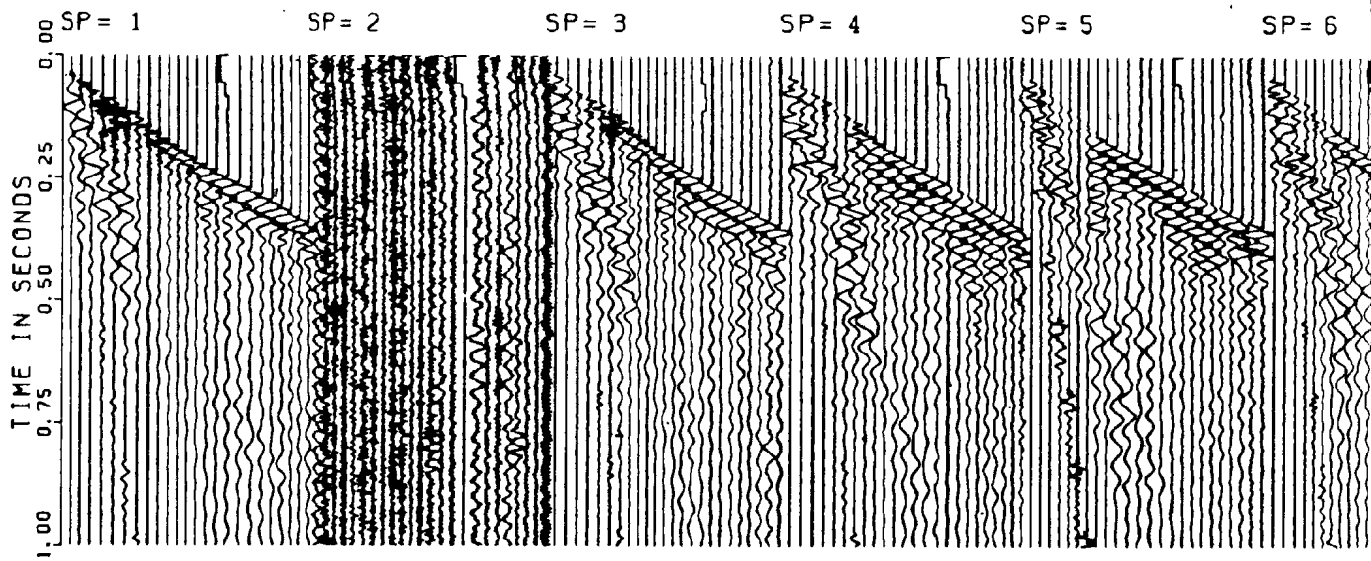


FIG. 3.1 PLOT OF DEMULTIPLEXED DATA

207

DEMULTIPLEXED DATA

SP= 6

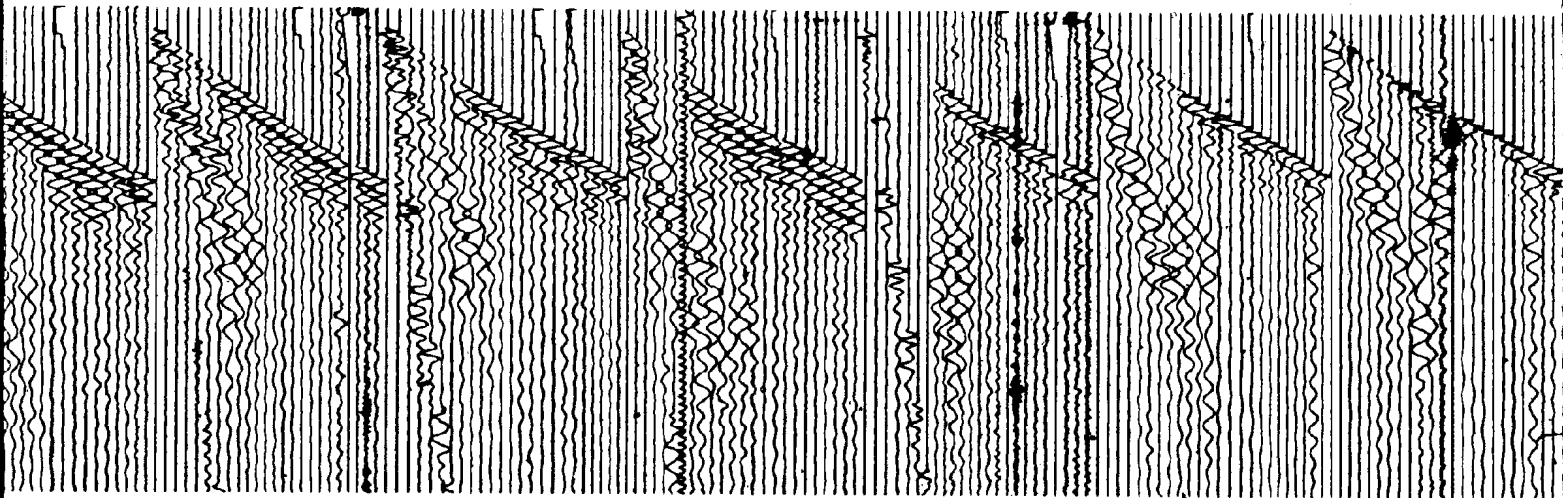
SP= 7

SP= 8

SP= 9

SP= 10

SP= 11



3 of 3

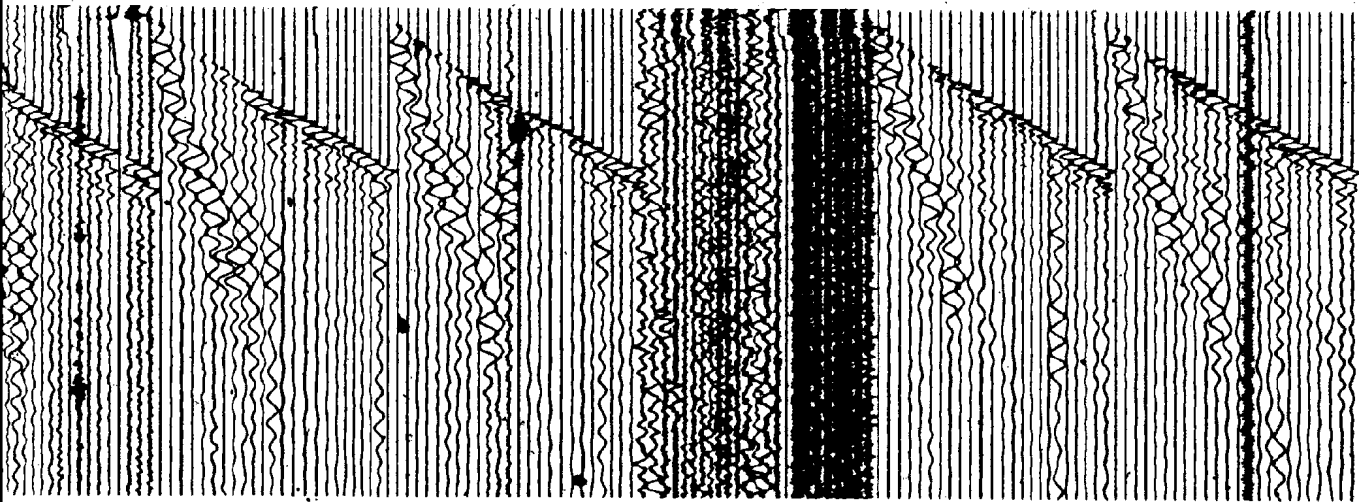
SP= 10

SP= 11

SP= 12

SP= 13

SP= 14



1 of

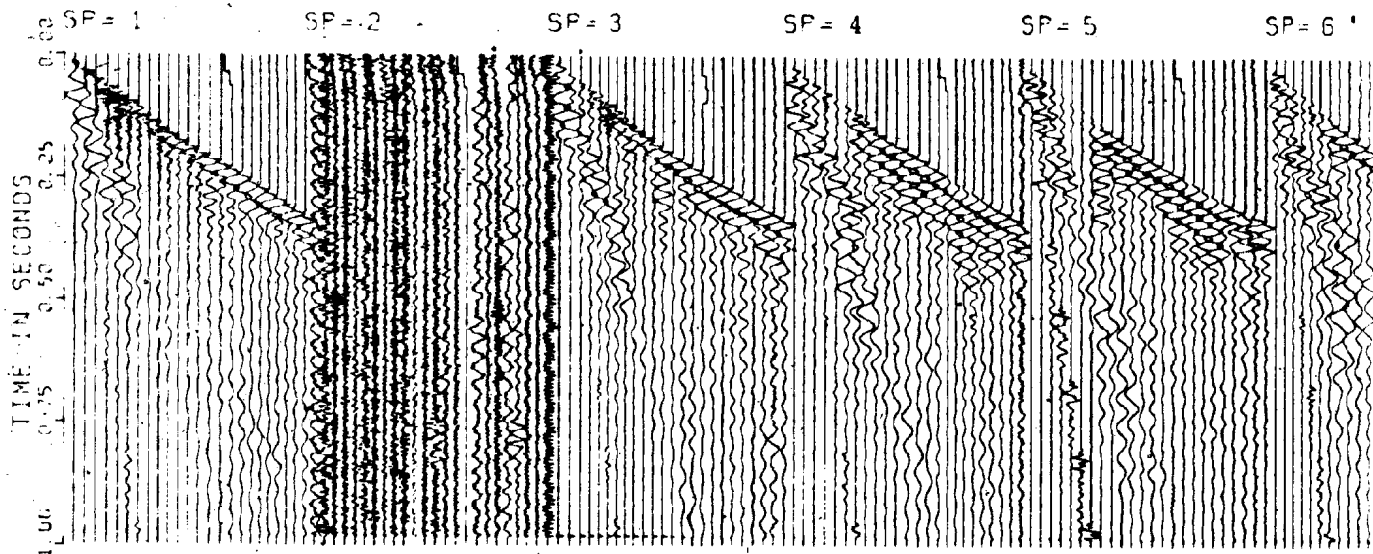
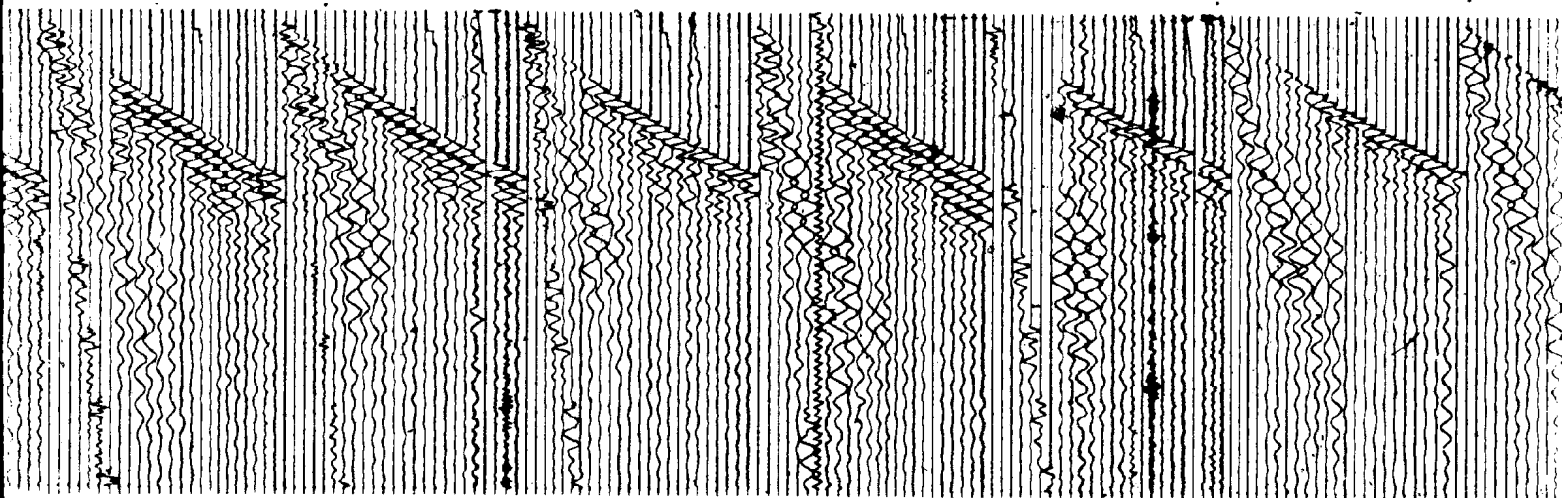


FIG. 3.2 PLOT OF STATIC CORRECTED DATA

207

STATIC CORRECTED DATA

SP = 5 SP = 6 SP = 7 SP = 8 SP = 9 SP = 10 SP = 11



3 of 3

DATA

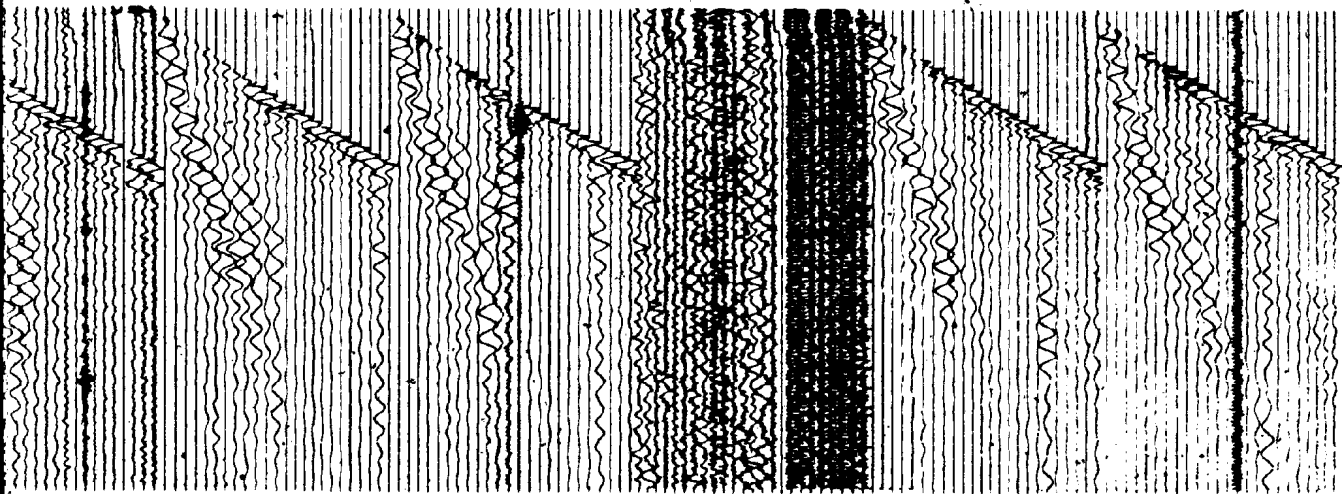
SP = 10

SP = 11

SP = 12

SP = 13

SP = 14



1 of 7

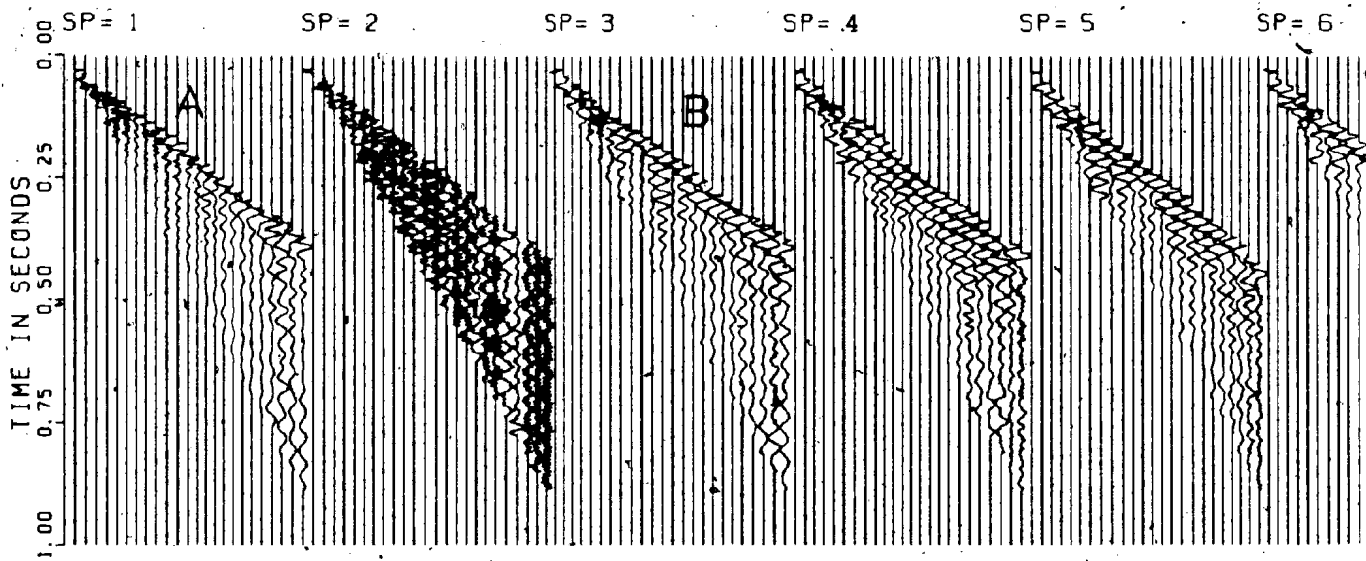
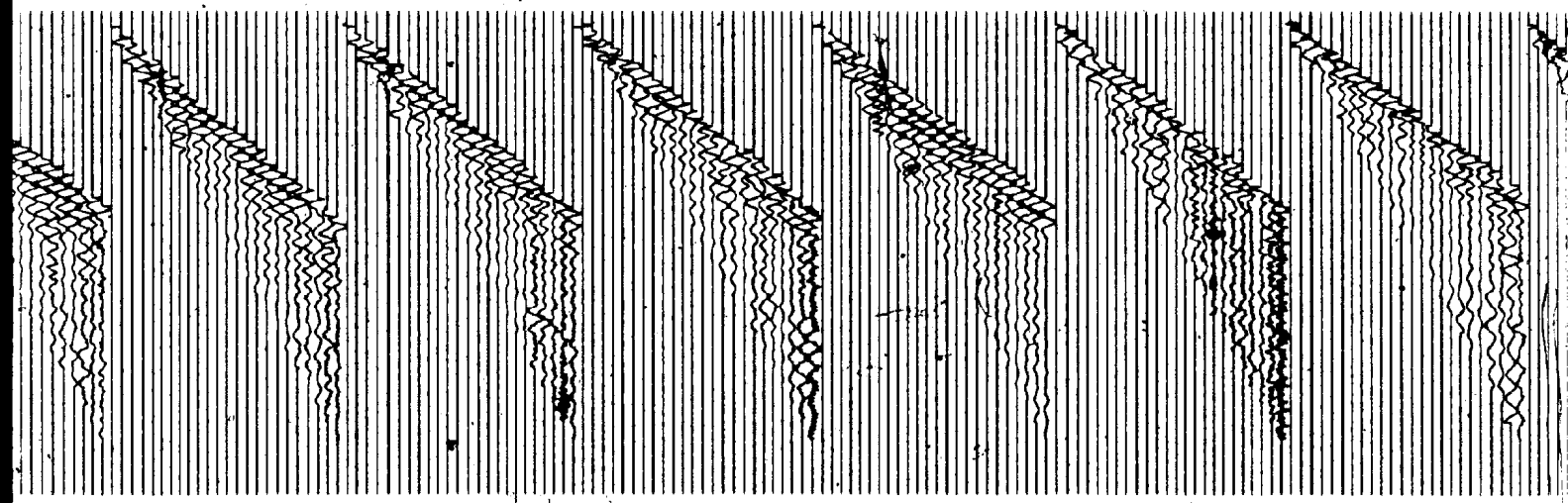


FIG. 3.3 PLOT OF MUTED DATA

207.

MUTED DATA.

SP= 5 SP= 6 SP= 7 SP= 8 SP= 9 SP= 10 SP=



3 of 3

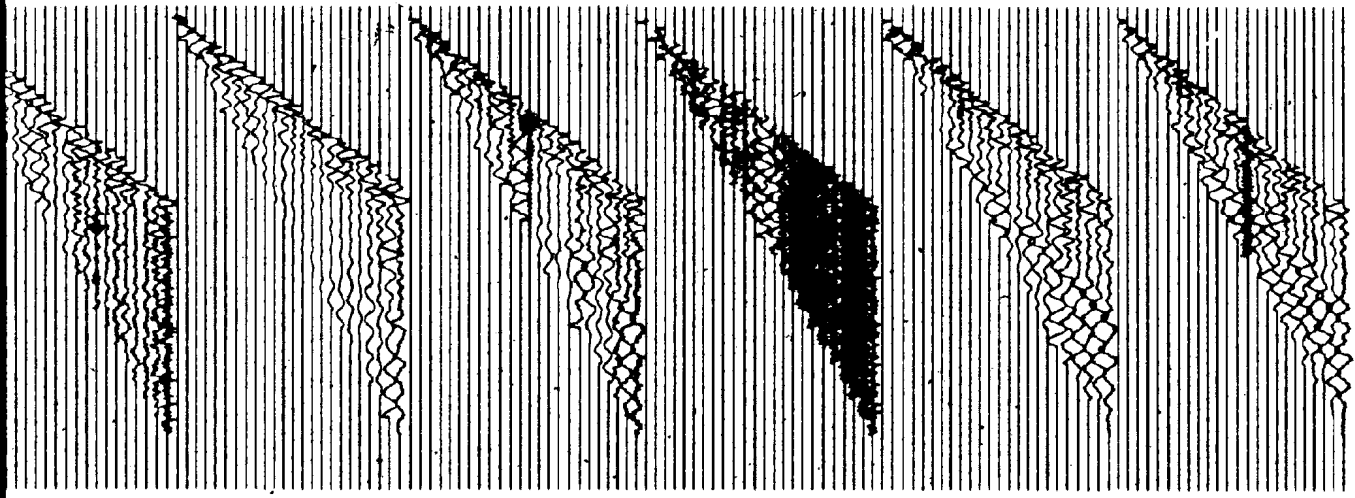
SP= 10

SP= 11

SP= 12

SP= 13

SP= 14



1 of

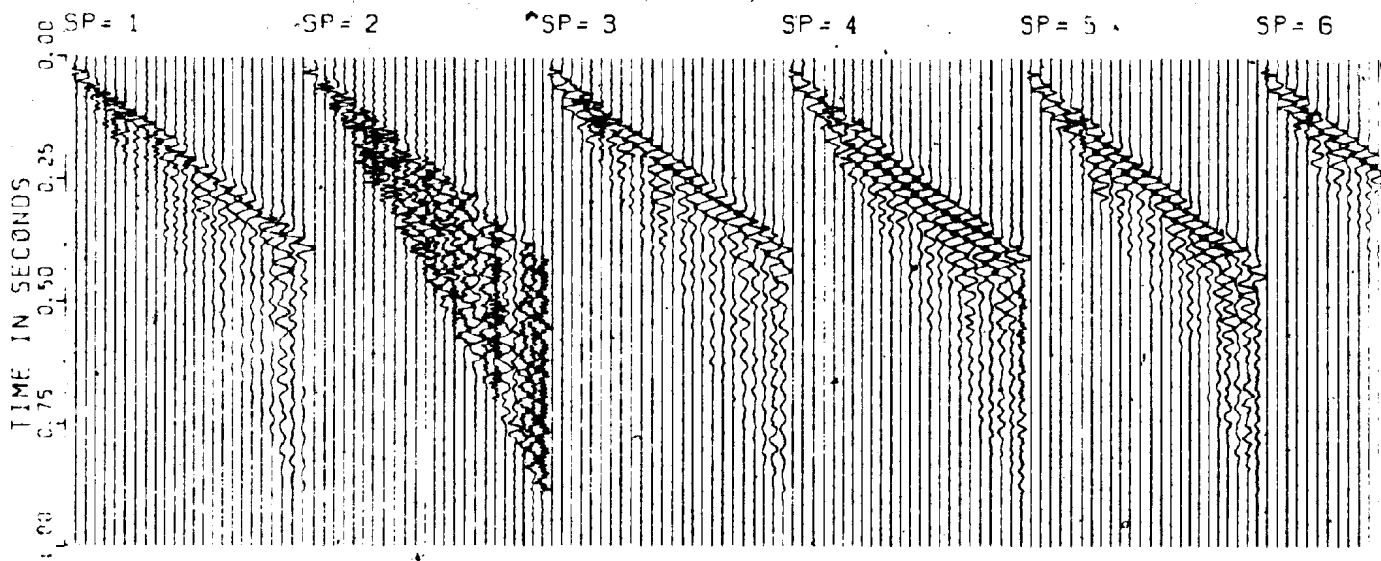


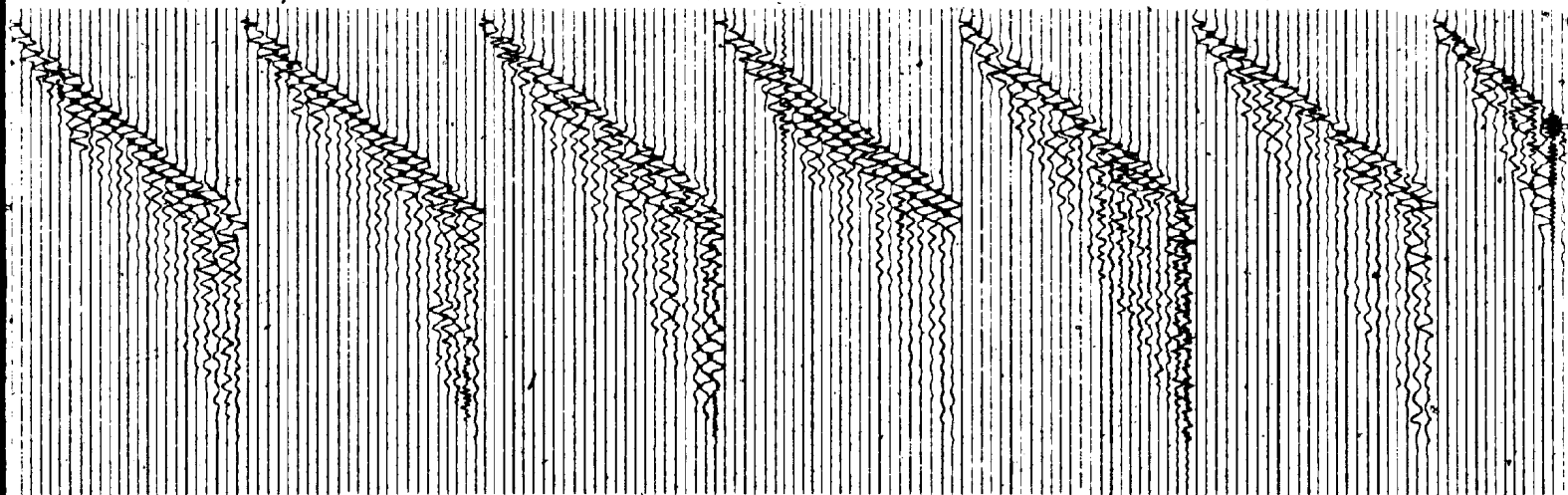
FIG. 3.5 PLOT OF FILTERED DATA

207

FILTERED DATA

60 HZ NOTCH & 20-120 HZ BAND-PASS

SP = 5 SP = 6 SP = 7 SP = 8 SP = 9 SP = 10 SP = 11



3 of 3

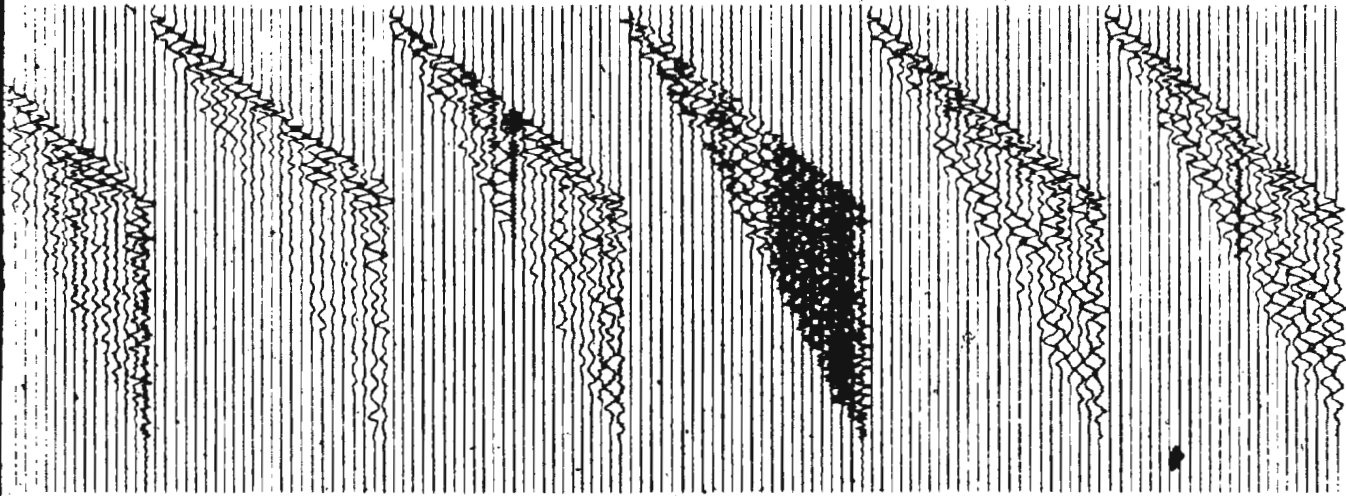
SP= 10

SP= 11

SP= 12

SP= 13

SP= 14



2

1 of

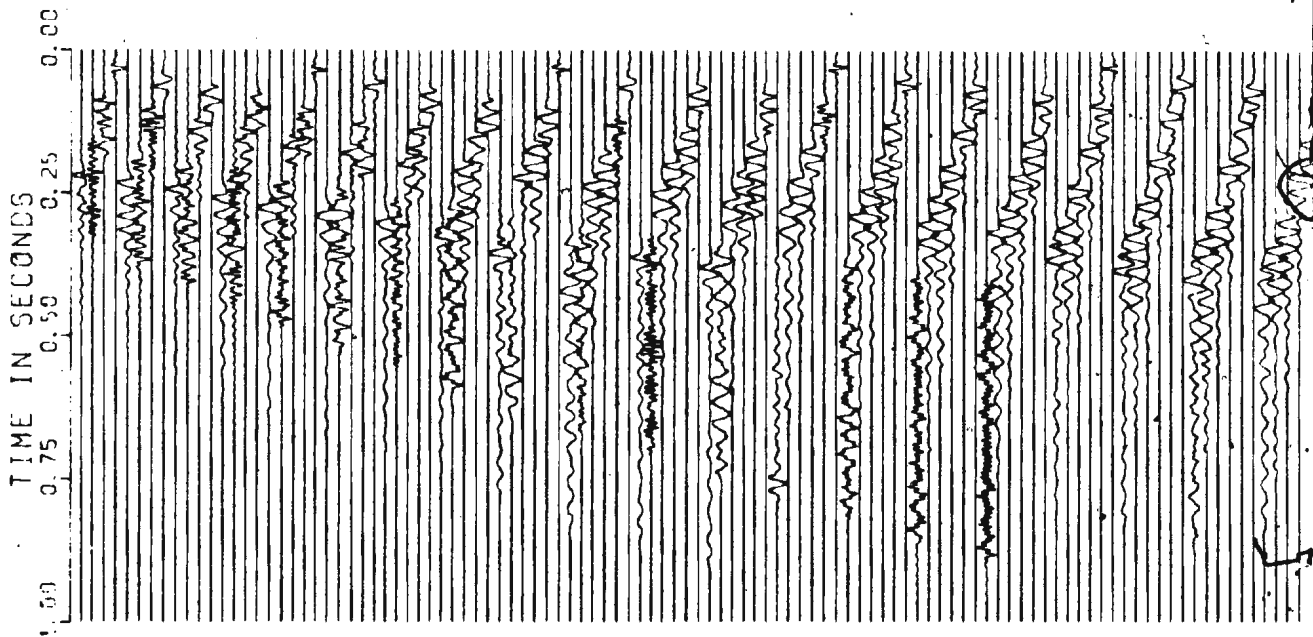
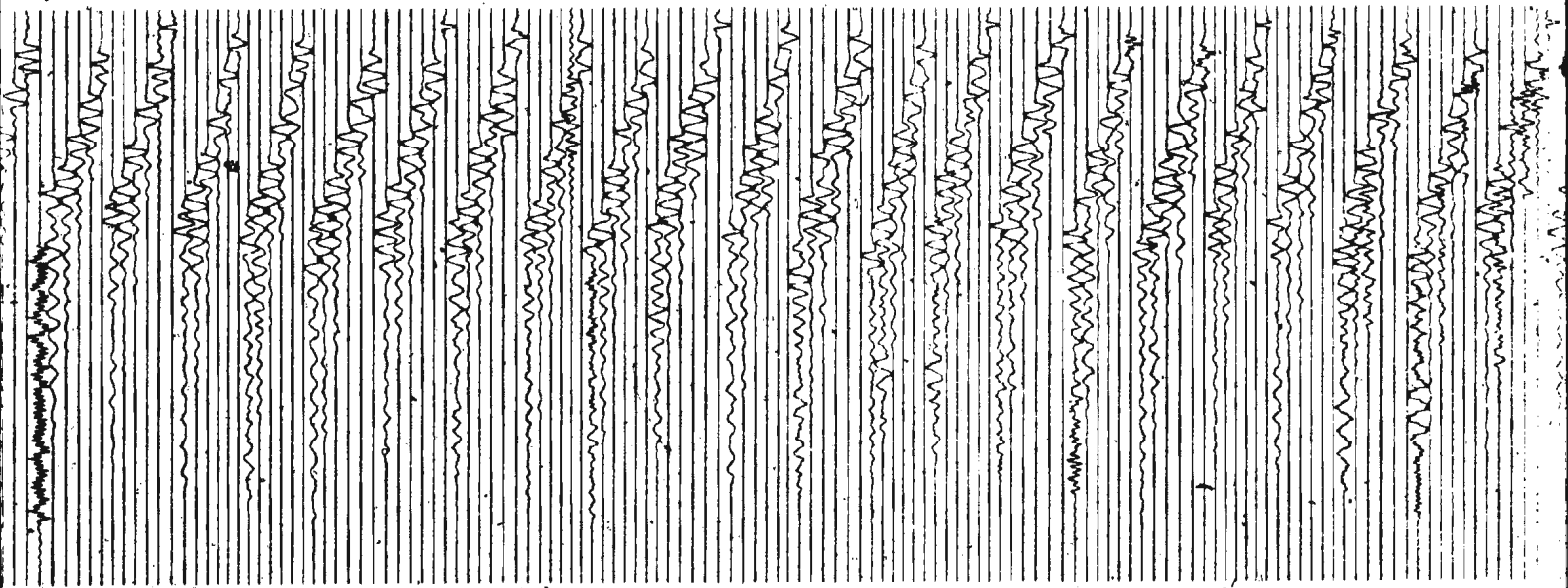


FIG. 3.8 PLOT OF COP GATHER DATA

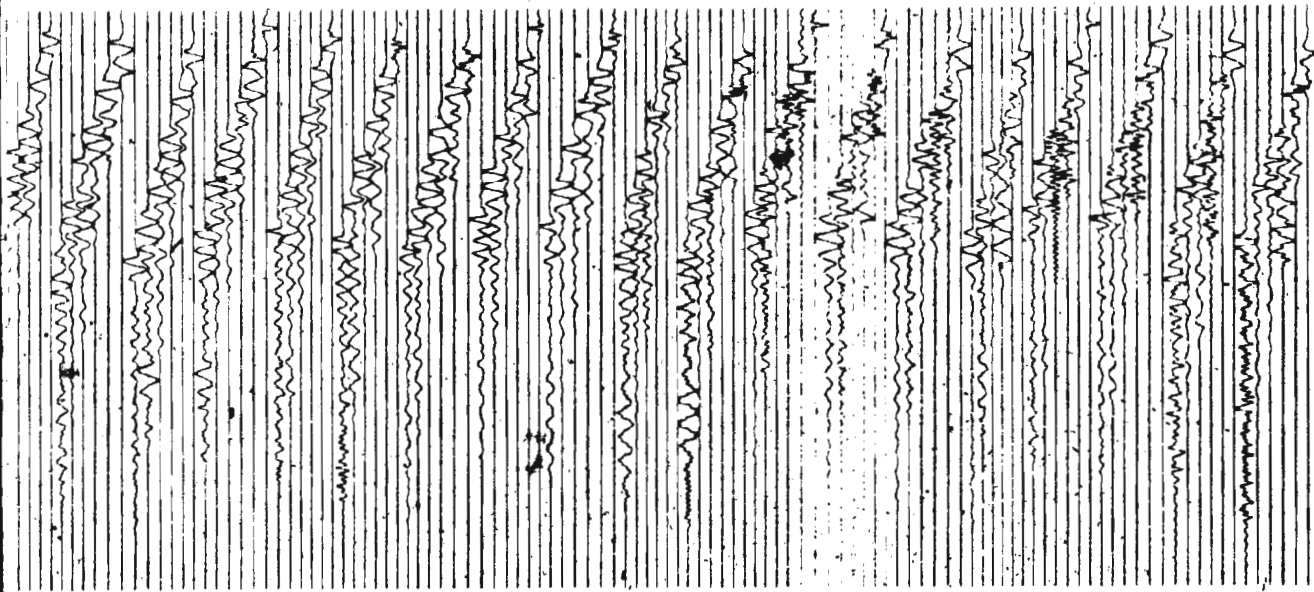
207

CDP GATHER DATA



3 of 3

DATA



1 of

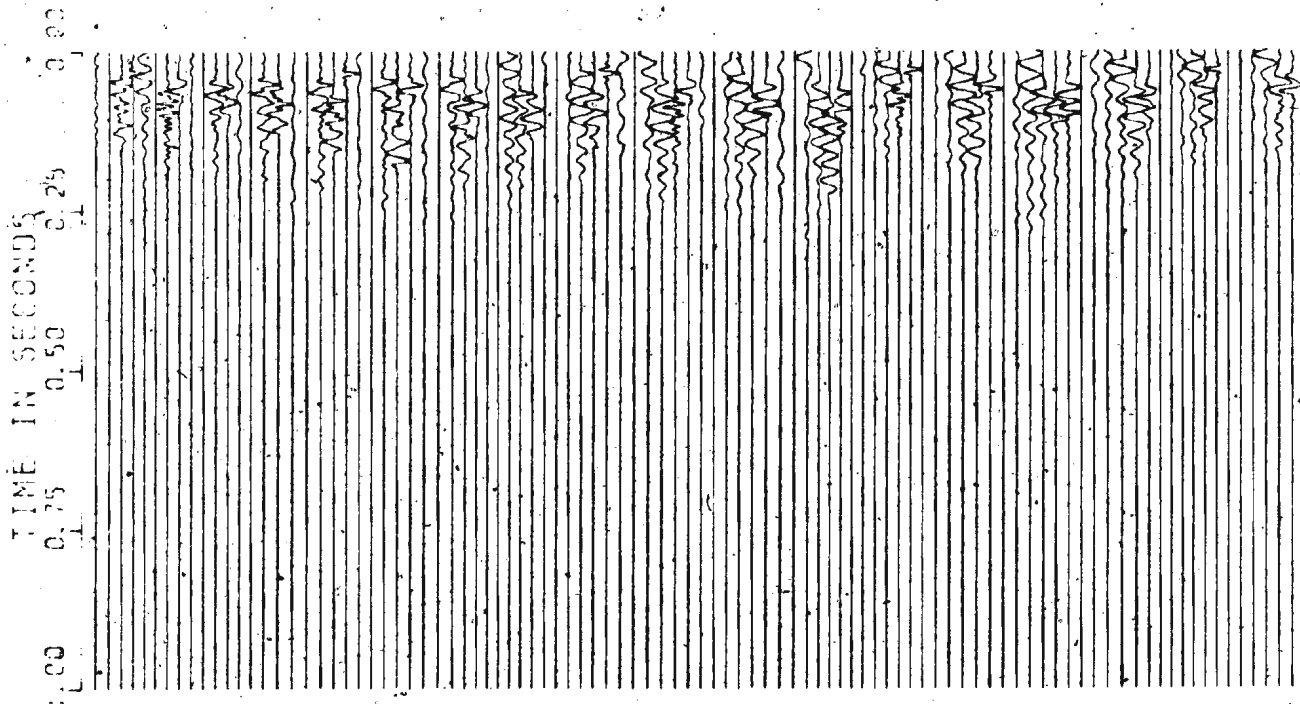
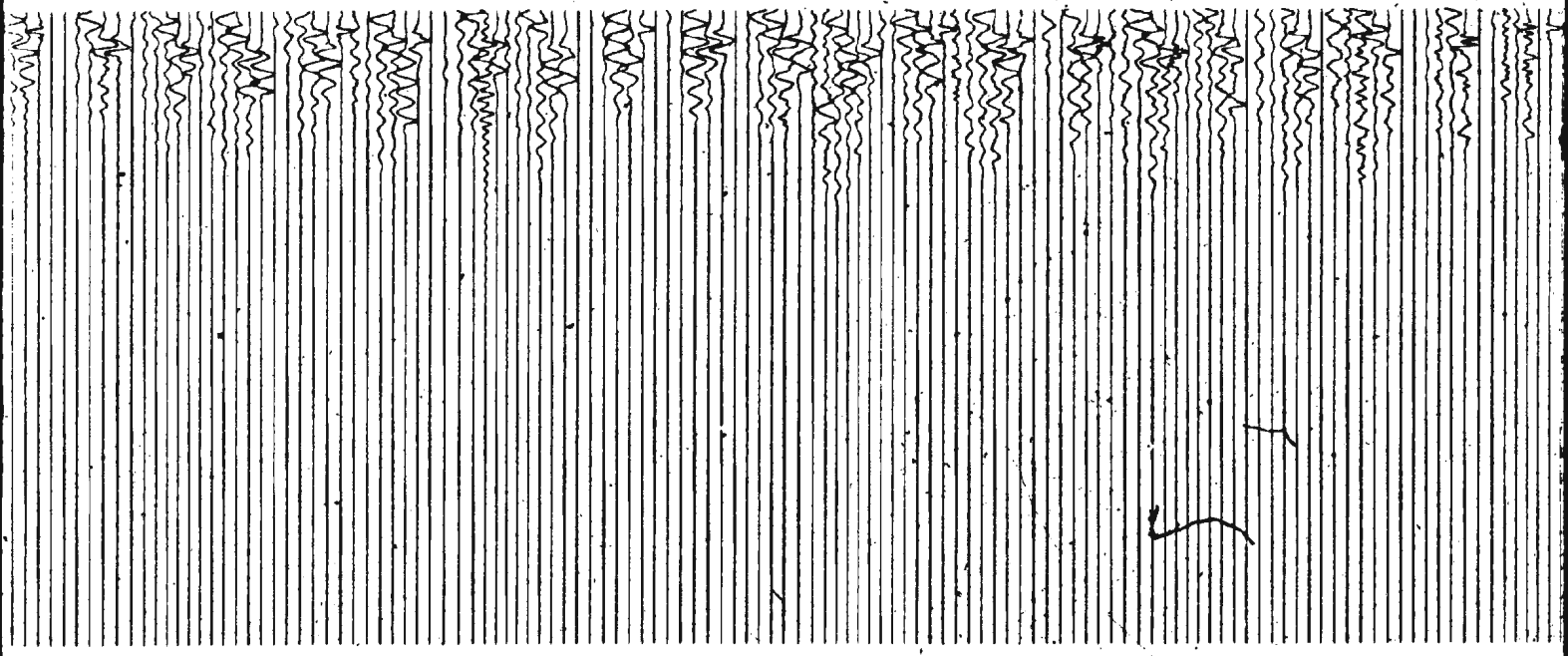


FIG. 3.9 PLOT OF DATA AFTER NMO CORRECTION

207

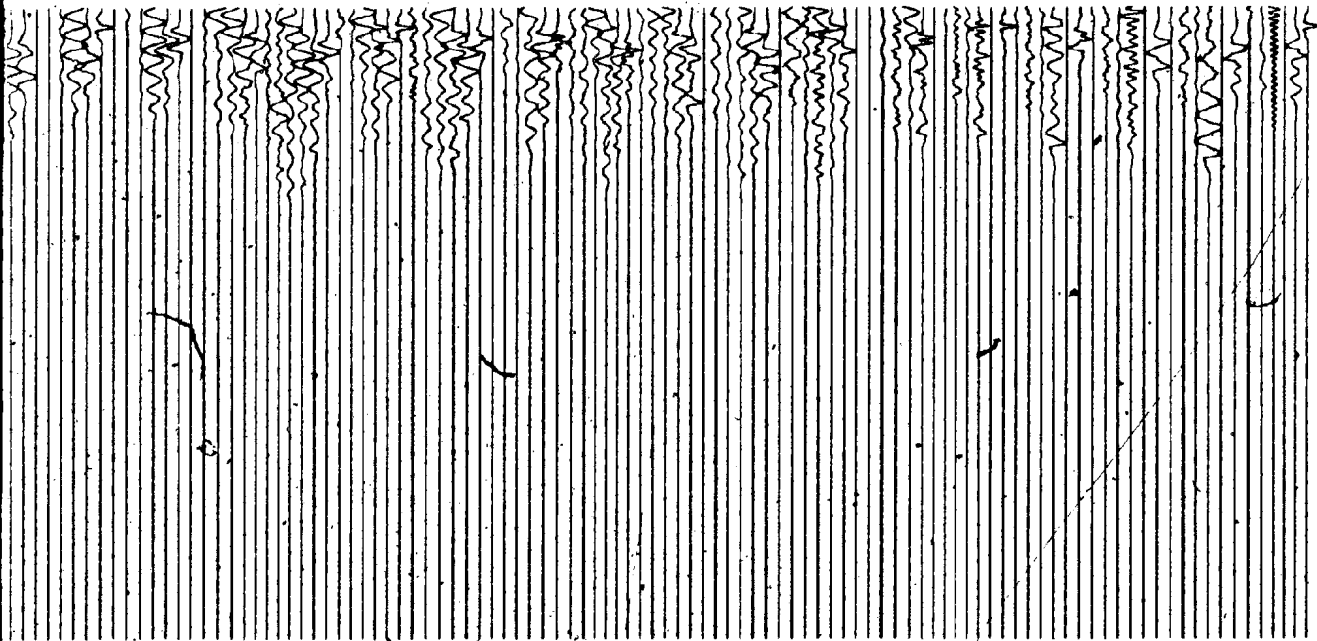
2

DATA AFTER NMO CORRECTION



3 of 3

DATA AFTER NMO CORRECTION



1 of

STACKE

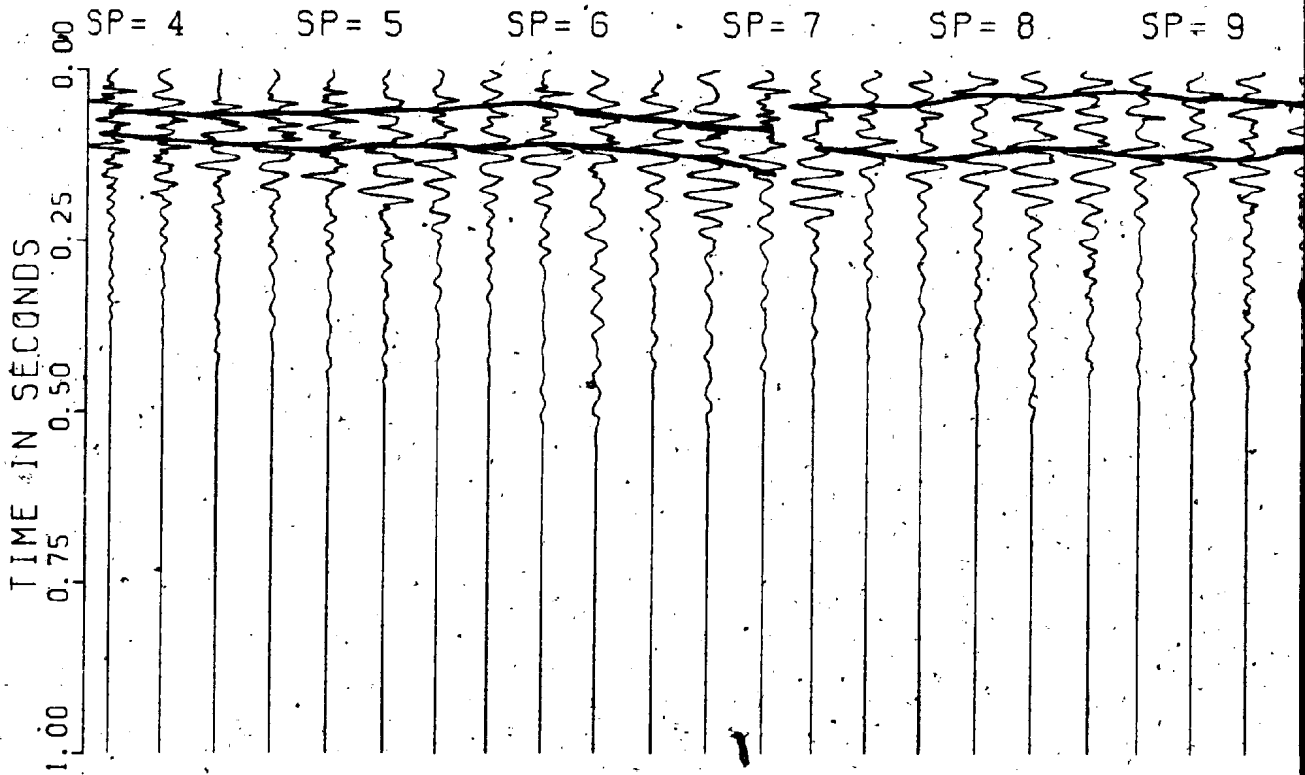
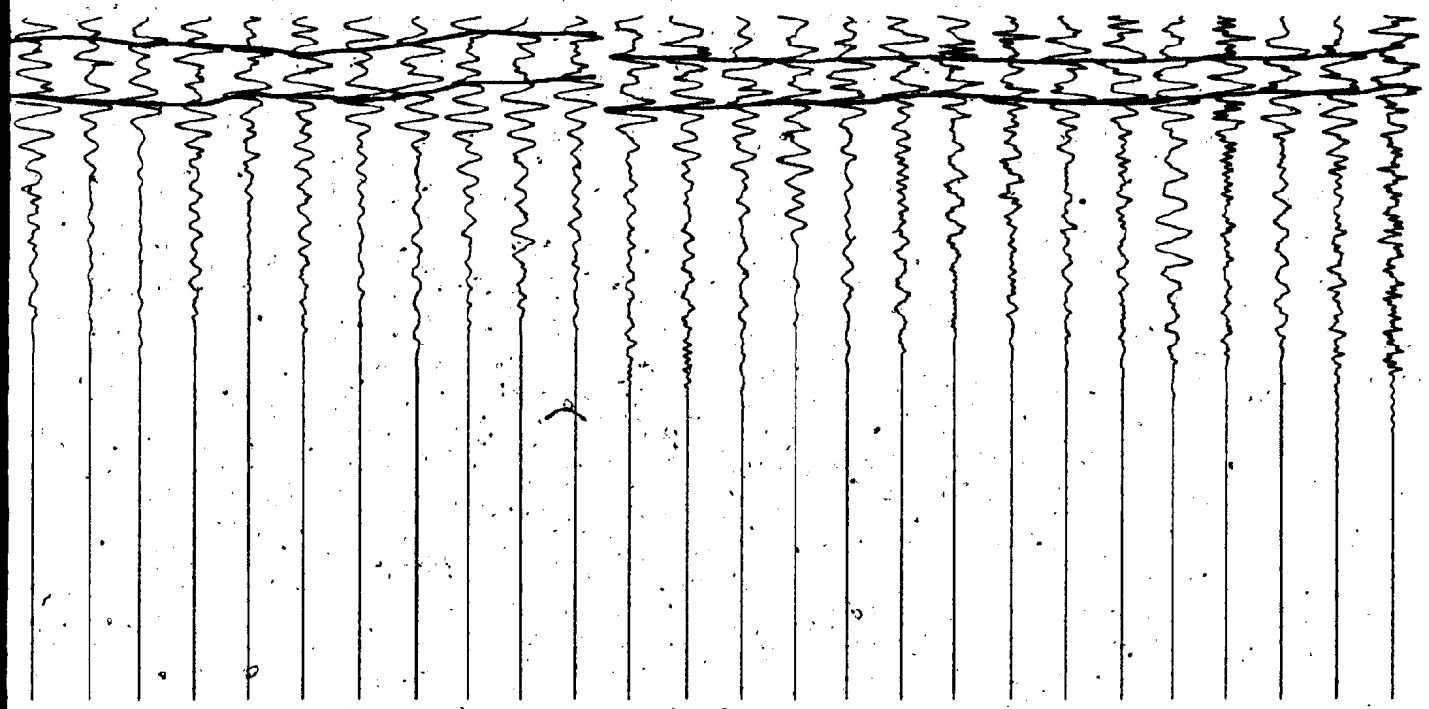


FIG. 3. 10 PLOT OF STACKED DATA

2 of 2 |

STACKED DATA

SP= 9 SP= 10 SP= 11 SP= 12 SP= 13 SP= 14



1 of 1

SYNTHETIC

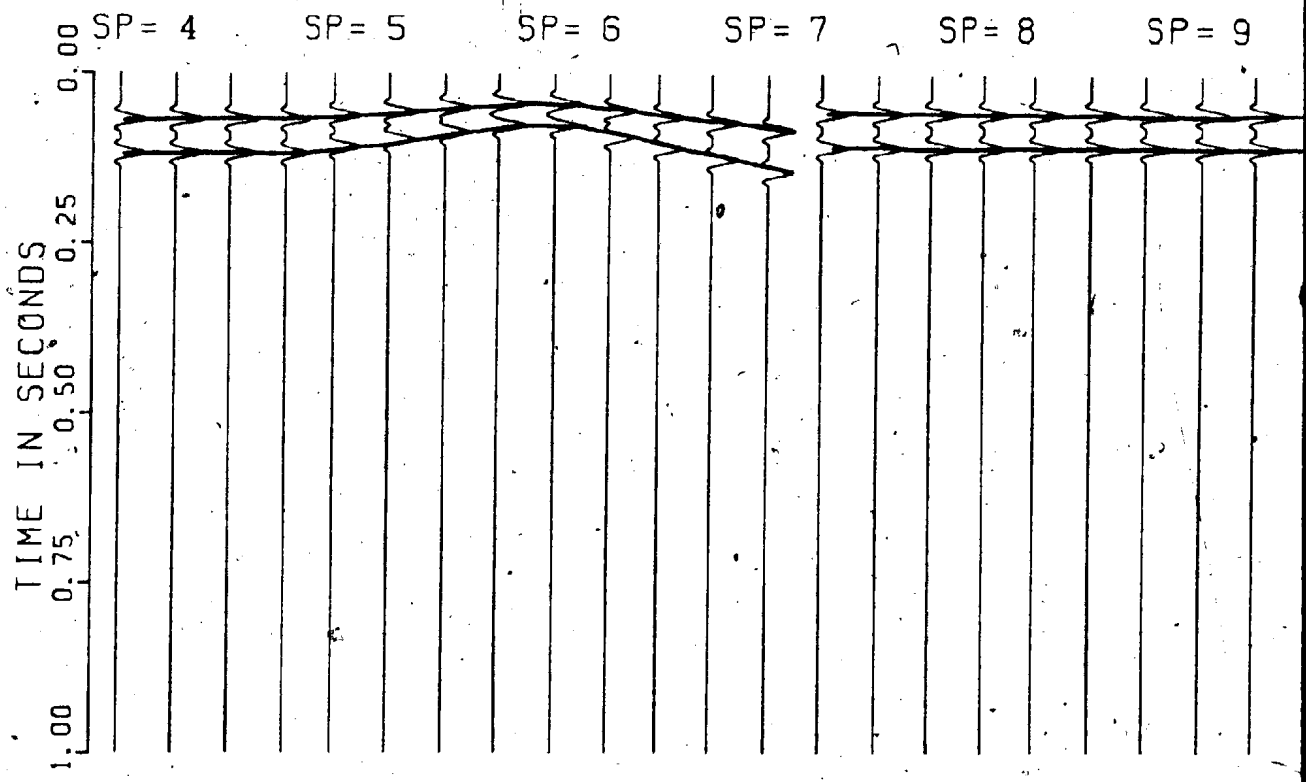
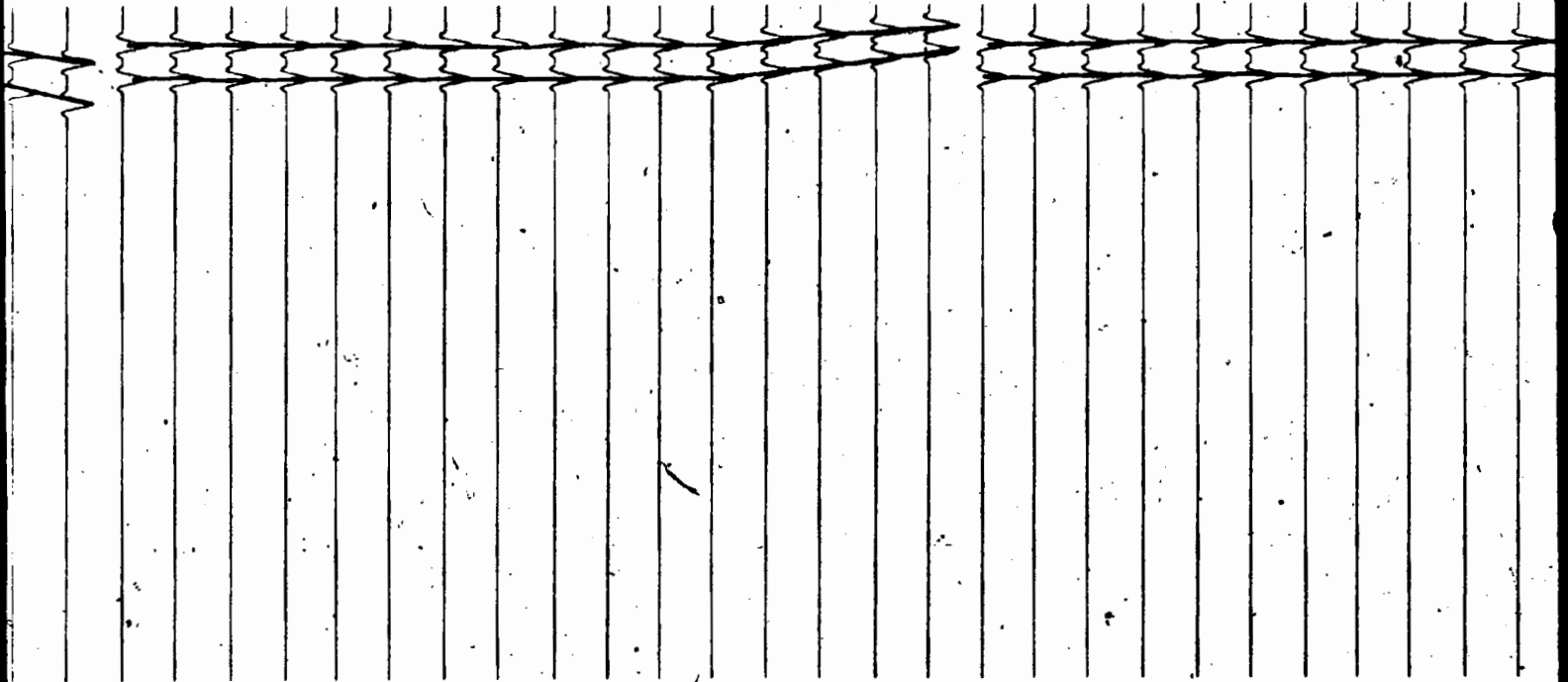


FIG. 4.1 PLOT OF SYNTHETIC STACKED DATA

207

SYNTHETIC STACKED DATA

SP= 7 SP= 8 SP= 9 SP= 10 SP= 11 SP= 12 SP= 13 SP=



STACKED DATA

3 of 3

IC STACKED DATA

P= 9 SP= 10 SP= 11 SP= 12 SP= 13 SP= 14

